AN ABSTRACT OF THE THESIS OF

George Modesto Adotevi-Akue for the DOCTOR OF PHILOSOPHY
(Name) (Degree)

in GEOPHYSICS presented on April 29, 1971
(Major) (Date)

Title: ON THE NUMERICAL INTERPRETATION OF GRAVITY AND OTHER POTENTIAL FIELD ANOMALIES CAUSED BY LAYERS OF VARYING THICKNESS

Abstract approved: Redacted for Privacy

This thesis involves the interpretation of gravity and other potential field anomalies caused by layers of varying thickness. The partial differential equations of potential field theory are reviewed for gravitational and magnetic force fields. A similar review is carried out for steady-state heat transport and diffusion processes. For the gravitational force fields, solutions of the partial differential equations are listed in integral form for the following cases: single body with given constant density, infinitely thin sheet with variable mass density, two homogeneous layers with a slowly undulating interface and two layers with a vertically-constant-density lower layer. The solutions give the gravity anomaly in terms of the parameters of the source body. Heat transport phenomena of a similar nature are also discussed.

The general expression obtained for the two homogeneous layers

with a slowly undulating interface is used as an integral equation and applied to the derivation of crustal thickness variation in Oregon on the basis of two different computational methods. The first method, called the digitized algebraic method, solves the quasi-linearized form of the general integral equation by an iterative technique for three reference values of the mean depth of the crust-mantle interface, viz., 25 km, 30 km, and 35 km. The second approach, called the second derivative approximation method, gives a solution by the Fourier transform technique to the linearized form of the general integral equation for the same three reference values of the mean depth of the crust-mantle interface.

The above results as to the depth of the crust-mantle interface are compared with recent results with seismic refraction and dispersion data obtained along a profile in eastern Oregon. The value of the reference depth d which best reconciles with the above results and the seismic results turns out to be 30.25 km for the depth data on the basis of the algebraic method and 28.90 km for the depth data obtained with the second derivative approximation method.

On the Numerical Interpretation of Gravity and Other Potential Field Anomalies Caused by Layers of Varying Thickness

by

George Modesto Adotevi-Akue

A THESIS

submitted to

Oregon State University

in partial fulfillment of
the requirements for the
degree of

Doctor of Philosophy

June 1972

APPROVED:

Redacted for Privacy

Professor of Mathematics and Geophysics

in charge of major

Redacted for Privacy

Chairman of Department of Oceanography

Redacted for Privacy

Dean of Graduate School

Date thesis is presented April 9, 1971

Typed by Clover Redfern for George Modesto Adotevi-Akue

ACKNOWLEDGMENT

With appreciation to:

Professor Gunnar Bodvarsson for selecting the project and for his willing cooperation in directing it.

Dr. Donald F. Heinrichs and Dr. Richard W. Couch for reading the manuscript and making many valuable suggestions for improvement.

Mr. Walter M. Pawley and Mr. Ken Keeling for their ready help with computer programming.

And finally to my wife, Ellen, for her companionship and unfailing moral support.

TABLE OF CONTENTS

LIST OF FIGURES

LIST OF TABLES

ON THE NUMERICAL INTERPRETATION OF GRAVITY AND OTHER POTENTIAL FIELD ANOMALIES CAUSED BY LAYERS OF VARYING THICKNESS

INTRODUCTION

The last three decades have seen tremendous progress in exploration geophysics. More accurate field measurements are being made by well trained observers using equipment of high precision. A considerable amount of geologic data is being obtained, thereby increasing knowledge of the subsurface geology and providing the control which is needed to surmount the difficulty arising from the inherent ambiguity of potential field interpretation. Recently various types of electronic computers have been put into use that provide rapid means of carrying out the numerous repetitive computations that attend geophysical data analysis.

Corresponding progress has been made in the analysis and interpretation of the field data. Regional-residual, various derivative, downward and upward continuation calculations have received increasing attention. In addition to the indirect method of interpretation (Grant and West, 1965), various direct procedures have received recognition (Tsuboi and Fuchida, 1937; Tsuboi, 1938; Bullard and Cooper, 1948; Tomoda and Aki, 1955; Bott, 1969, 1967). The aim of this study is the solution by two different computational methods of an

inverse problem in gravity that involves obtaining the variation of the crustal thickness in Oregon on the basis of observed surface data. One approach will be based on a method of solving a system of quadratic algebraic equations. The inversion of a linear integral equation of the first kind by the Fourier transform technique will form the basis of the second approach; the finite solution involves the computation of the second vertical derivative and the upward continuation of the gravity field.

The review of the applicable partial differential equations of potential theory and scalar fields and their solutions for various source bodies provides the point of departure for this study.

THE POTENTIAL EQUATION IN APPLIED GEOPHYSICS

Force Fields

In potential theory, if an attractive force $\vec{F}$ over a region of space can be expressed as the negative gradient of a scalar function, i.e.,

$$\vec{F} = -\nabla\phi \tag{1.1}$$

then $\vec{F}$ is called a conservative force; the function ϕ is known as a scalar potential function and can be shown to satisfy certain partial differential equations of the second order known as Poisson and Laplace's equations (Kellogg, 1929; MacMillan, 1958). Certain geophysical force fields can be described in terms of the potential function. As examples of these, the gravitational and magnetic fields will be considered and the relevant equations derived for them.

Gravitational Fields

The law of gravitation discovered by Newton is that two particles attract each other with a force which is directly proportional to the product of the masses of the particles and inversely proportional to the square of the distance between them. Thus if m_P and m_Q are the masses of two particles situated at the points P and Q respectively and if r_{PQ} is their separation, the magnitude of the

force of attraction between them is

$$F = \gamma \frac{m_P m_Q}{r_{PQ}^2} \tag{1.2}$$

where γ is the universal constant of gravitation. Now let $\vec{r}_{PQ}$ be the vector joining the points P and Q, its direction being $Q \rightarrow P$. In vector notation, the force of attraction exerted by the mass m_Q on m_P is given by

$$\vec{F}(P) = -\gamma \frac{m_P m_Q}{r_{PQ}^3} \vec{r}_{PQ} \tag{1.3}$$

the minus sign indicating that the direction of the force is opposite to that of the vector $\vec{r}_{PQ}$. In the above equation if $m_P = 1$, then we have

$$\vec{g}(P) = -\gamma \frac{m_Q}{r_{PQ}^3} \vec{r}_{PQ} \tag{1.4}$$

where $\vec{g}(P)$ is referred to as the gravitational acceleration due to the particle of mass m_Q at P. Define the quantity

$$U(P) = -\gamma \frac{m_Q}{r_{PQ}} \tag{1.5}$$

It is easily seen that

$$\vec{g}(P) = -\nabla_P U(P) \tag{1.6}$$

and hence $U(P)$ is a gravitational potential and the form of the expression (1.5) gives the potential of the particle m_Q at P.

Although Newton's law as stated above applies to particles, it holds also for bodies with a continuous distribution of matter. In Equation (1.5), let B be a body with a continuous distribution of matter represented by the density function $\rho(P)$. The total mass within B is

$$m_B = \int_B \rho(Q) dV_Q$$

and by the principle of superposition we have

$$U(P) = -\gamma \int_B \frac{\rho(Q)}{r_{PQ}} dV_Q \tag{1.7}$$

Equation (1.7) gives the expression for the gravitational potential due to a continuous distribution of matter represented by the density function $\rho(P)$. Assuming that B is finite, operate with the Laplacian on both sides of Equation (1.7)

$$\nabla^2 U(P) = -\gamma \nabla^2 \int_B \frac{\rho(Q)}{r_{PQ}} dV_Q$$

and interchange the integration and differentiation, which is permissible when $\rho(P)$ and B are bounded

$$\nabla^2 U(P) = -\gamma \int_B \rho(Q) \nabla_P^2 \left(\frac{1}{r_{PQ}}\right) dV_Q \tag{1.8}$$

We then have (Duff and Naylor, 1966)

$$\nabla_P^2 \left(\frac{1}{r_{PQ}}\right) = -4\pi\delta(P-Q)$$

where $\delta(P-Q)$ is the three-dimensional Dirac delta function. Substitute into Equation (1.8)

$$\nabla^2 U(\delta) = 4\pi\gamma \int_B \rho(Q)\delta(P-Q) dV_Q$$

or

$$\nabla^2 U(P) = 4\pi\gamma\rho(P) \tag{1.9}$$

This result is Poisson's equation. If the point P is located in a region of space in which there is no mass distribution, then $\rho(P) = 0$ and we have

$$\nabla^2 U(P) = 0 \tag{1.10}$$

which result is the well known Laplace equation.

Magnetic Fields

Assuming for convenience that magnetic monopoles exist, the fundamental law of magnetic force is that a magnetic pole of strength m_P at a point P in the field of another pole of strength m_Q at a point Q and at a distance r_{PQ} experiences a force $\vec{F}$ whose magnitude is given by

$$F = \frac{m_P m_Q}{r_{PQ}^2} \tag{1.11}$$

the force being attractive if the poles are of opposite polarity and repulsive if the polarity is the same. In vector notation, define $\vec{r}_{PQ}$ as the vector joining the points P and Q, its direction being $Q \rightarrow P$. If the poles are of opposite polarity, the attractive force experienced by the pole at P is given by (m_Q is negative)

$$\vec{F}(P) = \frac{m_P m_Q}{r_{PQ}^3} \vec{r}_{PQ} \tag{1.12}$$

If in Equation (1.12), $m_P = 1$, we shall have

$$\vec{H}(P) = \frac{m_Q}{r_{PQ}^3} \vec{r}_{PQ} \qquad (1.12a)$$

in which $\vec{H}(P)$ is the magnetic field intensity at P due to the pole of strength m_Q. Define the quantity $A(P)$ by the relation

$$A(P) = \frac{m_Q}{r_{PQ}} \qquad (1.13)$$

It is seen that

$$\vec{H}(P) = -\nabla A(P) \qquad (1.14)$$

and hence $A(P)$ is a scalar magnetic potential function and the form (1.13) gives the scalar magnetic potential of an isolated magnetic pole.

Magnetic poles probably do not exist in nature. Magnetic fields are due to currents, and small current loops can be approximated by dipoles. A dipole or doublet comprises a pair of opposite pole strengths $-m$ and m at points $Q-$ and $Q+$ at a distance d apart, d being infinitesimal and m correspondingly large so that the product md has a finite value M. M is called the magnetic moment of the dipole and the line $Q-Q+$ is called the axis. The axis is considered as having the direction $\overrightarrow{Q-Q+}$. The moment can be specified by the vector $\vec{M}$ of magnitude M and direction $\overrightarrow{Q-Q+}$. If the vector $\overrightarrow{Q-Q+}$ is denoted $\vec{d}$, then

$$\vec{M} = m\vec{d} \qquad (1.15)$$

If the position of another point P relative to the dipole is specified by the position vector $\vec{r}_{PQ}$ and inclined at the angle θ to the axis, Q being the center of the dipole, then the scalar magnetic potential due to the dipole is given by (Chapman and Bartels, 1940)

$$A(P) = \frac{M \cos \theta}{r_{PQ}^2}$$

$$= -\vec{M} \cdot \nabla_P \left(\frac{1}{r_{PQ}}\right) \tag{1.16}$$

and the force experienced by a unit pole at P is

$$\vec{H}(P) = -\nabla_P A(P)$$

$$= \nabla_P \left(\vec{M} \cdot \nabla_P \left(\frac{1}{r_{PQ}}\right)\right) \tag{1.17}$$

Now suppose that a closed finite region B has a continuously distributed magnetic dipole moment per unit volume given by $\vec{M}$. Then by superposition, the scalar magnetic potential at a point P outside B is

$$A(P) = \int_B \vec{M}(Q) \cdot \nabla_Q \left(\frac{1}{r_{PQ}}\right) dV_Q$$

and since B is finite

$$A(P) = -\int_B \frac{(\nabla_Q \cdot \vec{M}(Q))}{r_{PQ}} dV_Q \tag{1.18}$$

Since B is finite, operate with the Laplacian on both sides of Equation (1.18)

$$\nabla^2 A(P) = -\nabla^2 \int_B \frac{(\nabla_Q \cdot \vec{M}(Q))}{r_{PQ}} dV_Q$$

$$= -\int_B (\nabla_Q \cdot \vec{M}(Q)) \nabla_P^2 \left(\frac{1}{r_{PQ}}\right) dV_Q \qquad (1.19)$$

As before, rewrite $\nabla_P^2 \left(\frac{1}{r_{PQ}}\right)$ in terms of the Dirac delta function, i.e.,

$$\nabla_P^2 \left(\frac{1}{r_{PQ}}\right) = -4\pi\delta(P-Q)$$

Substitute into Equation (1.19) and we have

$$\nabla^2 A(P) = 4\pi \int_B (\nabla \cdot \vec{M}(Q))\delta(P-Q) dV_Q$$

or

$$\nabla^2 A(P) = 4\pi \nabla \cdot \vec{M}(P) \qquad (1.20)$$

which is Poisson's equation for the magnetic case. If the point P is located in a region of space without dipole distribution, then $\vec{M}(P) = 0$ and we have that

$$\nabla^2 A(P) = 0 \qquad (1.21)$$

which is the Laplace equation.

Stationary Flows Without Vorticity

In discussing stationary conduction flows such as the flow of a fluid in porous, isotropic media, let $\vec{F}$ represent the rate of flow through unit area. Assuming the existence of a flow potential, we have for the stationary flow

$$\vec{F} = -K\nabla\phi \tag{1.22}$$

where K is known as the conductivity of the medium through which the flow takes place. ϕ is referred to in this case as the flow potential. For the flow across a closed surface enclosing a volume V, the equation of continuity applies, i.e.,

$$\int_S \vec{F}\cdot\vec{n}\,dS = \int_V A\,dV \tag{1.23}$$

where $\vec{n}$ is the outward normal to S and A is the source density. It represents the rate of generation or of decrease of the fluid inside V. From Gauss's law

$$\int_S \vec{F}\cdot\vec{n}\,dS = \int_V \operatorname{div}\vec{F}\,dV$$

and so by substituting for the left-hand side of Equation (1.23), we obtain

$$\int_V \text{div}\,\vec{F}\,dV = \int_V A dV \tag{1.23a}$$

Substitute from Equation (1.22) into (1.23a)

$$-\int_V \text{div}(K\nabla\phi)dV = \int_V A dV \tag{1.24}$$

The above equation holds for any volume V and so the integrands should be equal. Consequently

$$-\text{div}(K\nabla\phi) = A \tag{1.25}$$

which is a generalized potential equation. If K is constant, Equation (1.25) becomes

$$-K\nabla^2\phi = A \tag{1.26}$$

which is a potential equation of the Poisson type. As examples of stationary flow fields, heat transport and stationary diffusion fields will be considered.

Heat Transport Fields Including Convective Terms

Consider a body B of incompressible material in which the temperature at a point P and time t is $T(P,t)$. Assume that the material of the body is moving with velocity $\vec{U}(P,t)$ and that

heat is being generated in the material at the rate S per unit mass. Assume also that there is a fluid percolating through the material and whose velocity relative to the material at the point P and time t is $\vec{V}(P,t)$. With these assumptions, the rate of heat conduction, $\overrightarrow{dQ}_c$, through a surface element dA of the material is given by Fourier's law as

$$\overrightarrow{dQ}_c = -KdA \text{ grad } T \tag{1.27}$$

where grad T is the temperature gradient along the outward normal to the surface element and K is the thermal conductivity of the material. If the material is isotropic, K is a scalar quantity. For non-isotropic materials, however, it is a conductivity tensor.

The fluid percolating through dA in the material transports heat relative to it at the rate $\overrightarrow{dH}_f$ given by

$$\begin{aligned}\overrightarrow{dH}_f &= s\rho_f\vec{V}TdA \\ &= s\vec{M}_m TdA\end{aligned} \tag{1.28}$$

where

$\vec{M}_m = \rho_f\vec{V}$

s = specific heat of the fluid

ρ_f = density of the fluid

The total heat transport $\vec{Q}$ is the sum of $\overrightarrow{dQ}_c$ and $\overrightarrow{dH}_f$, i.e.,

$$\vec{Q} = -K \text{ grad } T + s\vec{M}_m T \tag{1.29}$$

On the basis of the above results and by standard method one obtains the heat transport equation (Bodvarsson, 1966)

$$\rho S + \text{div}(K \text{ grad } T) + s \text{ div}(\vec{M}_m T) = \rho c \frac{DT}{Dt} \tag{1.30}$$

Since the material of the body is moving with velocity $\vec{U}$, the quantity $\frac{DT}{Dt}$ has to be interpreted as the total derivative, i.e.,

$$\frac{DT}{Dt} = \frac{\partial T}{\partial t} + \vec{U} \cdot \text{grad } T \tag{1.31}$$

Assuming that the fluid is incompressible, $\text{div } \vec{M}_m = 0$ and hence

$$\text{div}(\vec{M}_m T) = \vec{M}_m \cdot \text{grad } T \tag{1.32}$$

Substitute from Equations (1.31) and (1.32) into Equation (1.30) and we have the final expression for the heat transport equation

$$\text{div}(K \text{ grad } T) + \rho S = \rho c \frac{\partial T}{\partial t} + \rho c \vec{f} \cdot \text{grad } T \tag{1.33}$$

where

$$\vec{f} = \vec{U} + \frac{s\vec{M}_m}{\rho c} \tag{1.34}$$

Equation (1.33) is the general heat transport equation.

In some aeolotropic media, the conductivity, K, is a diagonal matrix with elements which are the same in two directions but different in the third. If the elements are K_x, K_y and K_z, but with $K_x = K_y = K_o$, we have

$$\text{div}(K \text{ grad } T) = \frac{\partial}{\partial x}\left(K_o \frac{\partial T}{\partial x}\right) + \frac{\partial}{\partial y}\left(K_o \frac{\partial T}{\partial y}\right) + \frac{\partial}{\partial z}\left(K_z \frac{\partial T}{\partial z}\right) \tag{1.35}$$

and Equation (1.33) becomes

$$\frac{\partial}{\partial x}\left(K_o \frac{\partial T}{\partial x}\right) + \frac{\partial}{\partial y}\left(K_o \frac{\partial T}{\partial y}\right) + \frac{\partial}{\partial z}\left(K_z \frac{\partial T}{\partial z}\right) + \rho S = \rho c \frac{\partial T}{\partial t} + \rho c \vec{f} \cdot \text{grad } T \tag{1.36}$$

If the conducting material is at rest and there is no fluid motion through it, the transport vector $\vec{f}$ is zero and the equation is

$$\frac{\partial}{\partial x}\left(K_o \frac{\partial T}{\partial x}\right) + \frac{\partial}{\partial y}\left(K_o \frac{\partial T}{\partial y}\right) + \frac{\partial}{\partial z}\left(K_z \frac{\partial T}{\partial z}\right) + \rho S = \rho c \frac{\partial T}{\partial t} \tag{1.37}$$

Equations (1.36) and (1.37) describe non-stationary phenomena, i.e., those phenomena in which the temperature varies not only in space but also with time. In deriving them, the conducting medium has been considered to be aeolotropic. If $K_x = K_y = K_z = K$ and the material is homogeneous, then the heat transport equation becomes

$$K\nabla^2 T = \rho c \frac{\partial T}{\partial t} + \rho c \vec{f} \cdot \text{grad } T - \rho S \tag{1.38}$$

For stationary phenomena, $\frac{\partial T}{\partial t} = 0$ and we have

$$K\nabla^2 T = \rho c \vec{f} \cdot \text{grad } T - \rho S \qquad (1.39)$$

which result may be considered as an extended potential equation. If the conducting medium is at rest and there is no fluid motion through it, then $\vec{f} = 0$ and Equation (1.39) becomes

$$-K\nabla^2 T = \rho S \qquad (1.40)$$

which is a potential equation of the Poisson type. The corresponding heat flow is a potential flow.

Stationary Diffusion Fields

Consider a substance that is being transported by a simple diffusion process. Let its concentration and density be s kg/kg and S kg/m^3 respectively and $\vec{q}$ its flow in kg/m^2 sec. The density and diffusive conductivity of the solvent are respectively ρ kg/m^3 and K kg/m sec. Fick's law of diffusion gives the flow, $\vec{q}$, of the substance by the relation

$$\vec{q} = -K \text{ grad } s \qquad (1.41)$$

Put $s = \frac{S}{\rho}$ and assume that ρ is constant. We have

$$\vec{q} = -a \text{ grad } S \qquad (1.42)$$

where $a = \frac{K}{\rho}$ and is known as the diffusivity. Starting from Equation

(1.42), the derivation of the diffusion equation follows a pattern which is similar to that of heat transport fields. The resulting diffusion equation is (Sutton, 1953)

$$\frac{\partial}{\partial x}\left(a_x \frac{\partial S}{\partial x}\right) + \frac{\partial}{\partial y}\left(a_y \frac{\partial S}{\partial y}\right) + \frac{\partial}{\partial z}\left(a_z \frac{\partial S}{\partial z}\right) = \frac{\partial S}{\partial t} + \vec{V} \cdot \text{grad } S \qquad (1.43)$$

where $\vec{V}$ is the velocity with which the medium moves and a_x, a_y and a_z are the values of the diffusion coefficient in the x, y and z directions respectively. If the coefficients are constant along their respective axes, Equation (1.43) becomes

$$a_x \frac{\partial^2 S}{\partial x^2} + a_y \frac{\partial^2 S}{\partial y^2} + a_z \frac{\partial^2 S}{\partial z^2} = \vec{V} \cdot \text{grad } S + \frac{\partial S}{\partial t} \qquad (1.44)$$

For the stationary case in which there is a source of strength Q kg/m^3 sec and for which the diffusion coefficient is a constant, we obtain

$$-a\nabla^2 S = Q \qquad (1.45)$$

which result is a Poisson-type potential equation. It is thus seen that the stationary diffusion process with constant diffusivity is equivalent to a potential flow.

THE INTEGRAL EQUATIONS OF INTERPRETATION THEORY

The geophysical interpretation of potential field data involves essentially the determination of unknown source parameters from known field values. The problem is often referred to as the inverse problem of potential theory. The earliest approach to solving the problem is the indirect method, according to which theoretical field values are computed for assumed models of the source and compared with the observed values for a fit. Adjustments are then made to the model, if necessary, and the theoretical field values are recomputed until the best fit is obtained. An alternative is the direct method, which seeks solutions to the inverse problem by means of numerical and analytical techniques.

In general, the inverse problem of potential theory does not have a unique solution, for there is not enough information to determine the size and shape of the source completely and unambiguously from its potential field. In the simple cases in which unique solutions can be found, the direct method often involves the solution of certain integral equations in two or three dimensions. The integral equations derive from the general solutions of the equations whose derivations have been given in the previous chapter. In this chapter, the fundamental integral equations are established for some simple cases pertaining to gravitational and heat transport fields.

Gravitational Fields

Basic Theory

In the previous chapter, the gravitational potential due to a continuous distribution of matter has been shown to be (Equation (1.7))

$$U(P) = -\gamma \int_B \frac{\rho(Q)}{r_{PQ}} dV_Q \tag{2.1}$$

r_{PQ} being the distance from the field point P to the source point Q. The gravitational acceleration at P is derivable from $U(P)$ and is given by

$$\vec{g}(P) = -\nabla_P U(P)$$

or

$$\vec{g}(P) = \gamma \int_B \nabla_P \left(\frac{1}{r_{PQ}}\right) \rho(Q) dV_Q \tag{2.2}$$

which, in the case of an unknown density, is an integral equation in $\rho(P)$ and is the fundamental integral equation of interpretation theory. If $\vec{g}(P)$ is given outside B, as, for instance, on a plane not intersecting B, the problem of solving Equation (2.2) for $\rho(P)$ is underdetermined. The sphere of constant density provides a simple illustration of the underdetermined nature of the problem. The mass of the sphere can be considered as concentrated at its center without

changing the external gravitational field, i.e., the field in the space for which $r_{PO} > R$, R being the radius of the sphere and O its center (Garland, 1965). Thus for all points external to the sphere, the evaluation of the integral in Equation (2.1) gives (Garland, 1965)

$$U(P) = -\gamma \frac{M}{r_{PO}} \tag{2.3}$$

We then have

$$\vec{g}(P) = \gamma M \nabla_P \left(\frac{1}{r_{PO}}\right) \tag{2.4}$$

where M is the total mass of the sphere and is given by the expression

$$M = \frac{4}{3} \pi R^3 \rho \tag{2.5}$$

Whereas the total mass of the sphere is obtainable from Equation (2.4), it is not possible to uniquely determine ρ from M according to Equation (2.5), since different combinations of the values of ρ and R can be found to satisfy this equation. Hence the problem is underdetermined. There exist, however, some simple cases for which Equation (2.2) possesses unique solutions, provided that restrictions are imposed on some of the source parameters. The fundamental integral equations are established for these cases.

Single Body With Given Constant Density

The determination of the shape of a single body B, assumed to be of given constant density ρ, causing a gravitational field leads to the solution of the integral equation

$$\vec{g}(P) = \gamma\rho \int_B \nabla_P \left(\frac{1}{r_{PQ}}\right) dV_Q \tag{2.6}$$

for the form of B. The equation may be rewritten in the form

$$\vec{g}(P) = \gamma\rho \int_{space} \chi(Q) \nabla_P \left(\frac{1}{r_{PQ}}\right) dV_Q \tag{2.7}$$

which is an integral equation in $\chi(Q)$; $\chi(Q)$ is the characteristic function of the body and is defined as follows

$$\chi(P) = \begin{cases} 1 & \text{for P inside B} \\ 0 & \text{for P outside B} \end{cases}$$

Since two characteristic functions cannot be superposed, Equation (2.7) is a non-linear integral equation. By using the formula

$$\nabla_Q \left(\frac{\chi(Q)\rho(Q)}{r_{PQ}}\right) = \rho(Q)\chi(Q)\nabla_Q \left(\frac{1}{r_{PQ}}\right) + \frac{1}{r_{PQ}} \nabla(\chi(Q)\rho(Q)) \tag{2.8}$$

it is possible to recast the volume integral in Equation (2.6) into the surface integral (Bodvarsson, 1969)

$$g_k(P) = \gamma\rho \int_{\Sigma} \frac{\vec{k}\cdot\vec{n}(S)}{r_{PS}} \, dA_S \qquad (2.9)$$

where $\vec{k}$ is the unit vector in the direction of the gravitational acceleration, $\vec{n}$ the inward normal to the surface Σ of the body and S a point on the surface. The use of Equation (2.9) to compute the vertical acceleration of bodies bounded by vertical faces has the advantage that the product $\vec{k}\cdot\vec{n}$ is zero for these faces; consequently their contribution to the acceleration is zero. Equation (2.6) or equivalently (2.9) is the fundamental integral equation of the single body with constant density.

Infinitely Thin Sheet With Variable Mass Density

Let the sheet be represented by the surface Σ and let its mass density be $m(x, y)$. If $h(x, y)$ is the depth of the sheet, the mass density may be written in terms of the one-dimensional Dirac delta function, i.e., mass density $= m(x, y)\delta(z-h(x, y))$. Then by using Equation (2.2), the vertical acceleration $g(P)$ caused by the sheet is given by

$$g(P) = \gamma \int_{\text{space}} \frac{(z-\zeta)m(\xi, \eta)\delta(\zeta-h(x, y))}{r_{PQ}^3} \, dV_Q \qquad (2.10)$$

where

$$r_{PQ}^2 = (x-\xi)^2 + (y-\eta)^2 + (z-\zeta)^2$$

$$g(P) = \gamma \int_{\Sigma} \frac{(z-h(x, y))m(\xi, \eta)d\xi d\eta}{[(x-\xi)^2+(y-\eta)^2+(z-h(\xi, \eta))^2]^{3/2}} \qquad (2.11)$$

which is the fundamental equation for the infintely thin sheet.

Two Homogeneous Layers With a Slowly Undulating Interface

This case derives from the situation in which a layer, of constant density ρ_1, is underlain by a second layer, also of constant density ρ_2, the two layers being separated by a slowly undulating interface. It is assumed that ρ_2 is greater than ρ_1. The upper part of the top layer is assumed to be bounded by the plane $z = 0$, while the bottom of the lower layer is assumed to be a plane at a fixed depth. There is an average depth H to the interface such that

$$\frac{1}{A}\int D(S)dA_S = H \quad \text{for large } A \qquad (2.12)$$

where

dA_S = surface element at the point S on the interface

$D(S)$ = depth of the interface at the point S

The problem arising from this case is to calculate the relief amplitude $h(x, y)$ on the basis of observed surface anomalies and a given density contrast $\Delta\rho = \rho_2 - \rho_1$. Let d be a reference depth which is chosen to be of the same order as H. The model used is shown in Figure 1

below.

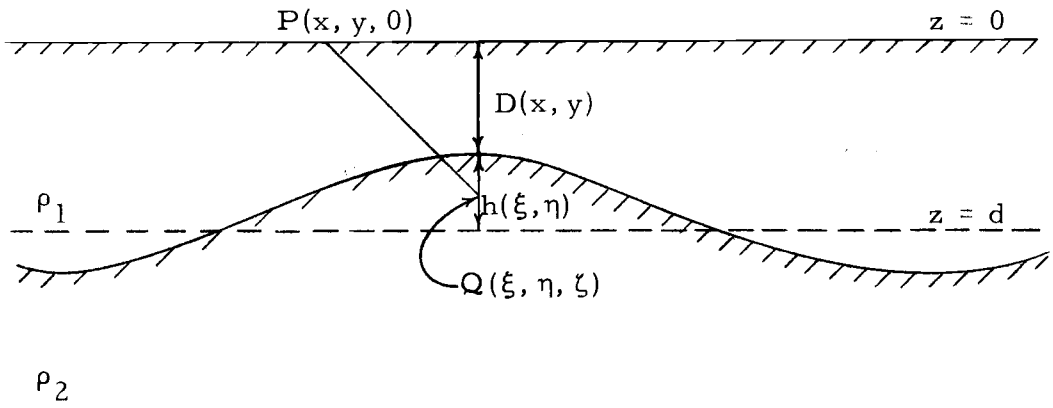

Figure 1. Illustration of the two homogeneous layers with a slowly undulating interface.

Since a slab of constant density does not produce a gravity anomaly, with reference to Figure 1, the vertical gravity anomaly at P is given by

$$g(P) = -\gamma\Delta\rho\frac{\partial}{\partial z}\int_{\xi}\int_{\eta}\int_{0}^{D(\xi,\eta)}\frac{d\xi d\eta d\zeta}{[(x-\xi)^2+(y-\eta)^2+(z-\zeta)^2]^{1/2}}$$

$$= \gamma\Delta\rho\int_{\xi}\int_{\eta}\int_{0}^{D(\xi,\eta)}\frac{(z-\zeta)d\xi d\eta d\zeta}{[(x-\xi)^2+(y-\eta)^2+(z-\zeta)^2]^{3/2}} \qquad (2.13)$$

If the point P is located on the surface, then $z = 0$ and the expression for the anomaly is

$$g(P) = -\gamma\Delta\rho \int_{\xi}\int_{\eta}\int_{0}^{D(\xi,\eta)} \frac{\zeta d\xi d\eta d\zeta}{[(x-\xi)^2+(y-\eta)^2+\zeta^2]^{3/2}} \qquad (2.14)$$

$D(x, y)$ may be written as

$$D(x, y) = d - h(x, y)$$

Substitute into Equation (2.14) and we have

$$g(P) = -\gamma\Delta\rho \int_{\xi}\int_{\eta}\int_{0}^{d-h(\xi,\eta)} \frac{\zeta d\xi d\eta d\zeta}{[(x-\xi)^2+(y-\eta)^2+\zeta^2]^{3/2}}$$

$$= -\gamma\Delta\rho \int_{\xi}\int_{\eta}\int_{0}^{d} \frac{\zeta d\xi d\eta d\zeta}{[(x-\xi)^2+(y-\eta)^2+\zeta^2]^{3/2}}$$

$$- \gamma\Delta\rho \int_{\xi}\int_{\eta}\int_{d}^{d-h(\xi,\eta)} \frac{\zeta d\xi d\eta d\zeta}{[(x-\xi)^2+(y-\eta)^2+\zeta^2]^{3/2}} \qquad (2.15)$$

The first integral on the right-hand side of Equation (2.15) is a constant since the limits of integration are fixed. Denote this integral by g_o. Then Equation (2.15) becomes

$$g(P) = g_o + \gamma\Delta\rho \int_{\xi}\int_{\eta} \left\{ \int_{d}^{d-h(\xi,\eta)} \frac{-\zeta d\zeta}{[(x-\xi)^2+(y-\eta)^2+\zeta^2]^{3/2}} \right\} d\xi d\eta$$

$$= g_o + \gamma\Delta\rho \int_{\xi}\int_{\eta} \left\{ \frac{1}{[(x-\xi)^2+(y-\eta)^2+(d-h)^2]^{1/2}} \right.$$

$$\left. - \frac{1}{[(x-\xi)^2+(y-\eta)^2+d^2]^{1/2}} \right\} d\xi d\eta \qquad (2.16)$$

Put

$$M = \frac{1}{[(x-\xi)^2+(y-\eta)^2+(d-h)^2]^{1/2}} - \frac{1}{[(x-\xi)^2+(y-\eta)^2+d^2]^{1/2}} \qquad (2.17)$$

$$= [(x-\xi)^2+(y-\eta)^2+d^2]^{-1/2}[1 - \frac{2dh-h^2}{[(x-\xi)^2+(y-\eta)^2+d^2]}]^{-1/2}$$

$$- [(x-\xi)^2+(y-\eta)^2+d^2]^{-1/2}$$

$$= R^{-1}[1 - \frac{2dh-h^2}{R^2}]^{-1/2} - R^{-1} \qquad (2.17a)$$

where

$$R^2 = (x-\xi)^2 + (y-\eta)^2 + d^2$$

The binomial expansion of the factor $[1 - \frac{2dh-h^2}{R^2}]^{-1/2}$ in Equation (2.17a) gives

$$[1 - \frac{2dh-h^2}{R^2}]^{-1/2} = 1 + \frac{1}{2}(\frac{2dh-h^2}{R^2}) + \frac{\frac{1}{2}x\frac{3}{2}}{2!}(\frac{2dh-h^2}{R^2})^2 + \ldots \qquad (2.18)$$

The right-hand side of (2.18) is an infinite series whose nth term is

$$U_n = \frac{\frac{1}{2}x\frac{3}{2}x\frac{5}{2}x \ldots x(\frac{2n-1}{2})}{(n-1)!}(\frac{2dh-h^2}{R^2})^{n-1} \qquad (2.19)$$

for $n > 1$

The (n+1)th term is

$$U_{n+1} = \frac{\frac{1}{2}x\frac{3}{2}x\frac{5}{2}x \ldots x(\frac{2n-1}{2})(\frac{2n+1}{2})}{n!} (\frac{2dh-h^2}{R^2})^n \qquad (2.20)$$

The ratio of the (n+1)th term to the nth term is

$$\frac{U_{n+1}}{U_n} = \frac{\frac{\frac{1}{2}x\frac{3}{2}x\frac{5}{2}x \ldots x(\frac{2n-1}{2})(\frac{2n+1}{2})}{n!} (\frac{2dh-h^2}{R^2})^n}{\frac{\frac{1}{2}x\frac{3}{2}x\frac{5}{2}x \ldots x(\frac{2n-1}{2})}{(n-1)!} (\frac{2dh-h^2}{R^2})^{n-1}}$$

$$= \frac{1}{n} (\frac{2n+1}{2})(\frac{2dh-h^2}{R^2})$$

$$= (1+\frac{1}{2n})(\frac{2dh-h^2}{R^2}) \qquad (2.21)$$

If it is assumed that $|h| \ll d$, then $dh - h^2 \approx dh$. The ratio $\frac{U_{n+1}}{U_n}$ becomes

$$\frac{U_{n+1}}{U_n} = 2(1+\frac{1}{2n})\frac{dh}{R^2}$$

$$\lim_{n \to \infty} \frac{U_{n+1}}{U_n} = \frac{2dh}{R^2} < 1$$

since R is much larger than both d and h. It follows that the series on the right-hand side of Equation (2.18) is convergent. Since

we have assumed $|h| \ll d$, we may terminate the binomial expansion at the third term and write

$$\left(1 - \frac{2dh - h^2}{R^2}\right)^{-1/2} = 1 + \frac{1}{2}\left(\frac{2dh - h^2}{R^2}\right) + \frac{\frac{1}{2} \times \frac{3}{2}}{2!}\left(\frac{2dh - h^2}{R^2}\right)^2 + E$$

$$= 1 + \frac{dh}{R^2} - \frac{h^2}{2R^2} + \frac{3d^2h^2}{2R^4} - \frac{3dh^3}{2R^4} + \frac{3h^4}{8R^4} + E$$

$$= 1 + \frac{dh}{R^2} + \frac{(3d^2 - R^2)h^2}{2R^4} - \frac{6dh^3 - 3h^4}{8R^4} + E$$

$$= 1 + \frac{dh}{R^2} + \frac{(3d^2 - R^2)h^2}{2R^4} + E' \qquad (2.22)$$

where

$$E' = E - \frac{6dh^3 - 3h^4}{8R^4} \qquad (2.23)$$

E being the error involved in terminating the expansion at the third term. The quantity M becomes

$$M = R^{-1}\left[1 + \frac{dh}{R^2} + \frac{(3d^2 - R^2)h^2}{2R^4} + E'\right] - R^{-1}$$

$$= \frac{dh}{R^3} + \frac{(3d^2 - R^2)h^2}{2R^5} + \frac{E'}{R} \qquad (2.24)$$

The gravity anomaly is then given by

$$g(P) = g_o + \gamma\Delta\rho \int_{\xi}\int_{\eta} \frac{h(\xi,\eta)}{R^3}\, d\xi d\eta$$

$$+ \gamma\Delta\rho \int_{\xi}\int_{\eta} \frac{(3d^2-R^2)h^2(\xi,\eta)}{2R^5} d\xi d\eta + \gamma\Delta\rho \int_{\xi}\int_{\eta} \frac{E'}{R}\, d\xi d\eta \qquad (2.25)$$

Put $g(P) - g_o = \Delta g(P)$ and the expression (2.25) becomes

$$\Delta g(P) = \gamma\Delta\rho \int_{\xi}\int_{\eta} \left\{ \frac{dh(\xi,\eta)}{R^3} + \frac{(3d^2-R^2)}{2R^5} h^2(\xi,\eta) \right\} d\xi d\eta$$

$$+ \gamma\Delta\rho \int_{\xi}\int_{\eta} \frac{E'}{R}\, d\xi d\eta \qquad (2.26)$$

which is a non-linear integral equation in $h(x, y)$. It is the fundamental integral equation for the two homogeneous layers with a slowly undulating interface. Equation (2.26) cannot be solved in its present form. To obtain a solution, it first has to be either quasi-linearized or linearized.

Two-Layer Case Having a Vertically-Constant-Density Lower Layer

This case consists of a layer with constant density ρ_1 overlying a second layer in which the density distribution is represented by $\rho_2(x, y)$, the vertical density contrast being $\Delta\rho(x, y) = \rho_2(x, y) - \rho_1$. The layers are separated by a slowly undulating interface. See the definition (2.12). The top layer is bounded at

its upper face by the plane $z = 0$ and the lower layer is bounded at its bottom face by the plane $z = H$. See Figure 2 for an illustration.

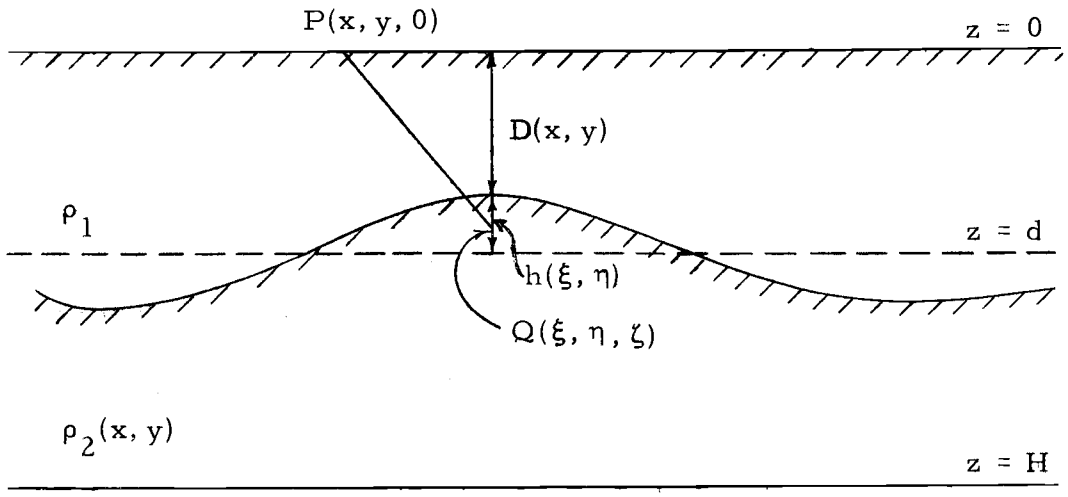

Figure 2. Illustration of the two-layer case having a vertically-constant-density lower layer.

The gravity anomaly at any point P is (see the explanation for the two homogeneous layers)

$$g(P) = -\gamma \frac{\partial}{\partial z} \int_{space} \frac{\Delta\rho(\xi, \eta)}{r_{PQ}} dV_Q$$

$$= \gamma \int_{\xi} \int_{\eta} \int_{D(\xi, \eta)}^{H} \frac{(z-\zeta)\Delta\rho(\xi, \eta) d\xi d\eta d\zeta}{[(x-\xi)^2+(y-\eta)^2+(z-\zeta)^2]^{3/2}} \qquad (2.28)$$

If the point P is located on the surface, then $z = 0$ and Equation (2.28) becomes

$$g(P) = -\gamma \int_{\xi} \int_{\eta} \int_{D(\xi,\eta)}^{H} \frac{\zeta \Delta\rho(\xi,\eta) d\xi d\eta d\zeta}{[(x-\xi)^2+(y-\eta)^2+\zeta^2]^{3/2}} \qquad (2.29)$$

From this point on, the derivation follows a pattern similar to that for the two homogeneous layers. The gravity anomaly is given by the expression

$$\Delta g(P) = \gamma \int_{\xi} \int_{\eta} \left\{ \frac{dh(\xi,\eta)}{R^3} + \frac{(3d^2-R^2)}{2R^5} h^2(\xi,\eta) \right\} \Delta\rho(\xi,\eta) d\xi d\eta$$

$$+ \gamma \int_{\xi} \int_{\eta} \frac{E'}{R} \Delta\rho(\xi,\eta) d\xi d\eta \qquad (2.30)$$

which is the fundamental integral equation for the two-layer case having a vertically-constant-density lower layer. It is non-linear in $h(x, y)$, but can be linearized if $|h| \ll d$.

Heat Transport Fields

Basic Theory

The interpretation of heat flow anomalies is done on the basis of solutions of the general heat transport equation with appropriate boundary conditions. Problems of this type are discussed by Shih (1968). The general heat transport equation has been found to be (see Equation (1.33))

$$\operatorname{div}(K \operatorname{grad} T) = \rho c \frac{\partial T}{\partial t} + \vec{f} \cdot \operatorname{grad} T - \rho S$$

or

$$\operatorname{div}(a \operatorname{grad} T) = \frac{\partial T}{\partial t} + \vec{f} \cdot \operatorname{grad} T - S/c$$

where $a = \frac{K}{\rho c}$ and is the diffusivity of the conducting medium. While no general solutions of this equation are known, solutions can be obtained by the perturbation method for those cases in which $\vec{f}$ is small or zero and variations in K or a are small. Let the conducting medium be an isotropic half-space in a steady state and let the heat production be zero, i.e., $S = 0$. We will assume that the thermal diffusivity may be considered as consisting of two terms, i.e.,

$$a = a_o + a_1 \quad \text{with} \quad |a_1| \ll |a_o|$$

where a_o is constant and a_1 is due to perturbation. It is assumed that $\vec{f}$ is small. The temperature is given to a first approximation by

$$T = T_o + T_1$$

where T_o is a solution of the Laplace equation and T_1 is the small temperature perturbation due to a_1 and $\vec{f}$. Substitute T into the heat transport equation and neglect second-order terms in T_1. There results the equation

$$\nabla^2 T_1 = -\frac{1}{a_o}[\mathrm{div}(a_1 \,\mathrm{grad}\, T_o) - \vec{f} \cdot \mathrm{grad}\, T_o] \qquad (2.32)$$

which is a Poisson-type equation. Suppose that the following boundary condition must be satisfied

$$T = 0 \quad \text{at} \quad z = 0$$

Then Equation (2.32) can be solved by the method of Green's function, the solution being

$$T_1 = -\frac{1}{a_o} \iiint F(Q)G(P,Q)dV_Q \qquad (2.33)$$

where

$$-F(Q) = \mathrm{div}(a_1 \,\mathrm{grad}\, T_o) - \vec{f} \cdot \mathrm{grad}\, T_o$$

$$G(P,Q) = \text{Green's function}$$

The Green's function for a homogeneous isotropic half-space with zero surface temperature is (Duff and Naylor, 1966)

$$G(P,Q) = \frac{1}{4\pi r_{PQ}} - \frac{1}{4\pi r_{PQ'}}$$

where Q' is the image in the upper half-space of the source point Q. The disturbed thermal gradient is

$$\frac{\partial T_1}{\partial z} = -\frac{1}{a_o} \iiint_{\text{space}} F(Q) \frac{\partial}{\partial z} G(P,Q)dV_Q \qquad (2.34)$$

$$g = g_o - \frac{1}{2\pi a_o} \iiint_{\text{space}} \frac{\frac{\partial a_1}{\partial \zeta} \frac{\partial T_o}{\partial \zeta} (z-\zeta) d\xi d\eta d\zeta}{r^3} \qquad (2.35)$$

$$r^2 = (x-\xi)^2 + (y-\eta)^2 + (z-\zeta)^2$$

Equation (2.35) is the fundamental equation that is applicable to problems involving the perturbation of the heat-flow fields. The problem of a basement rock covered by sediments with variable thickness and a flat surface is discussed below.

Basement Rock Covered by Sediments With Variable Thickness and a Flat Surface

The basement rock, of constant conductivity K_2, is covered with sediments, also of constant conductivity K_1 and a flat surface. It is assumed that $K_2 > K_1$. The interface separating the two layers is assumed to be a slowly undulating one at a mean depth d (see Equation (2.12)). See Figure 3 for an illustration of this case. The problem that arises from this case is to determine the relief amplitude $h(x, y)$ and hence the thickness of the sediments from the heat flow anomalies measured on the surface of the sedimentary layer.

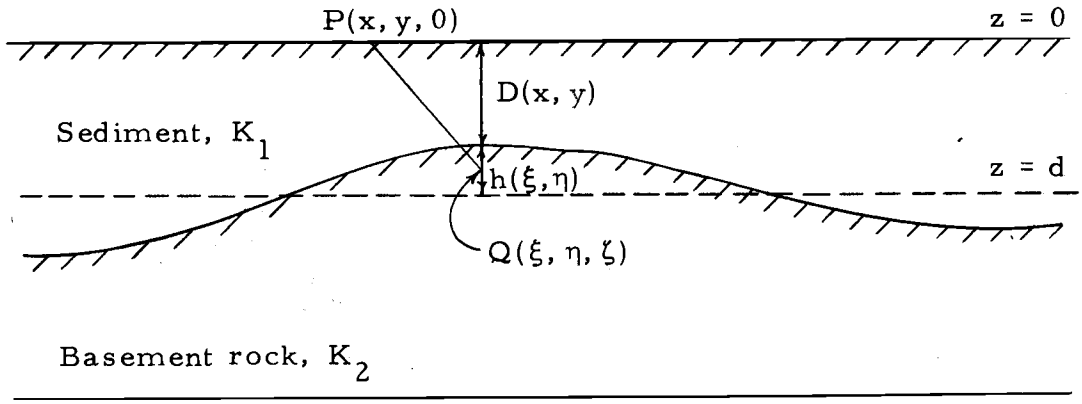

Figure 3. Illustration of basement rock covered by sediments with variable thickness and a flat surface.

Assume that the conducting layers are at rest and have no fluid moving through them, i. e., the transport vector $\vec{f}$ in Equation (1.35) is zero. If it is further assumed that the difference between the conductivities K_1 and K_2 is small, then the problem can be solved by the perturbation method and the approximate solution (2.35) is valid, viz.,

$$g = g_o - \frac{1}{2\pi a_o} \iiint_{\text{space}} \frac{\frac{\partial a_1}{\partial \zeta} \frac{\partial T_o}{\partial \zeta} (z-\zeta) d\xi d\eta d\zeta}{r^3} \qquad (2.35)$$

Write K with the help of $U(z)$, the unit step function, i. e.,

$$K = K_1 \left[1 + \left(\frac{K_2 - K_1}{K_1}\right) U(z-D)\right]$$

Differentiate with respect to z

$$\frac{\partial K}{\partial z} = K_1 \left(\frac{K_2 - K_1}{K_1}\right) \delta(z-D)$$

If the product ρc is assumed to be the same for both layers, we obtain by dividing both sides by ρc

$$\frac{\partial}{\partial z}\left(\frac{K}{\rho c}\right) = \frac{K_1}{\rho c}\left(\frac{K_2 - K_1}{K_1}\right) \delta(z-D)$$

or

$$\frac{\partial a}{\partial z} \approx a_o \left(\frac{K_2 - K_1}{K_1}\right) \delta(z-D)$$

Substitute into Equation (2.35) and integrate over the source half-space. One obtains for the surface thermal gradient at $z = 0$

$$g_{z=0} = g_o - \frac{1}{2\pi}\left(\frac{K_2 - K_1}{K_1}\right) g_o \int_{\xi}\int_{\eta} \frac{D(\xi,\eta)}{r^3}\, d\xi d\eta \qquad (2.36)$$

$$r^2 = (x-\xi)^2 + (y-\eta)^2 + D^2$$

Put $D(x,y) = d - h(x,y)$, and substitute into Equation (2.40)

$$g_{z=0} = g_o - \frac{1}{2\pi}\left(\frac{K_2 - K_1}{K_1}\right) g_0 \int_{\xi}\int_{\eta} \frac{(d-h(\xi,\eta))d\xi d\eta}{[(x-\xi)^2+(y-\eta)^2+(d-h(\xi,\eta))^2]^{3/2}} \qquad (2.37)$$

Carry out the series expansion along the same line as for (2.16) and neglect all terms containing $h(x,y)$ raised to the third power or

greater. The final expression is

$$g_{z=0} = g_o - \frac{1}{2\pi}\left(\frac{K_2-K_1}{K_1}\right) g_o$$

$$\times \int_{\xi}\int_{\eta} \left\{ \frac{d}{R^3} + \frac{(3d^2-R^2)}{R^5} h(\xi, \eta) + \frac{(15d^3-9dR^2)}{2R^7} h^2(\xi, \eta) \right\} d\xi d\eta \tag{2.37}$$

where

$$R^2 = (x-\xi)^2 + (y-\eta)^2 + d^2$$

which is a non-linear integral equation in $h(x, y)$. It is the fundamental integral equation for $h(x, y)$ in the case of a given surface temperature gradient.

APPLICATION TO A GRAVITY PROBLEM

Introduction

The two-layer homogeneous case is encountered in the earth, in which the curst overlies the mantle, the boundary between them being called the Mohorovicic discontinuity. According to the theories of isostasy (Airy, 1855; Pratt, 1857; Vening Meinesz, 1931), a variation in the thickness of the crust is to be expected in areas of varying topography, the thickness being greater under mountains and smaller under areas of low relief and valleys. Several studies have been undertaken with a view to testing the validity of these theories. (See, for example, Putnam and Gilbert, 1895; Hayford, 1906; Reid, 1911; Bowie, 1921, 1922; Washington, 1922; Byerly, 1937; Gutemberg, 1943; Woollard, 1962.) The various lines of evidence show that isostasy is true in general, although no one isostatic system is able to completely explain the actual conditions.

The problem tackled is the application of the results obtained above to the investigation of the variation of crustal thickness in Oregon by two different computation methods based on the fundamental Equation (2.26) derived for the two-layer case with constant densities. The crust and upper mantle are assumed to be homogeneous and two values are tentatively assumed for their density constrast, namely,

0.45 gm/cc and 0.60 gm/cc. The first value is adopted from Woollard (1969) and is the presently adopted value; while the second value is adopted from Coulomb and Jobert (1963) and is the previously adopted value. The undulating character of the crust-mantle interface and the density jump across it perturb the earth's gravity field. The perturbation is reflected in the form of variations in the gravity field. Assuming a slightly undulating interface then on the basis of equation 2.26, it is possible to investigate the variation of the crustal thickness and to obtain a model of the crust that is consistent with the known values of the Bouguer field and also with the crust-mantle density contrast and an assumed average depth of the crust-mantle interface.

The first method of analysis is the digitized algebraic method. It starts off by solving the quasi-linearized form of the fundamental equation (2.26) for the relief amplitude $h(x, y)$ by an iterative method. The solution is programmed for use in the Oregon State University CD 3300 computer. The values of $h(x, y)$ so obtained are converted into crustal thicknesses by addition to, or subtraction from, d, the assumed average depth of the crust-mantle interface. To check on the accuracy of the method of computation that has been designed, two two-layer models are constructed with the top layer varying in two dimensions in one case and in one dimension in the other. From the thicknesses of the top layers, gravity anomalies are

computed from which the thicknesses are recomputed. A comparison between the model thickness and the recomputed thickness provides a basis for making a judgment on the accuracy of the digitized algebraic method.

The second approach to the problem inverts a linearized form of Equation (2. 26) by the Fourier transform technique. The formal solution involves the second derivative of the regional field and its upward continuation. Computer programs are developed for performing these two operations and also for obtaining the final solution. A comparison is established between this method and the algebraic method, which is illustrated by means of critical cross-sections through the results obtained by the two methods.

Some results are available from previous investigations of the crustal thickness in Oregon by different methods. A comparison is established between these results and the results obtained from the present investigation.

Physiography of Oregon

The physiography of Oregon is characterized on the west by the Coast Range, to the south of which lie the Klamath Mountains. The general crestline of the former is about 455 meters in altitude while the latter show a maximum relief of about 1, 550 meters. The Willamette Valley is a depression with hills of moderate relief. It

separates the Coast Range from the Cascades, which extend the entire length of the state and whose eastern margin is marked by a crestline that averages a little more than 1,550 meters in altitude. The Cascade Range is studded with such peaks as Mount Hood, 3,420 meters; Mount Jefferson, 3,280 meters and the Three Sisters, of which the South Sister stands 3,240 meters high. East of the Cascades, the relief changes from 910 meters in the Deschutes-Umatilla Plateau to 1,550 meters in the Blue Mountains and dips to a moderate altitude in the High Lava Plains before rising to a little over 1,210 meters in the Basin and Range province and the Owyhee Plateau. The physiographic map, adopted from Baldwin (1964), is presented in Figure 4.

Data and Regional Field Separation

Source of Data

Some of the gravity data used in this investigation are the results of measurements made by the following organizations: The University of Wisconsin, U.S. Geological Survey, the University of Oregon, Southern Methodist University, Standard Oil of California and Humble Oil and Refining Company. Data from these sources were supplemented by measurements made by the Geophysics Group at Oregon State University at about 500 selected stations within the state.

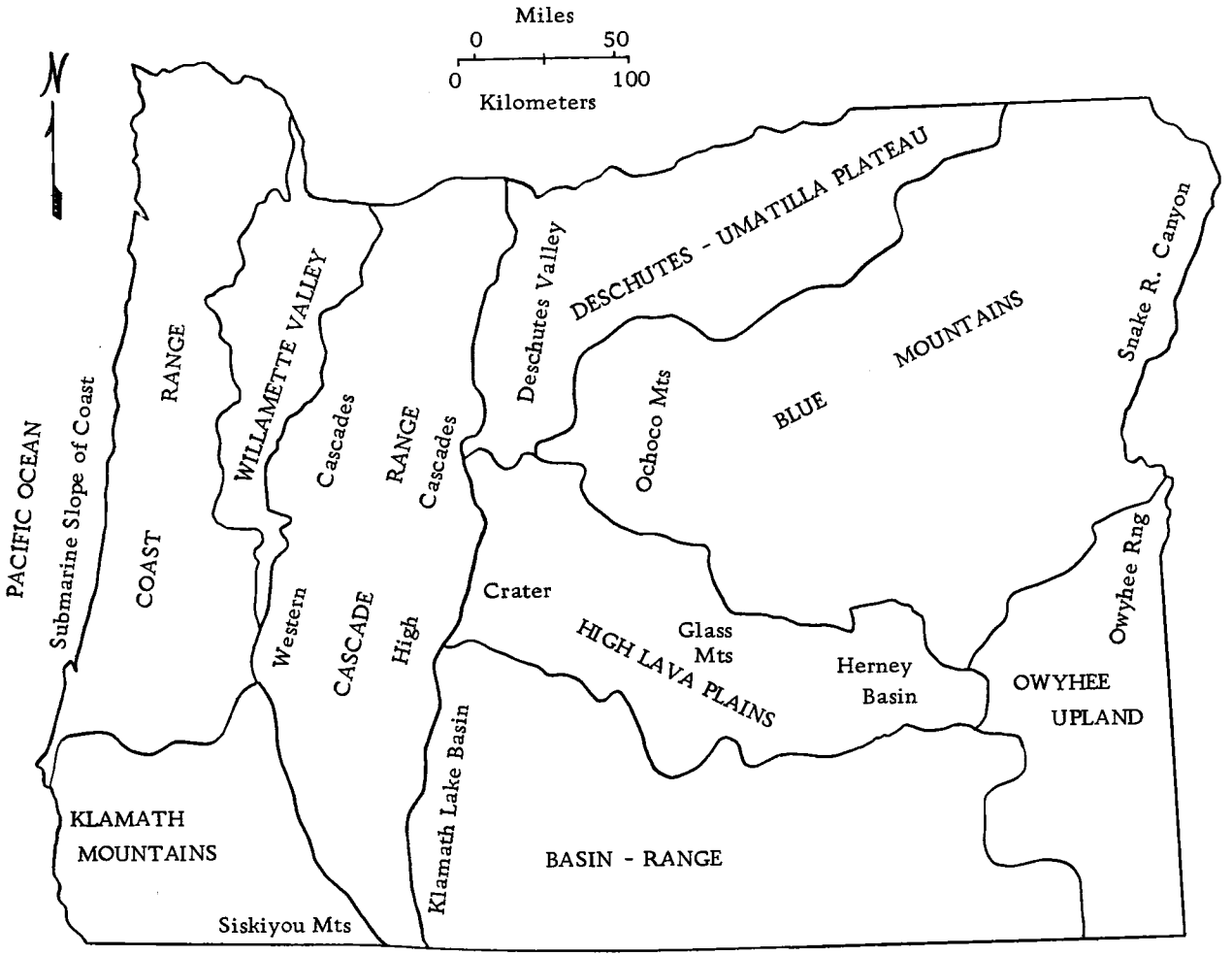

Figure 4. Physiographic divisions of Oregon. Reproduced from Baldwin.

Altogether 4,000 measurements were selected and adjusted, where necessary, to the gravity base stations in the state.

Complete Bouguer gravity anomalies are available, having been calculated using a crustal density of 2.67 gm/cc. Data from 460 stations have been terrain-corrected using Hammer's terrain correction chart for zones D through M (Hammer, 1939). Terrain corrections for many of the other stations have been achieved by interpolation. In southwestern Oregon, the stations have been individually terrain corrected by Blank (1965).

A Bouguer map can be regarded as consisting of two components. There are the larger features, characterized by smooth trends that extend over considerable areas. These may be considered as caused by deep-seated crustal features and are known as the regional field. Superimposed on these are the smaller disturbances of a more complicated configuration, caused by crustal structures that are close to the surface. These are the residuals. Within the context of the present investigation, the regional field is the more important and has to be separated from the complete anomaly field.

Regional Field Separation

There exist three well known methods for separating the regional field from the total anomaly field. These have been described by Peters (1949), Elkins (1951), Henderson and Zietz (1949), and

Simpson (1954). For the purpose of this investigation, a 10^{th}-degree polynomial map constructed by Thiruvathukal (1968) according to Simpson's least-square polynomial method was used. The resulting map is shown in Figure 5.

Calculations were carried out on 200 anomaly field values selected from corresponding points on the complete anomaly map and the regional map. According to the result, the regional field values showed a root-mean-square deviation of 13.79 mgls from the complete anomaly field. A comparison of the root-mean-square deviation with the regional field values showed that on the whole the regional field makes up a substantial part of the complete anomaly field.

Given the underdetermined nature of the problem of calculating the source parameters from known field values, the least-square polynomial method and, for that matter, any other method of separating a gravity field into regional and residual components is ambiguous. It has been argued, however, that the method is based on the assumption that the regional field is smooth enough to be represented by a low-degree polynomial surface while the residual is not. This argument has been assumed to be true to some extent in gravity surveys; and so the application of the least-square method can be relied upon to give useful results.

In the absence of lateral variations of density within the crust and upper mantle, the 10^{th}-degree polynomial surface will be assumed

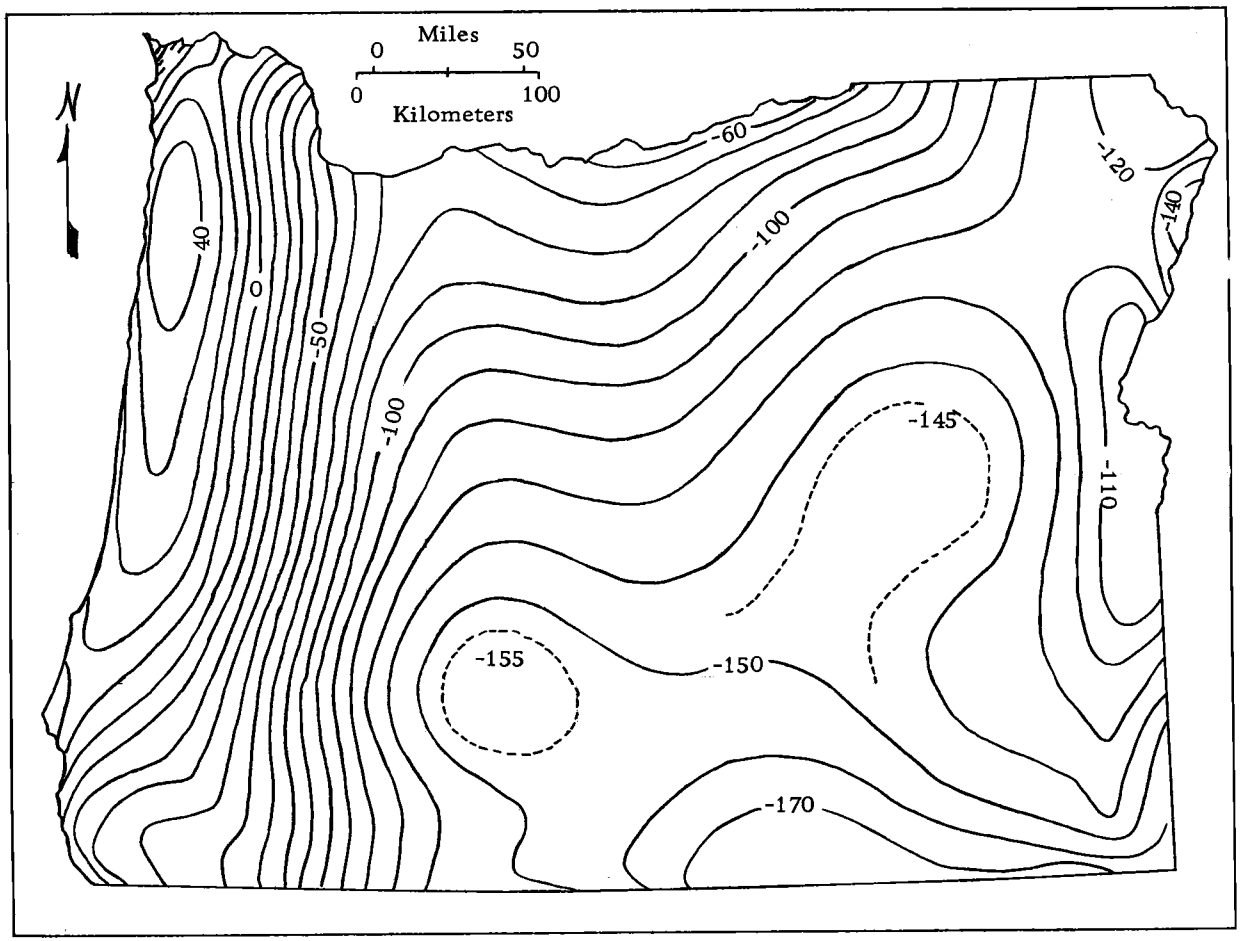

Figure 5. 10th degree least-square polynomial for the Bouguer gravity anomalies of Oregon. Contour interval 10 milligals. Reproduced from Thiruvathukal.

to reflect anomalies due to the density jump at the Mohorovicic discontinuity.

The Digitized Algebraic Method

The Working Equation

In Equation (2.26), since $|h| \ll d$, the second integral on the right-hand side can be ignored so that we have

$$\Delta g = \gamma \Delta \rho \int_{\xi} \int_{\eta} \left\{ \frac{d}{R^3} h(\xi, \eta) + \frac{(3d^2 - R^2)}{2R^5} h^2(\xi, \eta) \right\} d\xi d\eta \qquad (3.1)$$

which is the working equation for the algebraic method. Since $|h| \ll d$, the first term on the right-hand side is much larger than the second and Equation (3.1) may be called a quasi-linear integral equation in $h(x, y)$. It involves an error term which may be denoted by ϵ and which is given by the integral (see Equation (2.26))

$$\epsilon = \gamma \Delta \rho \int_{\xi} \int_{\eta} \frac{E'}{R} \, d\xi d\eta$$

where

$$E' = E - \frac{6dh^3 - 3h^4}{8R^4} \qquad \text{(see Equation (2.23))}$$

$$\approx E - 6\left(\frac{dh^3}{8R^4}\right)$$

E being the remainder that results from terminating the binomial expansion of the quantity $(1-\frac{2dh-h^2}{R^2})^{-1/2}$ at the third term. Arfken (1966) has shown that the binomial expansion of the function $f(x) = (1+x)^m$, where m is a negative integer or fraction, leaves a remainder R_n bounded by

$$|R_n| \leq |m(m-1)\ldots(m-n+1)\frac{x^n}{n!}|$$

if the expansion is terminated at the $(n-1)$th term. By comparison with the problem on hand, $m = -\frac{1}{2}$ and $x = \frac{2dh-h^2}{R^2}$ and so

$$|E| \leq |\frac{1\times3\times5\times7}{8\times4!}(\frac{dh-h^2}{R^2})^4|$$

$$= \frac{1\times3\times5\times7}{8\times4!}(\frac{dh}{R^2})(1-\frac{h}{d})^4$$

$$\approx \frac{1\times3\times5\times7}{8\times4!}(\frac{dh}{R^2}) \qquad \text{since} \quad 1 \gg h/d$$

We then have

$$|E'| \leq |\frac{1\times3\times5\times7}{8\times4!}(\frac{dh}{R^2}) - 6(\frac{dh^3}{8R^4})|$$

Consider an anomalous source point that is located directly under a field point. For this source point, $R = d$ and consequently the error at the field point is at most

$$\left| \frac{1 \times 3 \times 5 \times 7}{8 \times 4!} \gamma \Delta \rho \frac{h}{d^2} d\xi d\eta - \gamma \Delta \rho \frac{b}{d} \left(\frac{h}{2d}\right)^3 3\xi d\eta \right|$$

A calculation with the values of $\Delta\rho = 0.60$ gm/cc, $d = 25$ km and $\frac{h}{d} = \frac{1}{10}$ gives an error of not more than 3.50 mgals from the source point located directly under a field point. For the other source points, the error is very much smaller still, since R is always much larger than d and h, so that the total error at a field point should at most be comparable with the uncertainty involved in the regional field values used in this interpretation.

Transition into a Set of Algebraic Equations

In order to solve the working equation by an algebraic method, it first has to be transformed into a system of algebraic equations. To this purpose rewrite it in the form

$$\Delta g = c_1 \int_{\xi}\int_{\eta} K_1(x, y; \xi, \eta) h(\xi, \eta) d\xi d\eta$$

$$+ c_2 \int_{\xi}\int_{\eta} K_2(x, y; \xi, \eta) h^2(\xi, \eta) d\xi d\eta \qquad (3.2)$$

where

$$c_1 = \gamma \Delta \rho d$$

$$c_2 = \frac{\gamma \Delta \rho}{2}$$

$$K_1 = \frac{1}{R^3}$$

$$K_2 = \frac{3d^2 - R^2}{2R^5}$$

Since in practice we are dealing with a finite area, the integrals in Equation (3.2) may be replaced with a summation (Kantorovich and Krylov, 1958). Suppose that the integrals are carried out over the same intervals, say, (a, b). We shall then have

$$\Delta g = c_1 \int_a^b\int K_1(x, y; \xi, \eta)h(\xi, \eta)d\xi d\eta + c_2 \int_a^b\int K_2(x, y; \xi, \eta)h^2(\xi, \eta)d\xi d\eta \qquad (3.2a)$$

Divide the interval (a, b) into n equal sub-intervals of length $\frac{b-a}{n} = \Delta x = \Delta y = \Delta \xi = \Delta \eta$.

Put

$$K_1(a+p\Delta x, a+q\Delta y; a+r\Delta \xi, a+s\Delta \eta) = K_{1pqrs}$$

$$K_2(a+p\Delta x, a+q\Delta y; a+r\Delta \xi, a+s\Delta \eta) = K_{2pqrs}$$

$$h(a+r\Delta \xi, a+s\Delta \eta) = h_{rs}$$

$$h^2(a+r\Delta \xi, a+s\Delta \eta) = h^2_{rs}$$

$$\Delta g(a+p\Delta x, a+s\Delta y) = \Delta g_{pq}$$

where

$$p, q = 1, 2, \ldots, n$$

$$r, s = 1, 2, \ldots, n$$

Equation (3.2a) may now be replaced by

$$c_1 \sum_{r=1}^{n} \sum_{s=1}^{n} K_{1pqrs} h_{rs} \Delta\xi\Delta\eta + c_2 \sum_{r=1}^{n} \sum_{s=1}^{n} K_{2pqrs} h_{rs}^2 \Delta\xi\Delta\eta = \Delta g_{pq} \tag{3.3}$$

which is a set of n^2 quadratic equations in n^2 unknown h_{rs}. As $\Delta\xi$ and $\Delta\eta$ both tend to zero, the summation goes over into Equation (3.2a).

Solution by the Iterative Method

Since the main contribution to the Bouguer field is so much larger than the second-order effect, because $|h| \ll d$, and since the iterative method of solution that is envisaged is applicable only to linear systems, an approximate initial solution will be obtained by ignoring the quadratic term in Equation (3.3). We then have to solve the following equation for the approximate initial solution

$$c_1 \sum_{r=1}^{n} \sum_{s=1}^{n} K_{1pqrs} h_{rs} \Delta\xi\Delta\eta = \Delta g_{pq} \tag{3.4}$$

This is a set of linear algebraic equations in h_{rs} and will be solved

by the iterative method. This method gives the solution in the form of a sequence of certain vectors all constructed by a uniform process. In order to more easily discuss the process of constructing these vectors and to investigate the conditions under which the iterative method can be applied, rewrite Equation (3.4) in matrix form

$$K\vec{H} = \vec{G} \tag{3.5}$$

in which for simplicity the constant c_1 and the factor $\Delta\xi\Delta\eta$ in Equation (3.4) have been absorbed into the matrix of coefficients K. $\vec{H}$ is the vector of unknown and $\vec{G}$ the vector representing the observed values of the Bouguer field. Equation (3.5) may be transformed into the following form

$$(K-I)\vec{H} + \vec{H} = \vec{G} \tag{3.6}$$

where I is the unit matrix. By transposing terms, we have

$$\vec{H} = (I-K)\vec{H} + \vec{G} \tag{3.7}$$

Put $I - K = F$ and substitute

$$\vec{H} = F\vec{H} + \vec{G} \tag{3.8}$$

$\vec{H}$ is obtained by solving Equation (3.8). The uniform process referred to above goes as follows. Suppose that the solution is estimated to be $\vec{H} = \vec{H}^{(o)}$. Construct the following sequence of vectors

$$\vec{H}^{(1)} = F\vec{H}^{(o)} + \vec{G}$$

$$\vec{H}^{(2)} = F\vec{H}^{(1)} + \vec{G}$$

. . . . . .

$$\vec{H}^{(n)} + F\vec{H}^{(n-1)} + \vec{G}$$

It may be seen that the process computes the nth approximation to the h_{ij} component of $\vec{H}$ by means of the formula

$$h_{ij}^{(n)} = \sum_{k=1}^{n} \sum_{\ell=1}^{n} f_{ijk\ell} h_{k\ell}^{(n-1)} + g_{ij} \tag{3.9}$$

which does not take into account the already computed nth approximation to the components $h_{11}, h_{12}, \ldots, h_{i-1,j-1}$.

Now if the sequence $\vec{H}^{(o)}, \vec{H}^{(1)}, \ldots, \vec{H}^{(n)}$ has a limit $\vec{H}$, then this limit will be the solution of the system (3.8); for in the limit as n tends to infinity, the equation $\vec{H}^{(n)} = F\vec{H}^{(n-1)} + \vec{G}$ tends to $\vec{H} = F\vec{H} + \vec{G}$. The solution may also be rewritten in the form

$$\vec{H}^{(n)} = F^{n}\vec{H}^{(o)} + (I+F+F^{2}+\ldots+F^{n-1})\vec{G} \tag{3.10}$$

This form may be verified by the method of induction. It is evident from this last form of the solution that the iterative process converges if the matrix series $I + F + \ldots + F^{n-1}$ converges in a proper sense. For the convergence to take place with an initial vector $\vec{H}^{(o)}$ and

with the value of the vector $\vec{G}$, it is necessary and sufficient that the eigenvalues of the matrix F all have absolute values less than one (Fadddeeva, 1959). In order to verify this condition, it would be necessary to calculate the eigenvalues of F, which will be a tedious process. It is more convenient to judge the convergence in terms of the elements of F. Scarborough (1966) gives a sufficient, though not necessary, condition for the convergence as that the absolute value of the largest element in any row or column of F be greater than the sum of the absolute values of all the other elements in the same row or column. Because convergence is necessary for the existence of a solution to the system (3.8), it is important that this latter condition be verified once a computation scheme has been set up. Now suppose that an estimate of the solution to the system (3.8) were $\vec{H}^{(o)} = 0$. Then the first iteration would give $\vec{H}^{(1)} = \vec{G}$ and the second iteration $\vec{H}^{(2)} = F\vec{G} + \vec{G}$. If, on the other hand, the initial estimate were $\vec{H}^{(o)} = \vec{G}$, then the first iteration would give $\vec{H}^{(1)} = F\vec{G} + \vec{G}$, which would be the same as the result of the second iteration for the first estimate and the subsequent iterations would be one step ahead. The second estimate, therefore, makes for a reduction of the number of iterations necessary for convergence, which is an advantage. Another fact to note is that since the system (3.8) is linear in character, one would normally expect $\vec{H}$ to have the same variation as $\vec{G}$. It follows from this fact that a natural choice for the estimate is

$\vec{H}^{(o)} = \vec{G}$.

Equation (3.8) has a unique solution which may be written in the form $\vec{H} = K^{-1}\vec{G}$, provided that K is a non-singular matrix. In relation to the problem in hand, $\vec{G}$ consists of the observed regional gravity anomalies, which are subject to error. It is necessary to investigate the effect of this error on the solution. Let us call the error in $\vec{G}$ and the corresponding error in $\vec{H}$ $\vec{\delta G}$ and $\vec{\delta H}$ respectively. It can be shown (Forsythe and Moller, 1967) that

$$\frac{\|\vec{\delta H}\|}{\|\vec{H}\|} \leq \|K\| \; \|K^{-1}\| \frac{\|\vec{\delta G}\|}{\|\vec{G}\|} \qquad (2.11)$$

where the norms of the various quantities are involved. Define the condition number of K as

$$\text{cond}(K) = \|K\| \; \|K^{-1}\|$$

Then

$$\frac{\|\vec{\delta H}\|}{\|\vec{H}\|} \leq \text{cond}(K) \frac{\|\vec{\delta G}\|}{\|\vec{G}\|} \qquad (3.12)$$

$\frac{\|\vec{\delta G}\|}{\|\vec{G}\|}$ may be defined as a measure of the relative error in $\vec{G}$. In the same way, $\frac{\|\vec{\delta H}\|}{\|\vec{H}\|}$ can be interpreted as the relative error in $\vec{H}$. It follows that cond(K) binds the relative error in $\vec{H}$ to that of $\vec{G}$. If cond(K) = 1, then $\|\vec{\delta H}\|$ bears the same ratio to $\|\vec{H}\|$ that $\|\vec{\delta G}\|$ bears to $\|\vec{G}\|$; in other words, the relative error

in $\vec{H}$ is precisely the same as that of $\vec{G}$. If cond(K) is relatively small, the error in $\vec{G}$ does not have an appreciable effect on $\vec{H}$. K is then said to be well-conditioned with respect to the error in $\vec{G}$. If cond(K) is relatively large, the error in $\vec{G}$ does lead to an appreciably large error in $\vec{H}$ and K is said to be badly- or ill-conditioned with respect to the error in $\vec{G}$. In fact with large cond(K), the effect of the error in $\vec{G}$ is reflected in the form of high amplitude and high frequency noise in the solution. The noise can, however, be removed by first smoothing the input regional field. The point is elaborated by Bullard and Cooper (1948); Kreisel (1949); Philips (1962) and Baker (1964).

While discussing the sources of error in the solution of Equation (3.8), a second point that is worth looking into is the extent to which changes in the elements of K^{-1} affect the solution. Since K^{-1} is the inverse of K, the study of this effect reduces to a study of the sensitivity of the elements of K^{-1} to small changes in the elements of K. K^{-1} exists if the determinant of K is not zero. The elements of K are subject to rounding errors. In situations in which the determinant of K is not much different from zero, the rounding-off can change the elements in such a way as to yield a matrix with determinant equal to zero. This is equivalent to saying that small perturbations in the elements of a matrix may produce correspondingly large changes in the elements of its inverse. Under this condition, the

matrix is said to be unstable or ill-conditioned with respect to small changes in its elements. It turns out, however, that the determinant of a matrix of coefficients, such as K is, is not a reliable indicator of the stability of a system. A reliable indicator is the condition number of the matrix (Forsythe and Moller, 1967). We may then write

$$\frac{\|\overrightarrow{\delta H}\|}{\|\vec{H}\|} \leq \text{cond}(K) \frac{\|\delta K\|}{\|K\|} \tag{3.13}$$

Here also, $\text{cond}(K)$ binds the relative error in K to that of $\vec{H}$. It is clear, therefore, that $\text{cond}(K)$ is a reliable indicator of the stability of $\vec{H}$ with respect to changes in the elements of K and $\vec{G}$. When it is greater than about 100, this indicates a relatively unstable system (Emilia, 1968). A measure of the condition number is given by

$$\begin{aligned} \text{cond}(K) &= \|K\| \ \|K^{-1}\| \\ &= \frac{\mu_1}{\mu_n} \geq 1 \end{aligned} \tag{3.14}$$

where μ_1 and μ_2 are the largest and smallest eigenvalues of K respectively (Faddeeva and Faddeeva, 1963). Since K and hence $\text{cond}(K)$ are determined by the relative positions of the field points and the centers of the anomalous blocks, it is imperative that these positions be chosen in such a way as to make for a stable system.

The choice will be made so that the centers of the anomalous blocks are placed directly below the field points.

The method of solution discussed so far is known as the simple iterative method. As has been pointed out already, it gives the nth approximation to the h_{ij} component of $\vec{H}$ by means of the formula (see Equation (3.9))

$$h_{ij}^{(n)} = \sum_{k=1}^{n} \sum_{\ell=1}^{n} f_{ijk\ell} h_{k\ell}^{(n-1)} + g_{ij}$$

which does not take into account the already computed nth approximation to the components $h_{11}, h_{12}, \ldots, h_{i-1,j-1}$. Seydel's iterative method on the other hand takes these into account and gives the nth approximation to the component h_{ij} according to the formula (Faddeeva, 1959)

$$h_{ij}^{(n)} = \sum_{r=1}^{i-1} \sum_{s=1}^{j-1} f_{ijrs} h_{rs}^{(n)} + \sum_{r=i}^{n} \sum_{s=j}^{n} f_{ijrs} h_{rs}^{(n-1)} + g_{ij} \qquad (3.15)$$

The above formula has the advantage that it yields a more complete solution than that expressed in Equation (3.9). Consequently Seydel's method was adopted as the method of solution.

For reasons already stated, in seeking a solution to the working equation by the application of the iterative method, the non-linear

portion of the working equation has been ignored; it has also been pointed out that any solution so obtained is only an approximate one. However, such a solution can be improved upon by taking into account the quadratic term in Equation (3. 3) and using the following iterative improvement (Hertling, 1969). Call $\vec{h}_o$ any solution yielded by the Seydel's iterative method. Since it is only an approximation, it may be considered to be in error in relation to the complete solution of the working equation by $\vec{\Delta h}_o$, say, so that the complete solution is $\vec{h}_o + \vec{\Delta h}_o$. Substitute $\vec{h}_o + \vec{\Delta h}_o$ into a modified form of Equation (3. 3) in which the matrices K_1 and K_2 and their associated constant factors are replaced by the linear operators L_1 and L_2 respectively; at the same time make the approximation $(\vec{h}_o+\vec{\Delta h}_o)^2 \approx \vec{h}_o^2 + 2\vec{h}_o\vec{\Delta h}_o$ since $\vec{\Delta h}_o \ll \vec{h}_o$. The resulting equation is

$$L_1(\vec{h}_o+\vec{\Delta h}_o) + L_2((\vec{h}_o+\vec{\Delta h}_o)) = \vec{\Delta g}$$

$$L_1(\vec{h}_o) + L_2(\vec{h}_o) + L_1(\vec{\Delta h}_o) + L_2(\vec{\Delta h}_o) = \vec{\Delta g} \qquad (3.16)$$

Put

$$L_1(\vec{\Delta h}_o) + L_2(\vec{\Delta h}_o) = L_3(\vec{\Delta h}_o).$$

We then have

$$L_3(\vec{\Delta h}_o) = \vec{\Delta g} - L_1(\vec{h}_o) - L_2(\vec{h}_o) \qquad (3.17)$$

Equation (3. 17) is linear in $\vec{\Delta h}_o$. By solving for $\vec{\Delta h}_o$, we have the

first complete solution of the working equation, namely, $\vec{h}_1 = \vec{h}_o + \vec{\Delta h}_o$. This solution may itself be considered to be in error by $\vec{\Delta h}_1$, so that a more accurate solution is $\vec{h}_1 + \vec{\Delta h}_1$. This is in turn substituted into Equation (3.17) and the value of $\vec{\Delta h}_1$ is calculated. The iterative improvement is continued until it converges. In actual fact, the process may or may not converge. As Tanner (1967) has pointed out, instability arises when a solution is being sought for an assumed value of d that is too large. In view of this fact, non-convergence of the iterative improvement can be interpreted as a warning that the assumed value of d is on the high side.

Computation Scheme

The computer program that was developed to solve the working equation was designed to take all the foregoing considerations into account. First, the digitization of the regional anomaly field required that the digitizing intervals be specified both in the east-west or x direction and in the north-south or y direction.

Experience has shown that when the ratio of the digitzing interval to the depth of the source plane exceeds half, excessive oscillations begin to develop and the solution becomes unstable (Dix, 1964). This means in effect that for a stable solution the discrete representation of the input regional field should preferably be carried out in such a way that the interval between field points is at least twice d

the assumed depth of the source plane. The results of crustal studies undertaken in Oregon show a crustal structure with greater variation in the east-west direction than in the north-south, especially in the western half of the state. This makes the digitizing interval more critical in the former direction. Accordingly the interval was set at 80 km in this direction in order to allow the use of values of d of up to 40 km while at the same time satisfying the requirement that the digitizing interval should be at least twice as large as d. In the north-south direction, the interval was fixed at half-degree latitude, which was equivalent to a horizontal distance of about 55.50 km. The choice thus made allowed for a grid of 56 points aligned along eight lines running from east to west at a separation of half-degree latitude. Considerations of stability and the need not to force a solution on the system make it imperative that the position of the center of each source block be made to correspond with the position of a field point in both the x and y directions. First, the positions of the centers of the source blocks were fixed in the source plane so as to coincide with the grid points. Then the field points were selected in such a way as to coincide with the centers of the source blocks. Consequently there was the same number of source blocks as of field points.

The computer program written was identified as GRAVCALC and is reproduced in full in Appendix A. There were two parts to it. The first part was based on Seydel's method of solving a system of

linear algebraic equations. The solution obtained from this part of the program was called the initial solution and was fed as input to the second part, which performed the iterative improvement that takes the quadratic term in Equation (3.3) into account. Since both parts involved iterations, it was necessary to set a criterion for bringing the iterations to an end. Many possible mathematical criteria can be used. For instance, one can set such a criterion that the process is stopped when

$$\max \| G_{ij} - \sum_{k} \sum_{\ell} K_{ijk\ell} H_{k\ell} \| < E \qquad (3.18)$$

where E represents the error from measurement and data reduction. According to this criterion, the iteration is stopped when the absolute value of the maximum component of the residual vector is less than the estimated error in the input values. The disadvantage with this criterion is that it involves a lot of tedious computation, which is unnecessary. A second possibility is to set a criterion which involves the required vector $\vec{H}$. In this case, one can make the process stop when the Euclidean norm of the vector $\vec{H}^{(k)} - \vec{H}^{(K-1)}$ is less than some specified constant times the Euclidean norm of $\vec{H}^{(k-1)}$, i.e.,

$$\| \vec{H}^{(k)} - \vec{H}^{(k-1)} \| < \text{constant} \times \| \vec{H}^{(k-1)} \| \qquad (3.19)$$

The constant factor is chosen in view of the particular problem under consideration. This second criterion was applied and the constant factor was chosen to be 10^{-3}. In view of the expected magnitudes of the components of $\vec{H}$, this figure was judged to be convenient.

Such was the flexibility built into the program that it was possible to stop the computer at any stage during the iterative improvement and check on the results obtained after each iteration. Also, the program was designed to produce two sets of results, one set at the end of Seydel's iterative process and the second at the end of the iterative improvement. It was, therefore, possible to compare the two sets of results and to determine to what extent the iterative improvement modified the results obtained by the Seydel's iterative method.

Once the program was compiled inside the computer, the following tests were carried out. First for three values of d, viz., 25 km, 30 km and 35 km, corresponding values of cond(K) (see Equation (3.14)) were calculated. They were all found to be approximately one, indicating stable systems for all three values of d. Next the condition was tested as to whether the convergence of the Seydel's iterative process was possible. This condition was satisfied for all three values of d. So convergence was expected. The computations were carried out only after these tests had been made.

Since Oregon is part of a wider area, it was important to take

into account the gravitational effect of the surrounding area and to correct for it. To this effect, a boundary region was constructed around the state whose width was defined as the horizontal distance beyond which the source block with the largest value of h produced a gravitational effect equal to the estimated observational error involved in the regional field values. The width was calculated as follows. The gravitational effect due to a single block is given by

$$\overrightarrow{\Delta g} = \gamma \Delta \rho d \frac{h}{R^3} \Delta\xi \Delta\eta + \frac{\gamma \Delta \rho}{2} \frac{(3d^2 - R^2)}{R^5} h^2 \Delta\xi \Delta\eta \qquad (3.20)$$

where R represents the distance from the center of the block to the field point. Since the second term on the right-hand of Equation (3.20) is a small second-order effect, it can be neglected in this context and hence

$$\overrightarrow{\Delta g} = \gamma \Delta \rho d \frac{h}{R^3} \Delta\xi \Delta\eta \qquad (3.21)$$

The value of $\overrightarrow{\Delta g}$ was fixed at 0.25 mgal and for h the largest value from the already computed results was used. This value was 11 km. For $d = 35$ km, the value of R was calculated and from it the width of the boundary region was calculated, since

$$R^2 = d^2 + L^2$$

L being the horizontal distance between source point and field point

and hence the required width of the region. L was found to be 187 km. The grid covering the state was then extended into the region and for each grid point in the region crustal thicknesses were calculated according to the following scheme. First estimates of h for each grid point in the boundary region were made on the basis of a single block attraction given by Equation (3.21). In this connection, Δg was taken as the value of the regional field at the grid point. Each estimate of h was then improved by an iterative process in which the influences of the surrounding blocks were calculated on the basis of the results of the above first estimate and removed and a new value of h was computed from the recalculated field value. The process ran as follows. First, the estimate of h at a field point was corrected for the influence of the eight blocks immediately surrounding the field point. Then, the improved value of h was further improved by correcting for the influence of the next set of blocks. These are 16 in number. The process was continued until the magnitude of the influences of the farther blocks fell below the estimated observational error of the regional field values. The field values were obtained from Bouguer anomaly data published by Woollard and Rose (1963). The data had not been filtered into a 10^{th}-degree polynomial surface. However, they had first been subjected to a visual smoothing process from which emerged a set of contours that were continuous with the 10^{th}-degree polynomial surface used in the main

computation. The crustal thickness profiles obtained for the Oregon area are shown in Figures 6a to 8a for $\Delta\rho = 0.45$ gm/cc and in Figures 6b to 8b for $\Delta\rho = 0.60$ gm/cc.

Results and Discussion

Seydel's iterative process for solving the working equation converged for all three values of d. The process was supposed to stop at the criterion (see Equation (3.19)) or go to 21 iterations and to stop. It turned out that for the three values of d convergence was reached before the 21 iterations were carried out. The iterative improvement converged for $d = 25$ km and for $d = 30$ km after four iterations; it did not converge for $d = 35$ km, even after 21 iterations, so that the results obtained from the Seydel iterations were used in constructing the crustal thickness variation shown in Figures 8a,b. From the results for $d = 25$ km and $d = 30$ dm, it was found that the maximum change in crustal thickness brought about by the iterative improvement was about one part in 18. Consequently, the results shown in Figures 8a,b could be considered as approximately representative of the crustal thickness variation for $d = 35$ km. As Tanner has pointed out, the failure of the iterative improvement to converge can be interpreted as an indication that a solution is being sought for too high an assumed value of d. As a consequence, no values of d higher than 35 km were used for the computation.

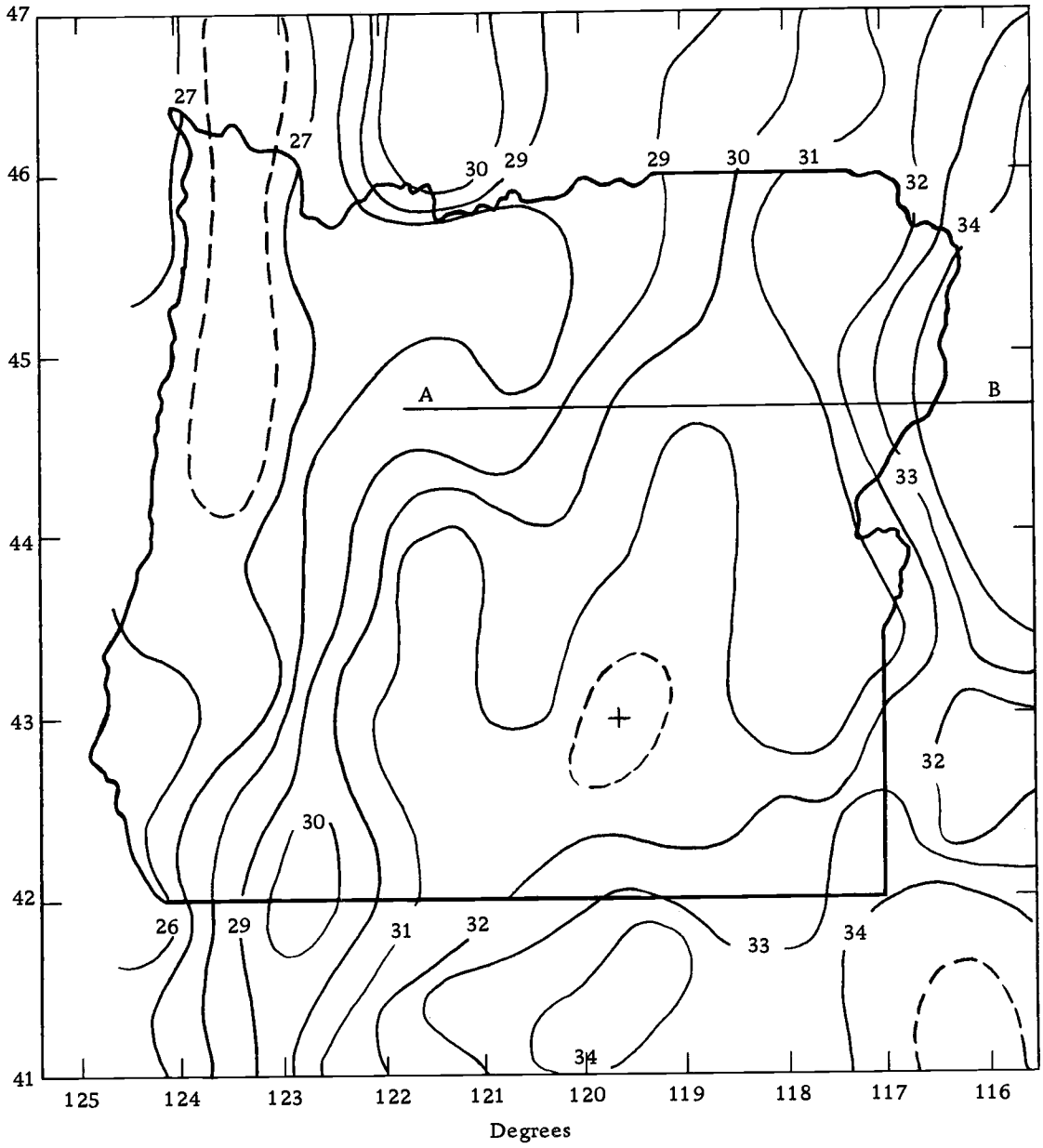

Figure 6a. Crustal thickness profiles for d = 25 km and $\Delta\rho$ = 0.45 gm/cc obtained by the digitized algebraic method. Contour interval: 1 km.

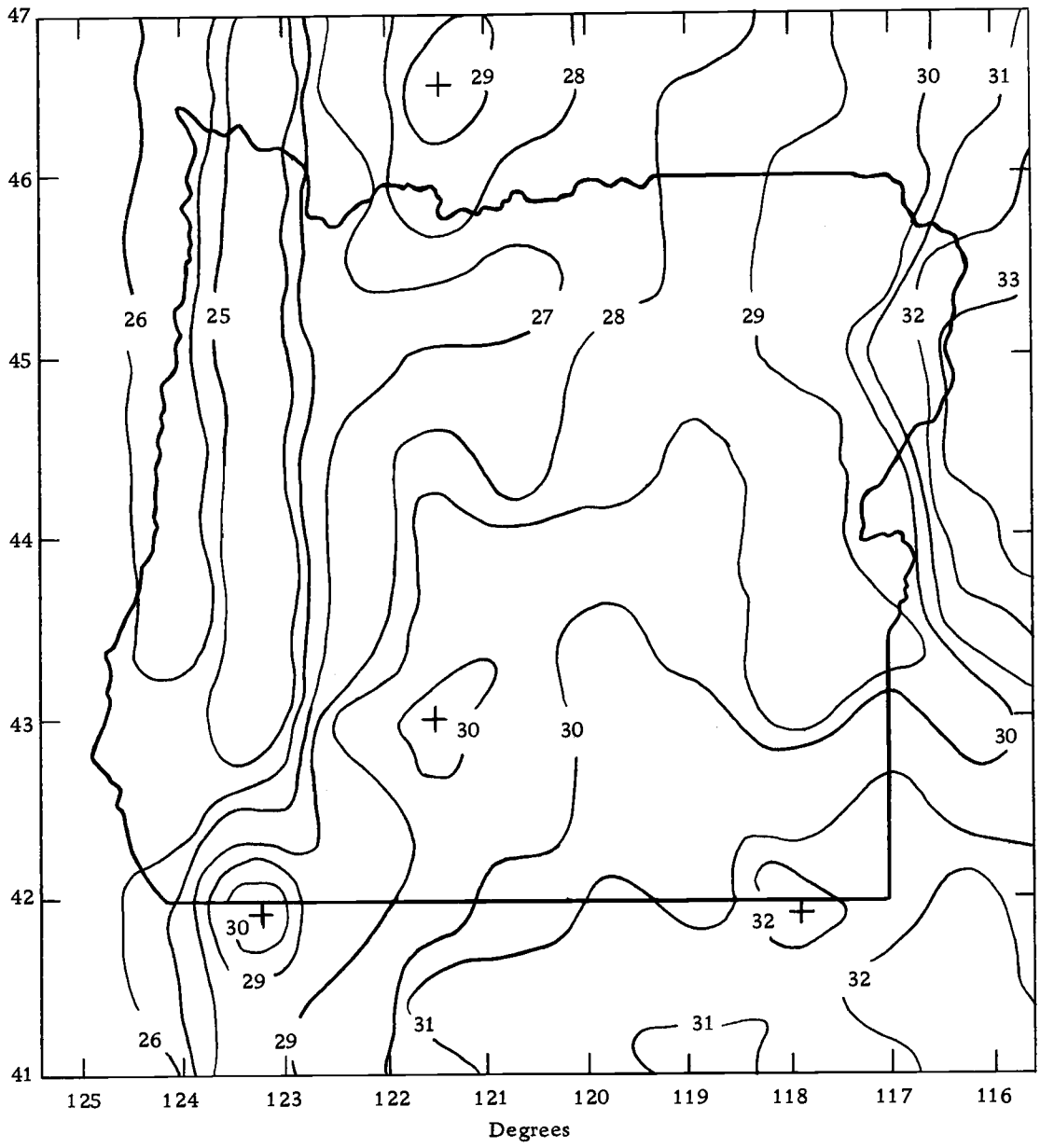

Figure 6b. Crustal thickness profiles for d = 25 km and $\Delta\rho$ = 0.60 gm/cc obtained by the digitized algebraic method. Contour interval: 1 km.

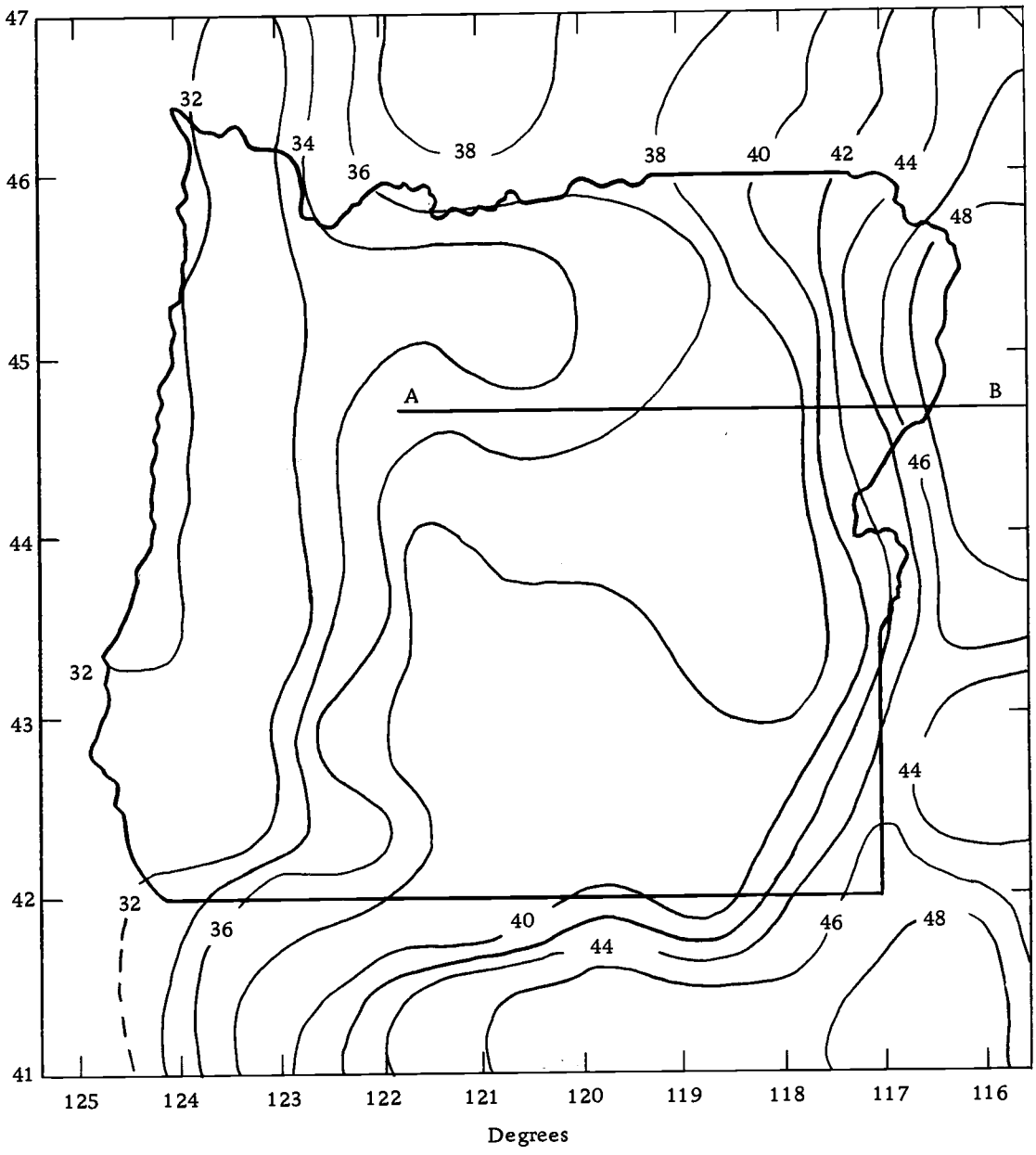

Figure 7a. Crustal thickness profiles for d = 30 km and $\Delta\rho$ = 0.45 gm/cc obtained by the digitized algebraic method. Contour interval: 2 km.

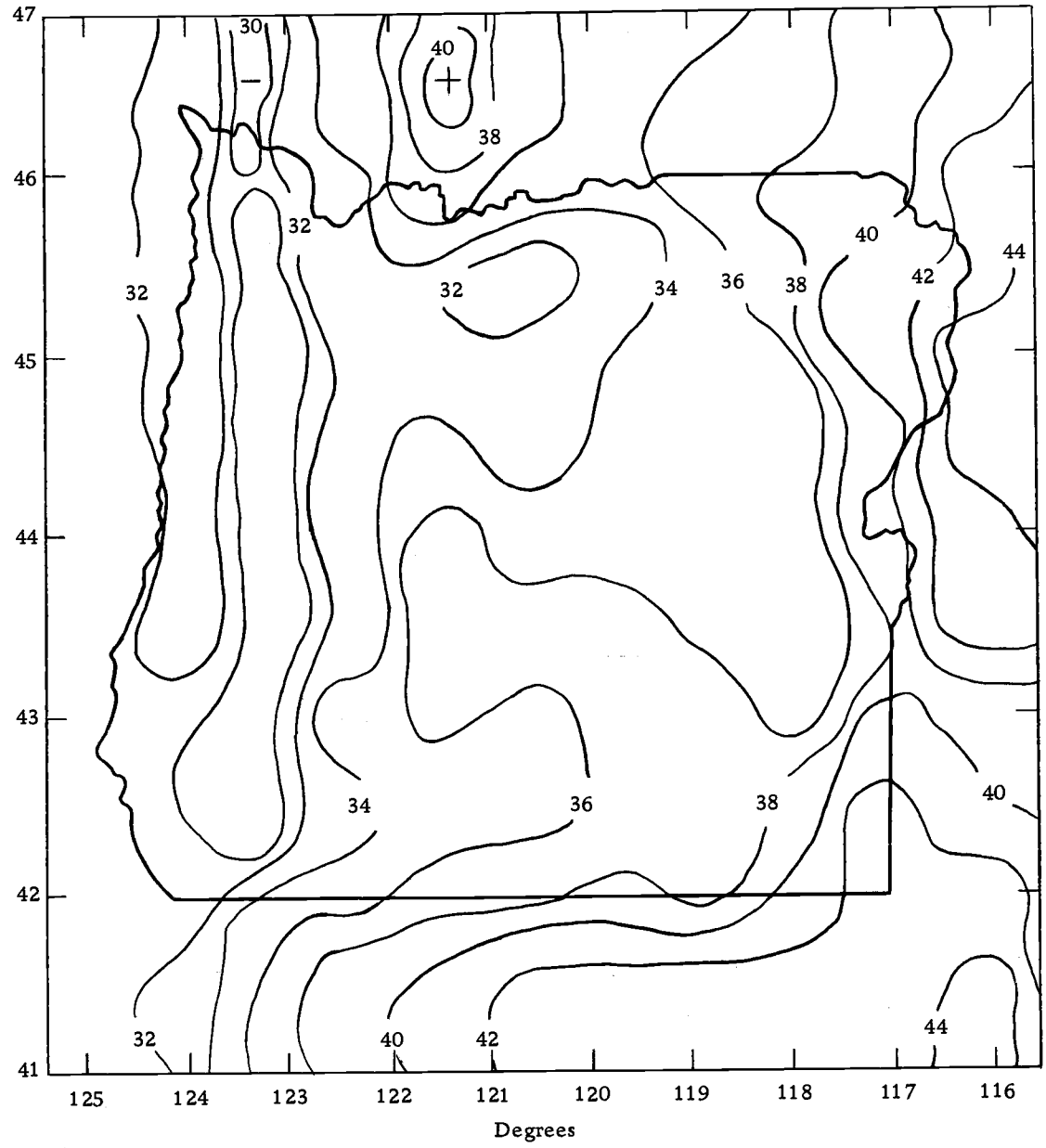

Figure 7b. Crustal thickness profiles for d = 30 km and $\Delta\rho$ = 0.60 gm/cc obtained by the digitized algebraic method. Contour interval: 2 km.

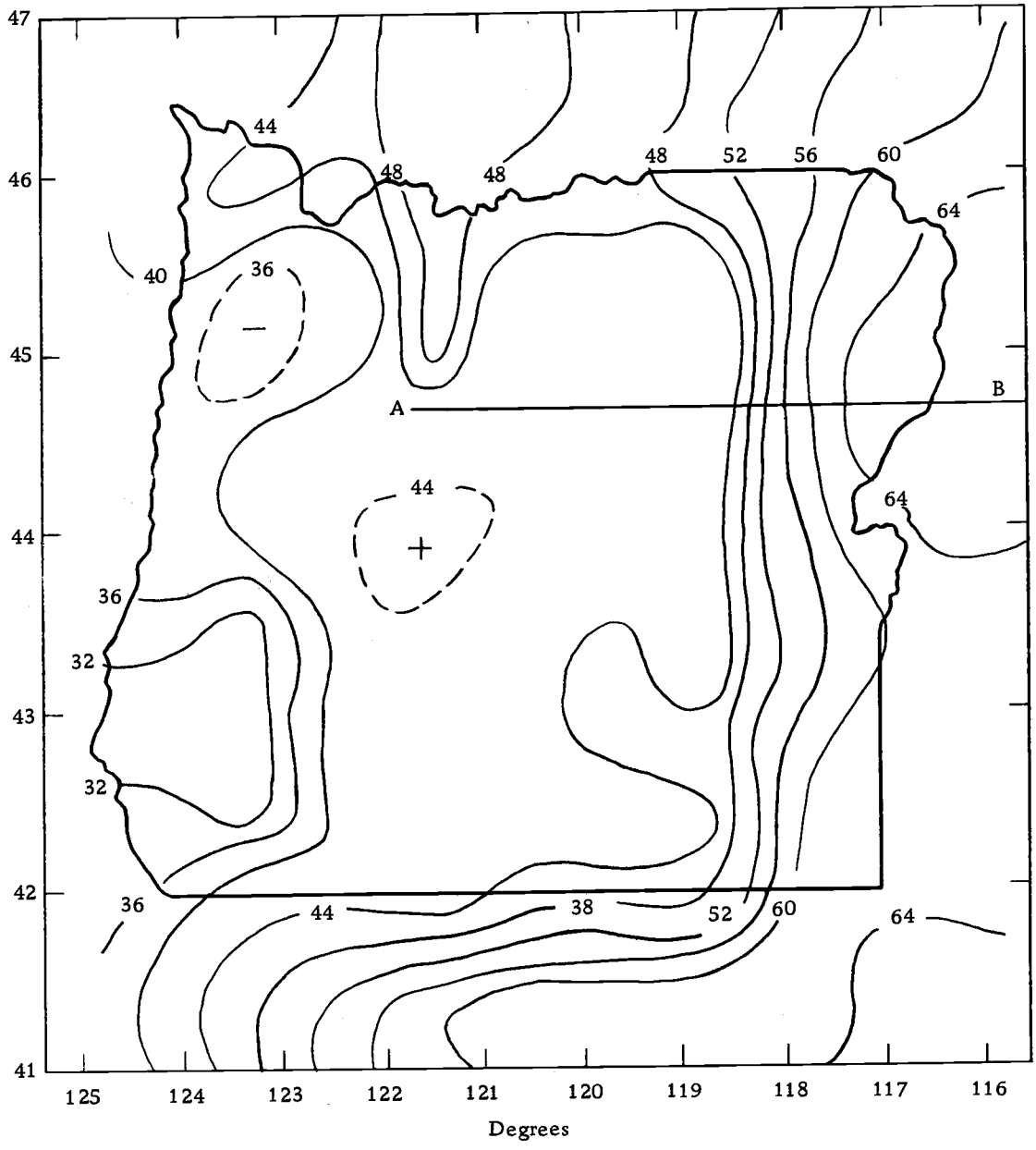

Figure 8a. Crustal thickness profiles for d = 35 km and $\Delta\rho$ = 0.45 gm/cc obtained by the digitized algebraic method. Contour intervals: 4 km.

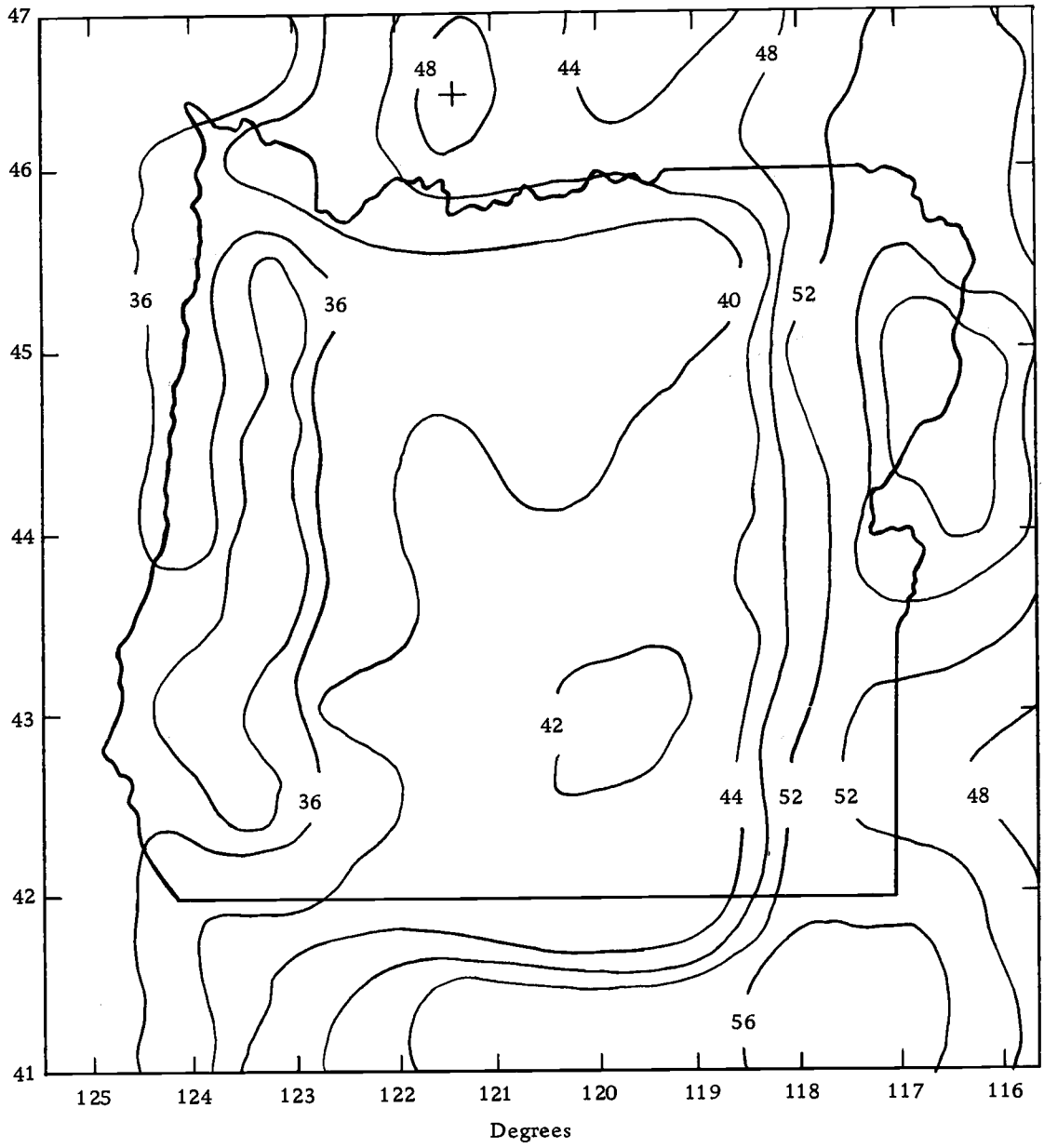

Figure 8b. Crustal thickness profiles for d = 35 km and $\Delta\rho$ = 0.60 gm/cc obtained by the digitized algebraic method. Contour interval: 4 km.

Values of d equal to 34 km, 33 km, 32 km and 31 km were tried in that order. For these, too, the iterative improvement failed to converge.

The physiographic map of Oregon shows a terrain that generally increases in relief gradually from west to east, if exception is made of the Willamette Valley. In accordance with the predictions of isostasy, one would normally expect a crustal thickness variation marked by a general gradual increase from west to east. This was borne out, as the results indicate. Since the Willamette Valley represents a structural depression between the Coast Range and the Cascades, one would expect a correspondingly thinner crust under the Valley than under most of the rest of the state. This was also borne out. In all six figures, the Valley stands out clearly as a contour low. The point needs stressing, however, that the thinner crust under the Valley obtained above may partially be a reflection of the assumption of constant crust-mantle density contrast made in computing the crustal thicknesses. It is entirely possible that if allowance is made for local changes in density within the crust and the mantle, the Valley may not be associated with a thinner crust than is the topography on either side of it.

As regards numerical values, for $d = 25$ km and $\Delta\rho = 0.45$ gm/cc (see Figure 7a), the thicknesses average about 26 km under the Coast Range, increasing to a little over 36 km under the Klamath Mountains,

which are due south of the Coast Range. The thickness ranges from about 27 km under the western margin of the Cascades to between 28 km and 30 km under the eastern margin. Thereafter, there is a gentle increase towards eastern Oregon, this increase becoming rather rapid near the Oregon-Idaho border. The thicknesses are correspondingly greater for $d = 30$ km and $d = 35$ km, but approximately the same trend is evident as for $d = 25$ km. The thickness profiles resulting from the use of $\Delta\rho = 0.60$ gm/cc in the computation also show the same trend as the above differing, as is to be expected, only in numerical values.

For Oregon and its surrounding areas, the following results on crustal thickness were obtained by investigators using different methods. On the basis of local travel-time curves, Dehlinger et al. (1965) obtained an average crustal thickness of 25 km to 30 km for the region west of the Cascades. Phase velocity dispersion studies carried out by Chiburis (1966) gave 38 km for the crustal thickness under the Coast Range. Bert et al. (1966) obtained about 16 km for the western edge of the northwestern Coast Range from seismic refraction studies. For eastern Oregon, Chiburis obtained an average depth to the Moho of 45 km, while Dehlinger et al. obtained an average of 35 km.

Studies of the crustal structure for an area extending from east of the Cascades into southern Idaho were undertaken by Pakiser and

Hill (1963), Hill and Pakiser (1966) and Hill (1970). Their results varied from 28-36 km under the Basin and Range province to 41-48 km in the Western Snake River Plain in southern Idaho. Near Baker in northeastern Oregon, Couch and Whitsett (1969) obtained a crustal thickness of 42 km using travel-time curves from the North Powder earthquake.

The most extensive seismic refraction and dispersion studies for the area under investigation were carried out by Dehlinger et al. (1968). Their results are presented in the cross-section in Figure 9. From this cross-section, one obtains for the Oregon region an average depth to the Moho of about 36 km. Since the results for seismic analyses are more absolute than the ones obtained from the present gravity method, this figure might be considered to be an appropriate value of d to be used in the two computational methods that have been the subject of application in the present investigation. However, the use of $d = 36$ km in the computations would have led to much larger crustal thicknesses in Eastern Oregon than the seismic analyses have yielded. This value of d will, therefore, have to be rejected for the present purpose. The discrepancy is possibly a reflection of the fact that the above computational model assumed a crust and a mantle of constant densities, which is a simplified model. For example, the regional field data used in the computations were not corrected for the anomalies resulting from the discontinuities in

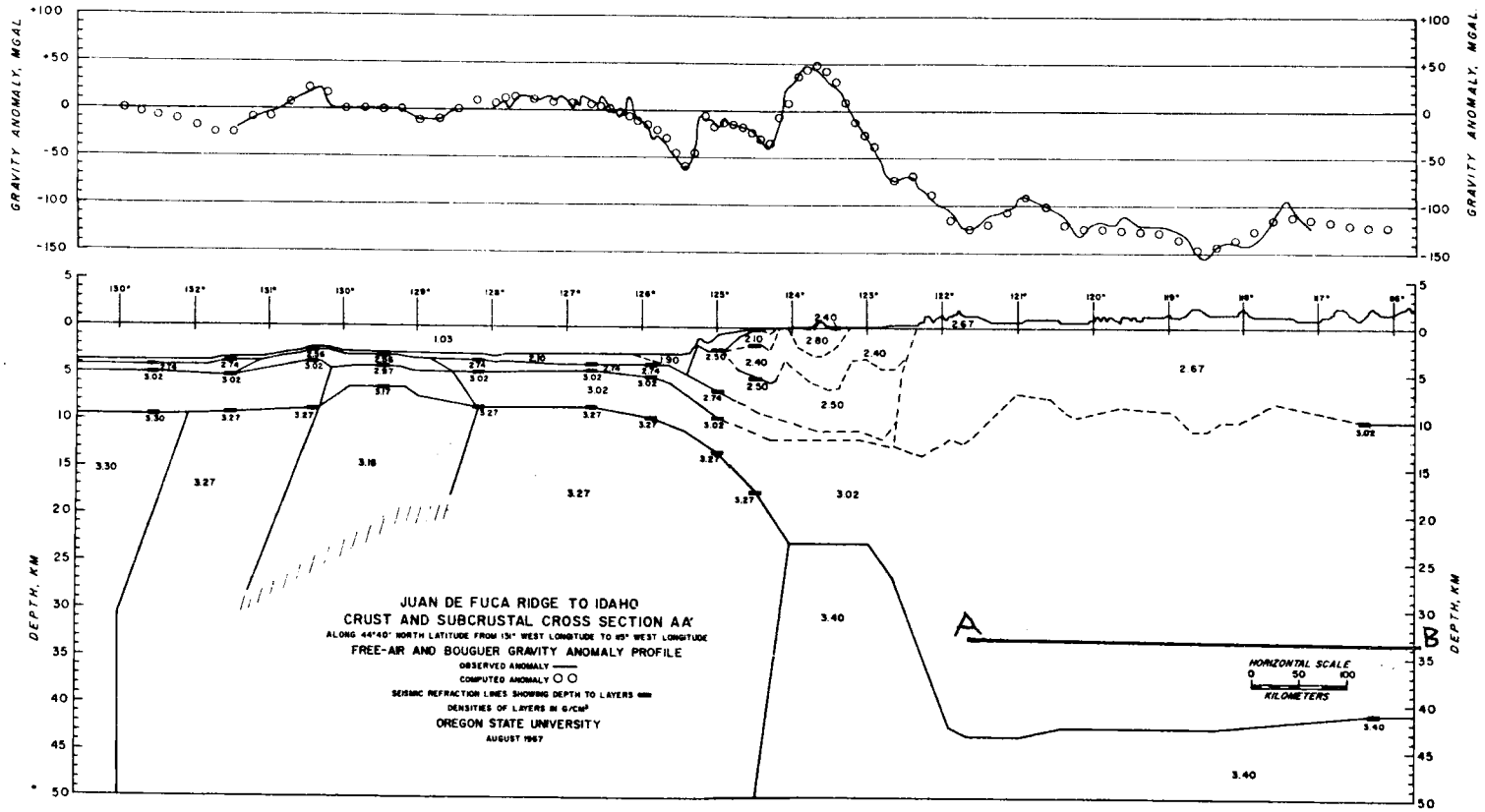

Figure 9. Crust and subcrustal cross-section along latitude 44° 40' N from longitude 131° W to 115° W. Reproduced from Dehlinger et al.

the crust evident in the cross-section in Figure 9. Such a correction would have been possible only if the two-dimensional structure of the discontinuities had been available.

By using the cross-section in Figure 9 and an average density contrast of 0.45 gm/cc as a standard of comparison, it is possible to interpolate between the assumed values of d and to arrive at a single value of d the best reconciles the above gravity and seismic results. Since there appear to be crustal density inhomogeneities west of the Cascades, this interpolation will be carried out only along the section of the seismic profile in Figure 10, extending from the Cascades into Idaho. The position of this section is indicated in Figures 6(a), 7(a), 8(a) and 9 by the line AB. The interpolation is carried out as follows. The average crustal thickness obtained for the section from the data in Figures 6(a), 7(a) and 8(a) is plotted in Figure 10 against the corresponding value of d. The three points can be connected by a straight line. The seismic data in Figure 9 yields an average depth of the Moho along the same section of 43 km. From Figure 10, we obtain the corresponding value of d equal to 30.25 km. On the presently available data, this value of d appears to be the most likely value for the reference crustal thickness to be applied as the basis of the present calculation.

In carrying out the iterative process in the boundary region, it was found that only the eight blocks immediately surrounding a field

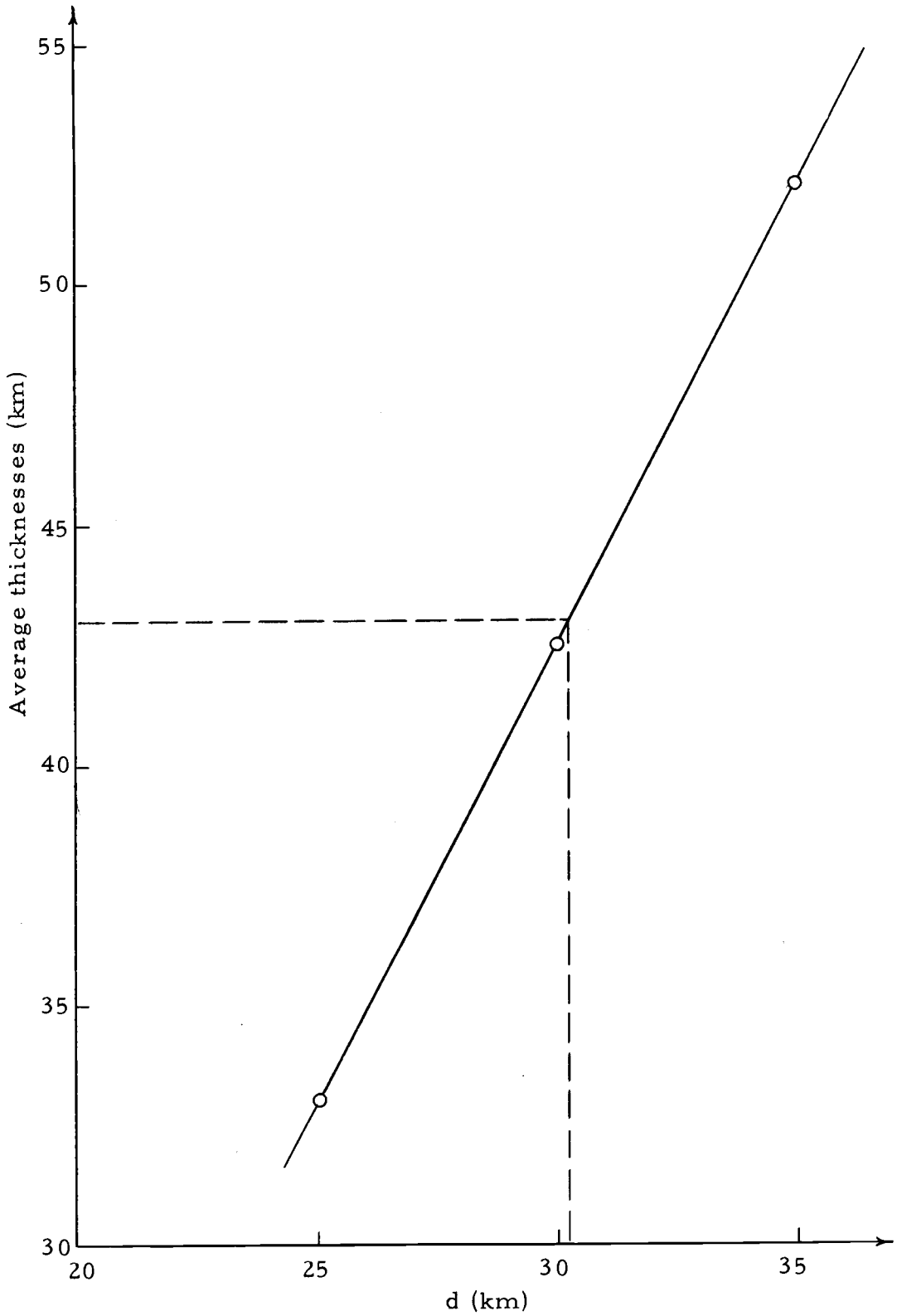

Figure 10. Graph of average thickness against assumed values of d, with $\rho = 0.45$ gm/cc.

point produced a significant effect there for those values of d equal to 25 km and 30 km. The effects were large enough to cause changes in the initial estimates of the crustal thickness of up to one part in 10. The farther blocks did not change the estimates to any significant extent; in most cases they either produced effects which were less than the estimated error of the input regional field or caused changes in crustal thickness of around one part in 50. For d = 35 km, the 16 blocks next to the eight immediately surrounding a field point produced effects which were greater than the estimated error of the input field. However, the farther blocks produced no significant influences, i.e., either their effects were small in comparison with the estimated error of the input field or they caused changes in the crustal thickness of not more than one part in 50.

Test of the Reliability of the Algebraic Method

In order to test the reliability of the computation method that had been developed, a two-layer model was constructed for an area the size of Oregon. The thickness of the upper layer of the model was made to vary in both the east-west and north-south directions, i.e., the model was two-dimensional. Table 1 shows the thickness of the top layer at the various grid points, while Figure 11 is the corresponding contour representation. Given the thicknesses, anomalies were calculated for each grid point on the basis of Equation (3.1). These

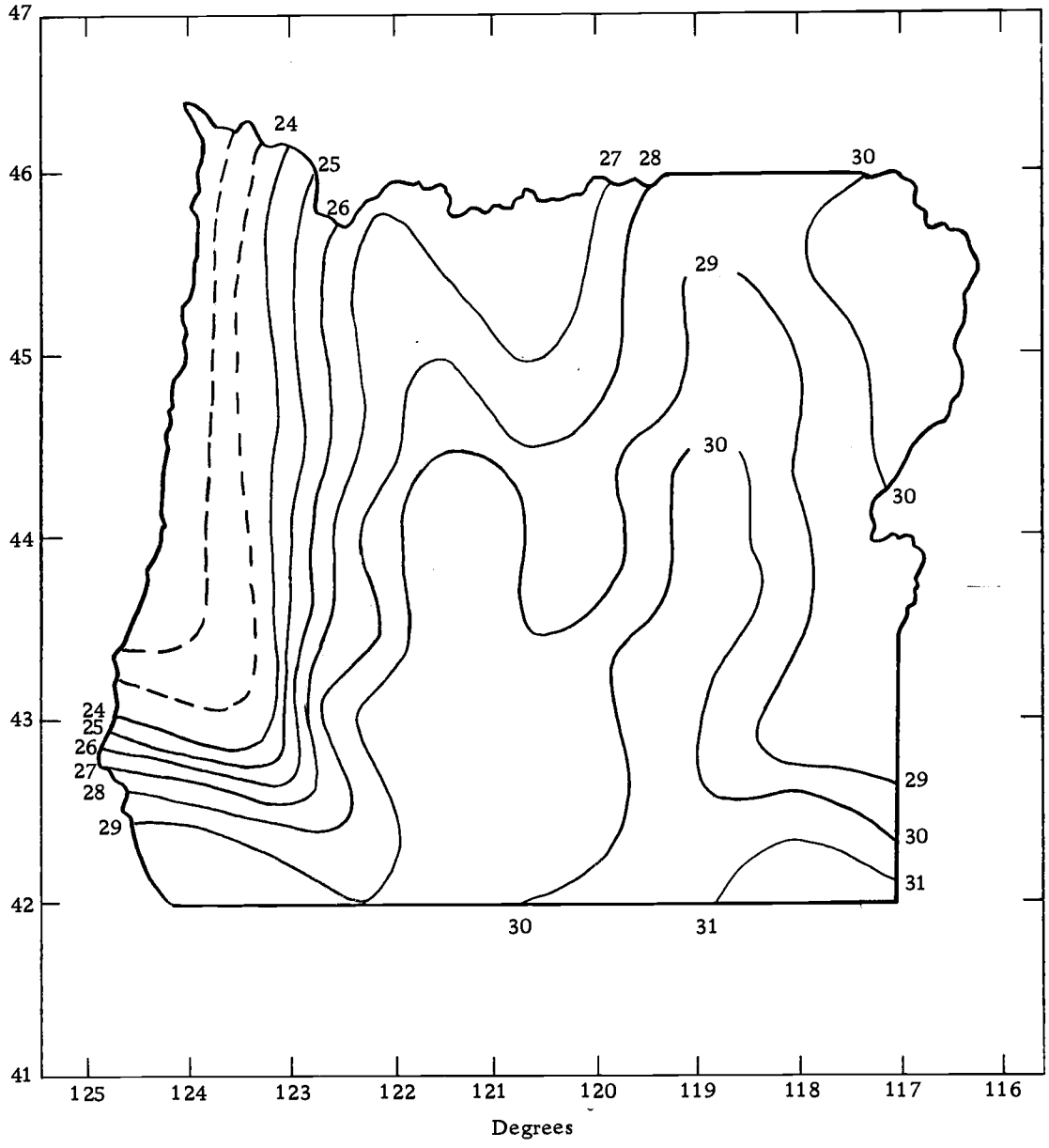

Figure 11. Contour representation of the top layer of two-dimensional model. Contour interval: 1 km.

anomalies constituted the input field to the computer program GRAVCALC. The results were compared with the model and a conclusion drawn as to the reliability of the algebraic method. This test was repeated for a second two-layer model in which the thickness of the top layer varied only in the east-west direction, a one-dimensional variation. Table 2 is a presentation of the values of the thicknesses at the grid points. An east-west cross-section is shown in Figure 12. The computations that followed were the same as for the two-dimensional model and the results were again used to establish a comparison with the original model.

Table 3 shows a comparison between the two-dimensional model and the computed results. The upper figures are the thicknesses of the top layer of the model, while the lower ones are the calculated results. The agreement between the two sets of figures is good. The maximum and minimum differences between the two have absolute values of 2.77 km and 0.02 km at points where the model has thicknesses of 34.00 and 23.50 km respectively. Figure 13 is a contour representation of the computed model. It shows nearly the same trends as are evident in the model, Figure 11.

In Table 4 are presented the corresponding results for the one-dimensional model. A comparison of east-west cross-sections is presented in Figure 14. Here also the agreement is good, the maximum difference having an absolute value of 1.63 km for a model

thickness of 29.00 km; the absolute minimum is 0.01 km where the model is again 29.00 km thick.

The close agreement between the models and the computed results does indicate that, with the proper choice of digitizing interval, the algebraic method can be relied upon to yield satisfactory values for those parameters of a source body that are sought. However, to what extent the results approximate the true geological situation, depends upon the restrictions that are placed upon the other unknown parameters of the source body.

Table 1. Thicknesses of the top layer of the two-dimensional two-layer model. Figures are in kilometers.

23.50	27.00	27.00	26.50	28.00	29.00	30.00
23.50	27.00	28.00	27.00	28.00	29.00	29.00
23.50	27.00	29.00	28.00	29.00	30.00	29.00
23.00	28.00	30.00	29.00	29.00	30.00	29.00
23.00	27.50	30.00	29.00	30.00	31.00	29.00
21.00	29.00	30.00	29.50	30.00	30.00	28.50
28.00	28.00	29.80	29.70	30.00	30.00	30.50
34.00	29.00	30.00	30.00	31.00	31.00	32.00

Table 2. Thicknesses of the top layer of the one-dimensional two-layer model.

23.00	21.00	24.00	29.00	26.00	29.00	30.00
23.00	21.00	24.00	29.00	26.00	29.00	30.00
23.00	21.00	24.00	29.00	26.00	29.00	30.00
23.00	21.00	24.00	29.00	26.00	29.00	30.00
23.00	21.00	24 00	29.00	26.00	29.00	30.00
23.00	21.00	24.00	29.00	26.00	29.00	30.00
23.00	21.00	24.00	29.00	26.00	29.00	30.00
23.00	21.00	24.00	29.00	26.00	29.00	30.00

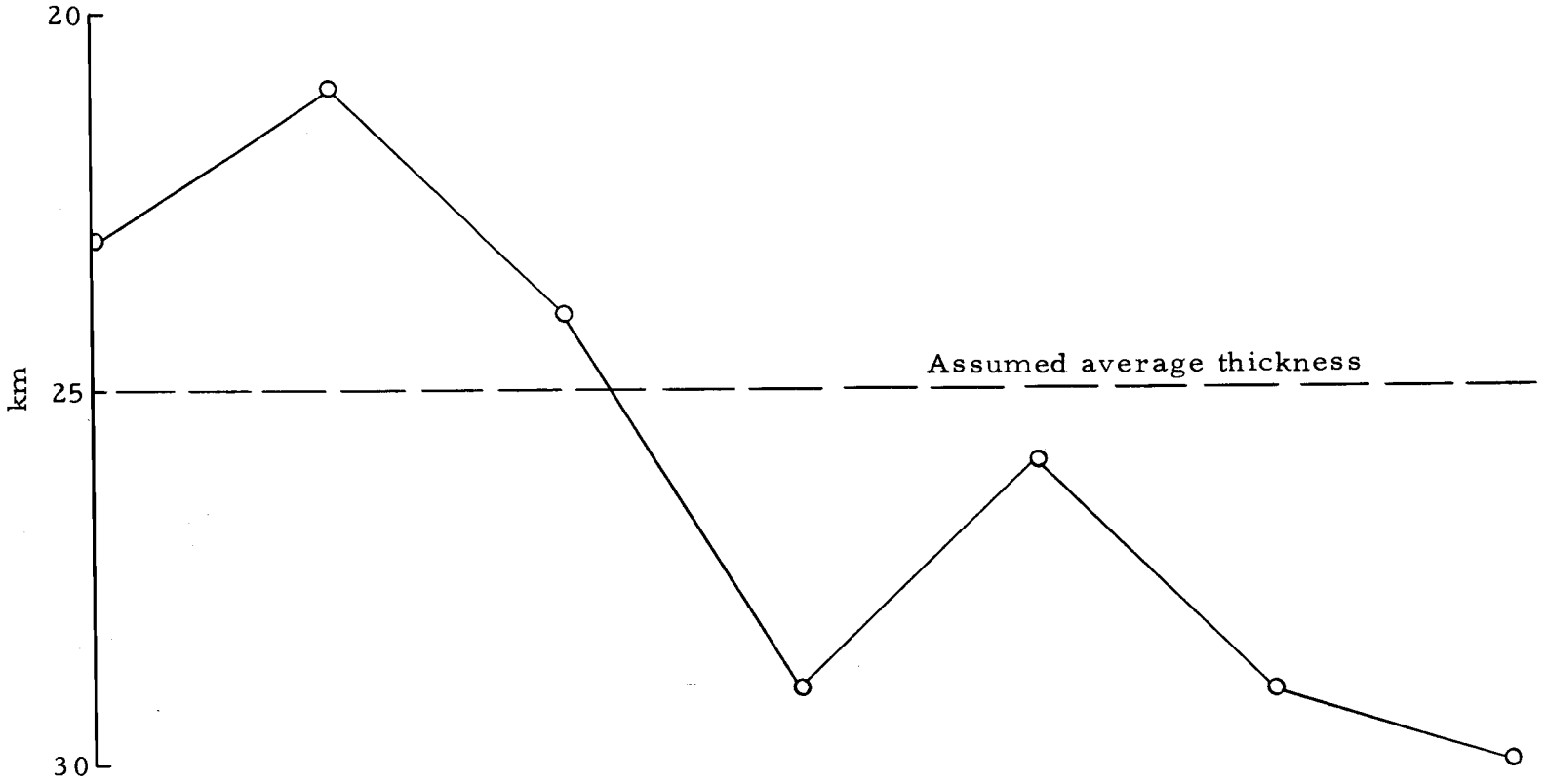

Figure 12. East-west cross-section through the top layer of the one-dimensional model.

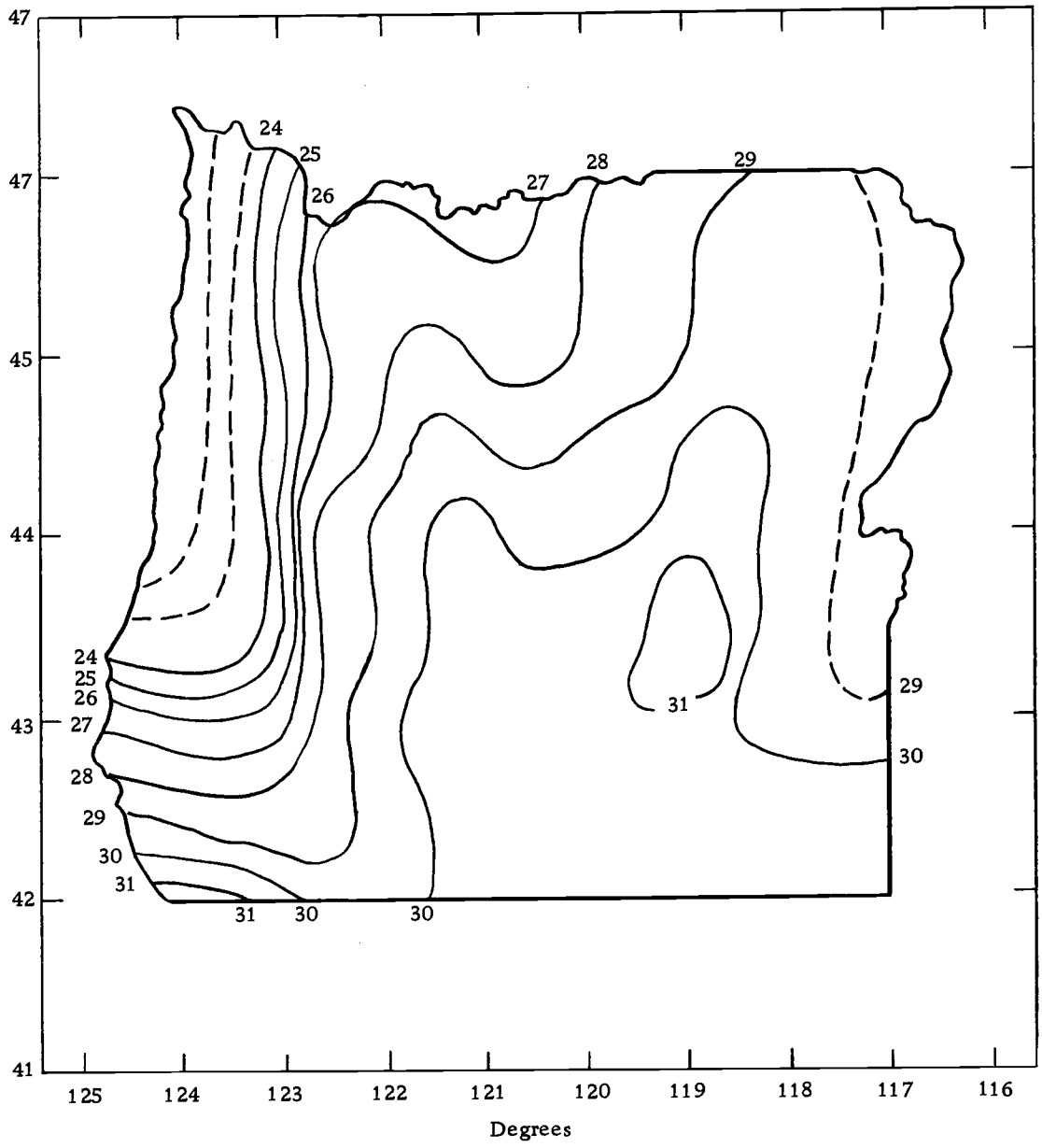

Figure 13. Recomputed thicknesses of the top-layer of the two-dimensional model. Contour interval: 1 km.

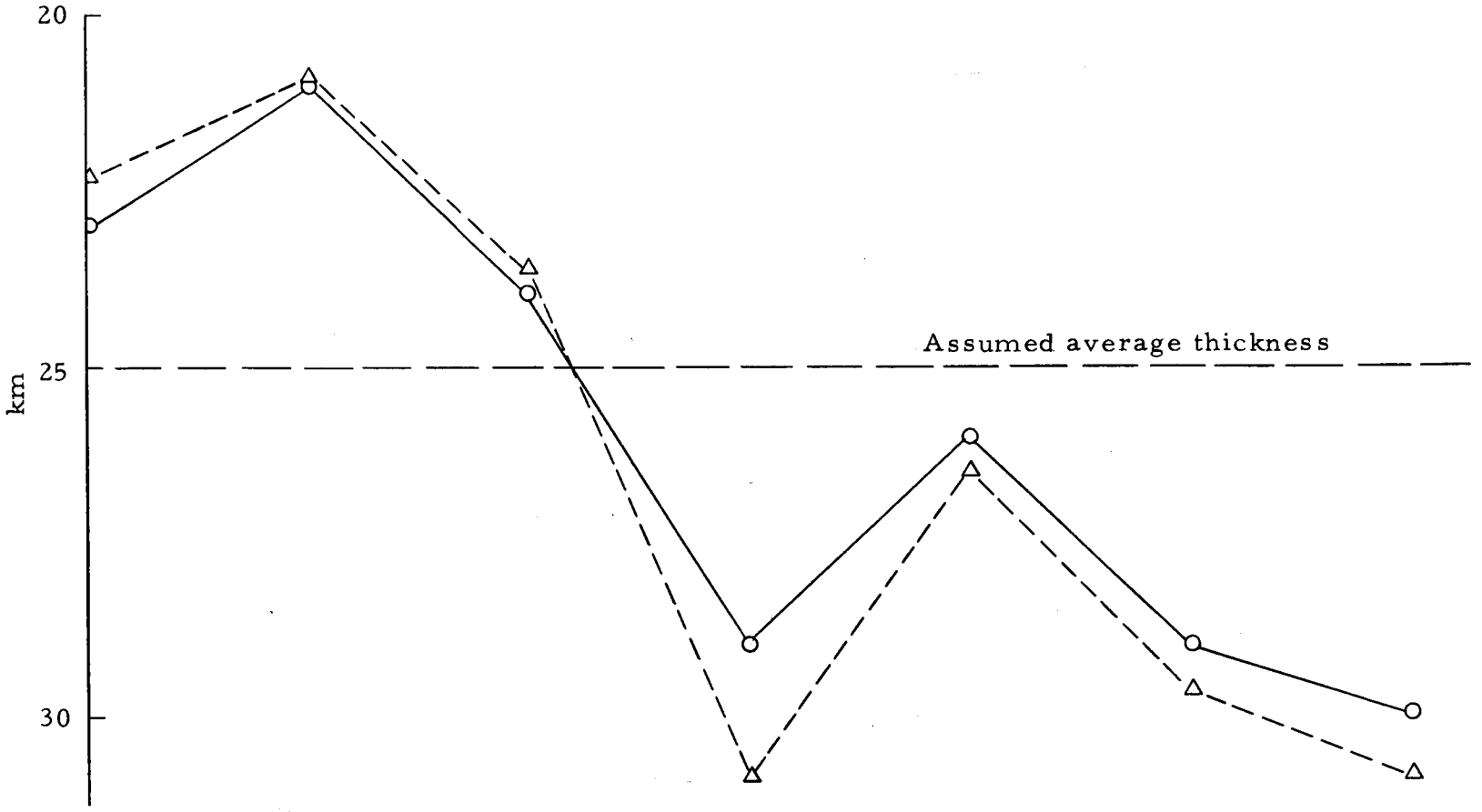

Figure 14. Comparison of the east-west cross-sections through the one-dimensional model (full line) and the recomputed model (broken line).

Table 3. Comparison between the thicknesses (upper figures) of the top layer of the two-dimensional two-layer model and the thicknesses (lower figures) recomputed by the algebraic method.

23.50	27.00	27.00	26.50	28.00	29.00	30.00
23.48	27.17	27.43	27.05	28.39	29.22	29.68
23.50	27.00	28.00	27.00	28.00	29.00	29.00
23.43	27.41	28.55	27.85	28.87	29.75	29.50
23.50	27.00	29.00	28.00	29.00	30.00	29.00
23.43	25.57	29.57	28.94	29.75	30.52	29.54
23.00	28.00	30.00	29.00	29.00	30.00	29.00
23.43	28.42	30.38	29.85	30.03	30.73	29.61
23.00	27.50	30.00	29.00	30.00	31.00	29.00
22.86	28.24	30.52	30.03	30.73	31.26	29.61
21.00	29.00	30.00	29.50	30.00	30.00	28.50
29.92	29.33	30.59	30.38	30.80	30.80	29.40
28.00	28.00	29.80	29.70	30.00	30.00	30.50
28.39	28.90	30.42	30.49	30.77	30.77	30.63
34.00	29.00	30.00	30.00	31.00	31.00	32.00
31.23	29.29	30.03	30.14	30.73	30.77	30.94

Table 4. Comparison between the thicknesses (upper figures) of the top layer of the one-dimensional two-layer model and the thicknesses (lower figures) recomputed by the algebraic method.

23.00	21.00	24.00	29.00	26.00	29.00	30.00
22.52	21.27	23.75	29.19	26.32	29.12	30.35
23.00	21.00	24.00	29.00	26.00	29.00	30.00
22.34	21.13	23.64	30.07	26.47	29.50	30.84
23.00	21.00	24.00	29.00	26.00	29.00	30.00
22.31	20.99	23.62	30.63	26.51	29.57	30.94
23.00	21.00	24.00	29.00	26.00	29.00	30.00
22.30	20.96	23.61	30.91	26.52	29.61	30.94
23.00	21.00	24.00	29.00	26.00	29.00	30.00
22.30	20.96	23.61	30.91	26.52	29.61	30.94
23.00	21.00	24.00	29.00	26.00	29.00	30.00
22.31	20.99	23.62	30.63	26.51	29.57	30.94
23.00	21.00	24.00	29.00	26.00	29.00	30.00
22.34	21.13	23.64	30.07	26.47	29.50	30.84
23.00	21.00	24.00	29.00	26.00	29.00	30.00
22.52	21.27	23.75	29.19	26.32	29.12	30.35

A Second Derivative Approximation Method

The Working Equation

The working equation for this method is

$$\Delta g(x, y, 0) = \gamma \Delta \rho d \int_{\xi} \int_{\eta} \frac{h(\xi, \eta) d\xi d\eta}{[(x-\xi)^2+(y-\eta)^2+d^2]^{3/2}} \tag{3.22}$$

which is the linear approximation to the fundamental Equation (2.26), which is valid for $|h| \ll d$. Equation (3.22) is an integral equation of the first kind and may be rewritten in the form

$$\Delta g(x, y, 0) = c \int_{-\infty}^{\infty} \int K(x, y; \xi, \eta) h(\xi, \eta) d\xi d\eta \tag{3.23}$$

where

$$c = \gamma \Delta \rho d$$

$$K = \frac{1}{[(x-\xi)^2+(y-\eta)^2+d^2]^{3/2}}$$

A method of solution which immediately suggests itself derives from the nature of kernel $K(x, y; \xi, \eta)$. It is symmetric in its variables, continuous and square integrable. Consequently, for the finite domain that we are here dealing with, it has eigenvalues λ_i and corresponding eigenfunctions ϕ_i in terms of which $\Delta g(x, y, 0)$ and $h(x, y)$ may be expanded (Morse and Feshback, 1953; Sobolev, 1964).

By carrying out this expansion, Equation (3.23) is transformed into the following equation

$$\sum_{i=1}^{\infty} c_i \phi_i = \sum_{i=1}^{\infty} \lambda_i h_i \phi_i$$

The required solution is given by

$$h = \sum_{i=1}^{\infty} \frac{c_i \phi_i}{\lambda_i}$$

provided that $\lambda_i \neq 0$. This method is somewhat tedious to apply. Instead a solution is adopted that is based on the inversion of Equation (3.22) by the Fourier transform technique and that involves the computation of the second derivative and the upward continuation of the regional field.

Solution by the Fourier Transform Method

If $G(\omega_1, \omega_2)$ is the two-dimensional Fourier transform of $\Delta g(x, y, 0)$, we have

$$G(\omega_1, \omega_2) = \underset{\substack{X \to \infty \\ Y \to \infty}}{\text{Limit}} \frac{1}{2\pi} \int_{-X}^{X} \int_{-Y}^{Y} \Delta g(x, y, 0) e^{-i(\omega_1 x + \omega_2 y)} dxdy$$

where $(-X, X)$ and $(-Y, Y)$ are the gravity profile dimensions in

the x and y directions. If $H(\omega_1, \omega_2)$ is the corresponding transform of $h(x, y)$, then the transformed version of Equation (3.22) takes the form

$$G(\omega_1, \omega_2) = 2\pi\gamma\Delta\rho \exp(-d\sqrt{\omega_1^2+\omega_2^2})H(\omega_1, \omega_2) \tag{3.24}$$

whose formal solution is

$$H(\omega_1, \omega_2) = \frac{1}{2\pi\gamma\Delta\rho} \exp(d\sqrt{\omega_1^2+\omega_2^2})G(\omega_1, \omega_2) \tag{3.25}$$

Inverting (3.25) should yield $h(x, y)$. A difficulty is posed by the presence on the right-hand side of the exponential which is unbounded and consequently prevents the inversion from being carried out unless the function $G(\omega_1, \omega_2)$ attenuates rapidly for large wave numbers. Due to errors of measurement, the $\Delta g(x, y, 0)$ data invariably contain components with large wave numbers which are magnified out of proportion. A smoothing of the observed field values $\Delta g(x, y, 0)$ enables one to circumvent this difficulty. However, smoothing removes useful information in the form of short-wave components and an inversion of Equation (3.25) on the basis of smoothed data will, therefore, yield an incomplete solution. A useful solution may yet be obtained by expanding the exponential factor in Equation (3.25) into a power series. Such an expansion would involve odd powers of $\sqrt{\omega_1^2+\omega_2^2}$, which are somewhat unpleasant terms to handle. However,

they can be avoided by a method used by Snow (1923) and later by Bateman (1946) which consists of adding and subtracting the term

$$\frac{1}{2\pi\gamma\Delta\rho} \quad \exp(-d\sqrt{\omega_1^2+\omega_2^2})G(\omega_1,\omega_2) \tag{3.26}$$

on the right-hand side of Equation (3.25). The addition of this term leads to a term including the factor

$$[\exp(d\sqrt{\omega_1^2+\omega_2^2}) + \exp(-d\sqrt{\omega_1^2+\omega_2^2})]G(\omega_1,\omega_2) \tag{3.27}$$

which, when expanded into series, contains only even powers of $\sqrt{\omega_1^2+\omega_2^2}$, i.e., terms of the form

$$(\omega_1^2+\omega_2^2)^{2n}G(\omega_1,\omega_2) \tag{3.28}$$

where n is a positive integer. These terms inverted into (x, y) space give the terms

$$(-\nabla^2)^n \Delta g(x, y, 0)$$

Thus is obtained the Snow-Bateman form of the solution of the integral Equation (3.22)

$$h(x,y) = \frac{1}{\gamma\Delta\rho}\left[\frac{1}{\pi}\sum_{n=0}^{\infty}\frac{d^{2n}}{(2n)!}(-\nabla^2)^n\Delta g(x,y,0) - \frac{d}{(2\pi)^2}\iint_{-\infty}^{\infty}\frac{\Delta g(\xi,\eta)d\xi d\eta}{[(x-\xi)^2+(y-\eta)^2+d^2]^{3/2}}\right] \quad (3.29)$$

in which the last term on the right-hand side is the inverse Fourier transform of the expression (3.26). This solution includes an infinite series in the Laplacian derivatives of $\Delta g(x,y,0)$. The series will diverge in the general case, but if $\Delta g(x,y,0)$ is a band-limited function with cut-off limit ω_o, the series will converge (Bodvarsson, 1971), the convergence being rapid when

$$2d^2\omega_o < 1$$

Under this condition, the Snow-Batemen solution is applicable. For the relatively long wave components in $h(x,y)$, the series can be truncated after the second term to yield the solution

$$h(x,y) = \frac{1}{\pi\gamma\Delta\rho}\left[\Delta\bar{g}(x,y,0) - \frac{d^2}{2}\nabla^2(\Delta g(x,y,0)) - \frac{d}{4\pi}\iint_{-\infty}^{\infty}\frac{\Delta g(\xi,\eta)d\xi d\eta}{[(x-\xi)^2+(y-\eta)^2+d^2]^{3/2}}\right] \quad (3.30)$$

in which the term $\nabla^2(\Delta\bar{g}(x,y,0))$ represents the second derivative

of the observed regional field and

$$\frac{d}{2\pi}\int_{-\infty}^{\infty}\int\frac{\Delta g(\xi,\eta)d\xi d\eta}{[(x-\xi)^2+(y-\eta)^2+d^2]^{3/2}}$$

represents the upward continuation of the regional field to the plane at a height d above its plane of observation. As Bodvarsson (1971) has shown, the solution expressed in Equation (3.30) is valid only for wavelengths of the undulating interface equal to or greater than $4d$ to $6d$.

Computation Scheme

There were three parts to the computation. The first was the calculation of the second derivative. The schemes designed for this calculation reduce to this general formula (Dobrin, 1960)

$$\frac{\partial^2}{\partial z^2}(\Delta g) = \frac{C}{s^2}[W_o\Delta g_o + W_1\overline{\Delta G}_1 + W_2\overline{\Delta G}_2 + \ldots] \qquad (3.31)$$

where Δg_o is the value of the regional field at the point where the second derivative is required; $\overline{\Delta g_1}, \overline{\Delta g_2}, \ldots$ are the averages of the field values along circles of radii $s, s\sqrt{2}, \ldots$ respectively. C is a numerical constant. $W_o, W_1, W_2, \ldots$ are weighting factors for the respective gravity values. Some of them are positive, others are negative and their algebraic sum is zero. The theory behind the above

general formula has been discussed by Peters (1949). The specific formula used in calculating the second derivative was Griffin's (1949) center-point-and-one-ring formula which gives the second derivative as

$$\frac{\partial^2}{\partial z^2}(\Delta g) = \frac{4}{s^2}(\Delta g_o - \overline{\Delta g(s)}) \qquad (3.32)$$

Since the above equation does not contain d, the second derivative had to be calculated only once. The second part of the computation involved the upward continuation, which was performed by a computer program called UPWARD, reproduced in Appendix B. The calculation was carried out for the three values of 25 km, 30 km and 35 km. Finally a computer program, identified as SUM and reproduced in Appendix C, was written to calculate the values of $h(x, y)$ in accordance with Equation (3.30). One of the functions of this program was to first compute the second derivatives with the appropriate values of Δg_o and $\overline{\Delta g(s)}$ as input (see Equation (3.32)). The values of $h(x, y)$ were converted into crustal thicknesses by addition to, or subtraction from, d. The results are shown in Figures 15a through 17b.

Results and Discussion

The broad features discernible in the crustal thicknesses obtained by the algebraic method are also evident in the results yielded by the present method. The Willamette Valley again stands

out as a trough. The same gradual increase in thickness towards the eastern margin of the state is also evident. On the whole, the results for $d = 25$ km and $d = 30$ km agree better with the corresponding results by the algebraic method than do the results for $d = 35$ km.

In order to arrive at the best value of d, the same method of interpolation was used as for the algebraic method. Averages were calculated from the results shown in Figures 15(a)-17(a) and plotted against the corresponding values of d. From the graph, which is presented in Figure 18, the value of d that best reconciles the above gravity results and the seismic results in Figure 9 was found to be 28.90 km.

The cross-sections in Figures 19-21 present a comparison of the results obtained from the algebraic and the second derivative approximation methods. The divergence that they show may be accounted for by the fact that the second derivative approximation method is based in part on the computation of the second vertical derivative of the regional gravity field. As has been pointed out by several workers (see, for instance, Rosenbach, 1953; Nettleton, 1954; Mesko, 1965, 1966; Skeels, 1967), the second derivative cannot be accurately calculated. Not only is it sensitive to grid spacing, but it also varies with the radii of the circles used in computing it. In practice, the second derivative has been found to relate more closely

to the residual than to the regional field that has been the basis of this investigation. As Peters (1949) points out, the schemes for calculating the second derivative are only approximations and give results which are more qualitative than quantitative.

From the foregoing discussion, it is safe to conclude that the second derivative approximation method should be expected to yield somewhat less accurate results than the algebraic method.

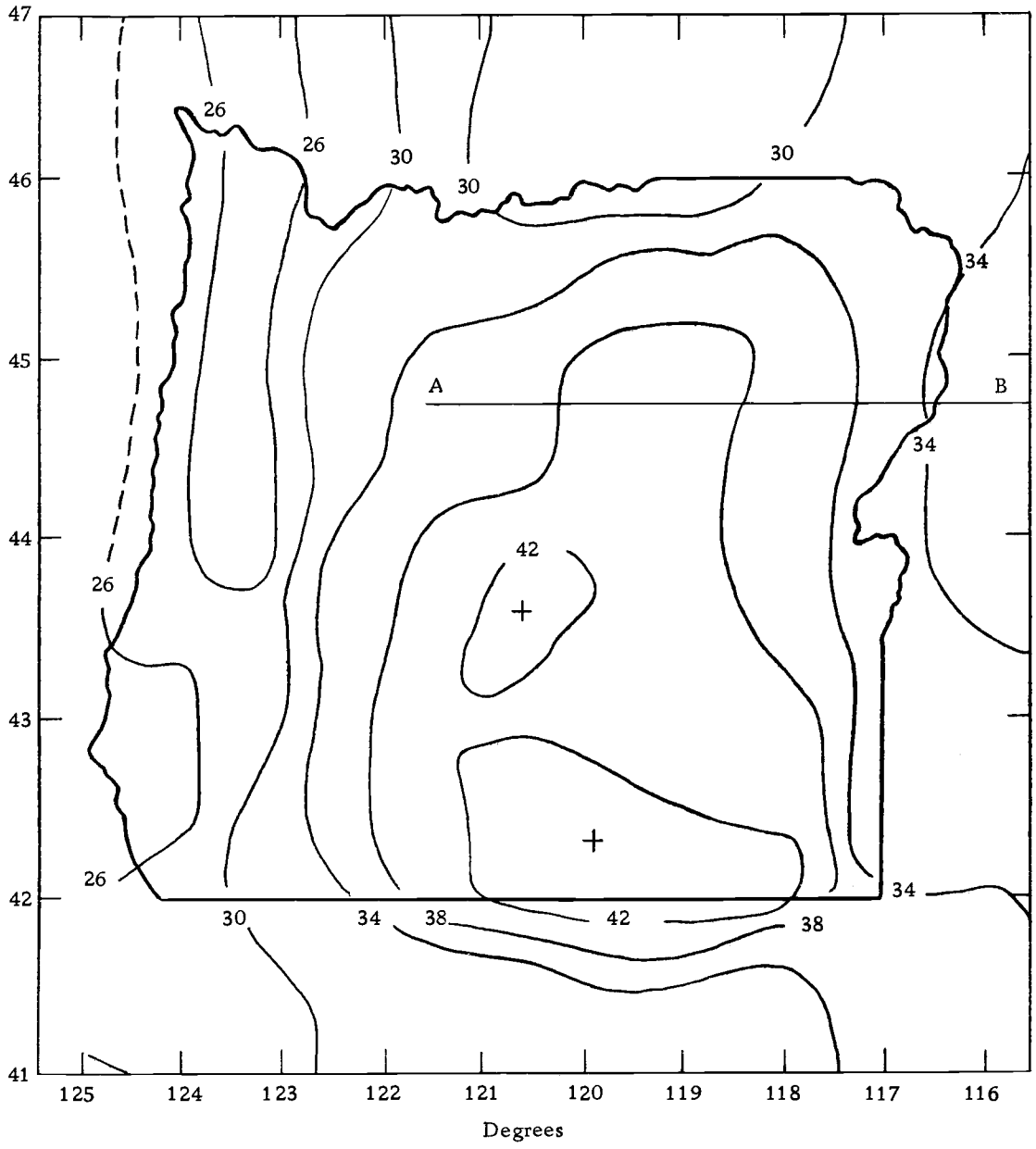

Figure 15a. Crustal thickness profiles for d = 25 km and $\Delta\rho$ = 0.45 gm/cc obtained by the second derivative approximation method. Contour interval: 4 km.

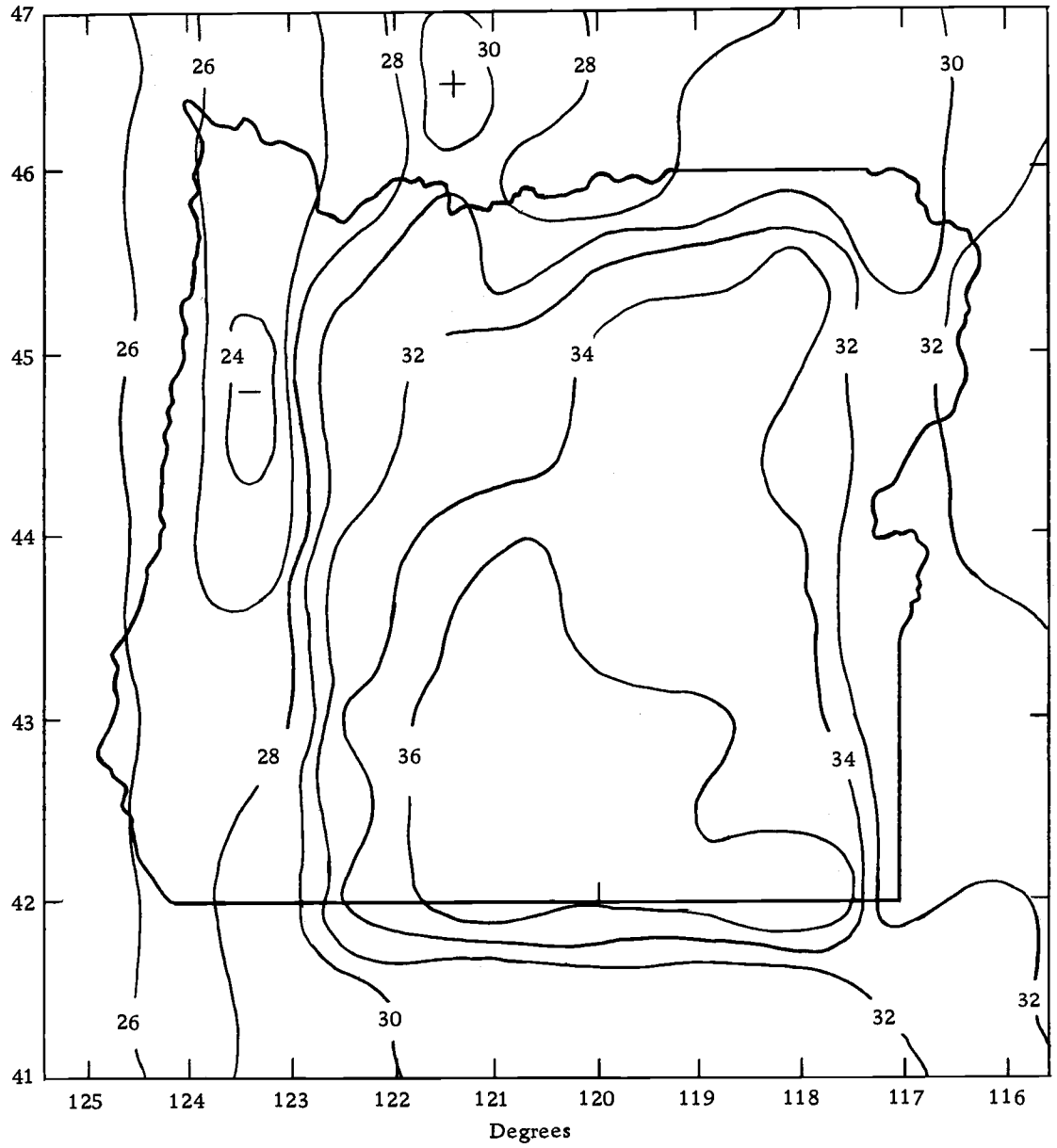

Figure 15b. Crustal thickness profiles for d = 25 km and $\Delta\rho$ = 0.60 gm/cc obtained by the second derivative approximation method. Contour interval: 2 km.

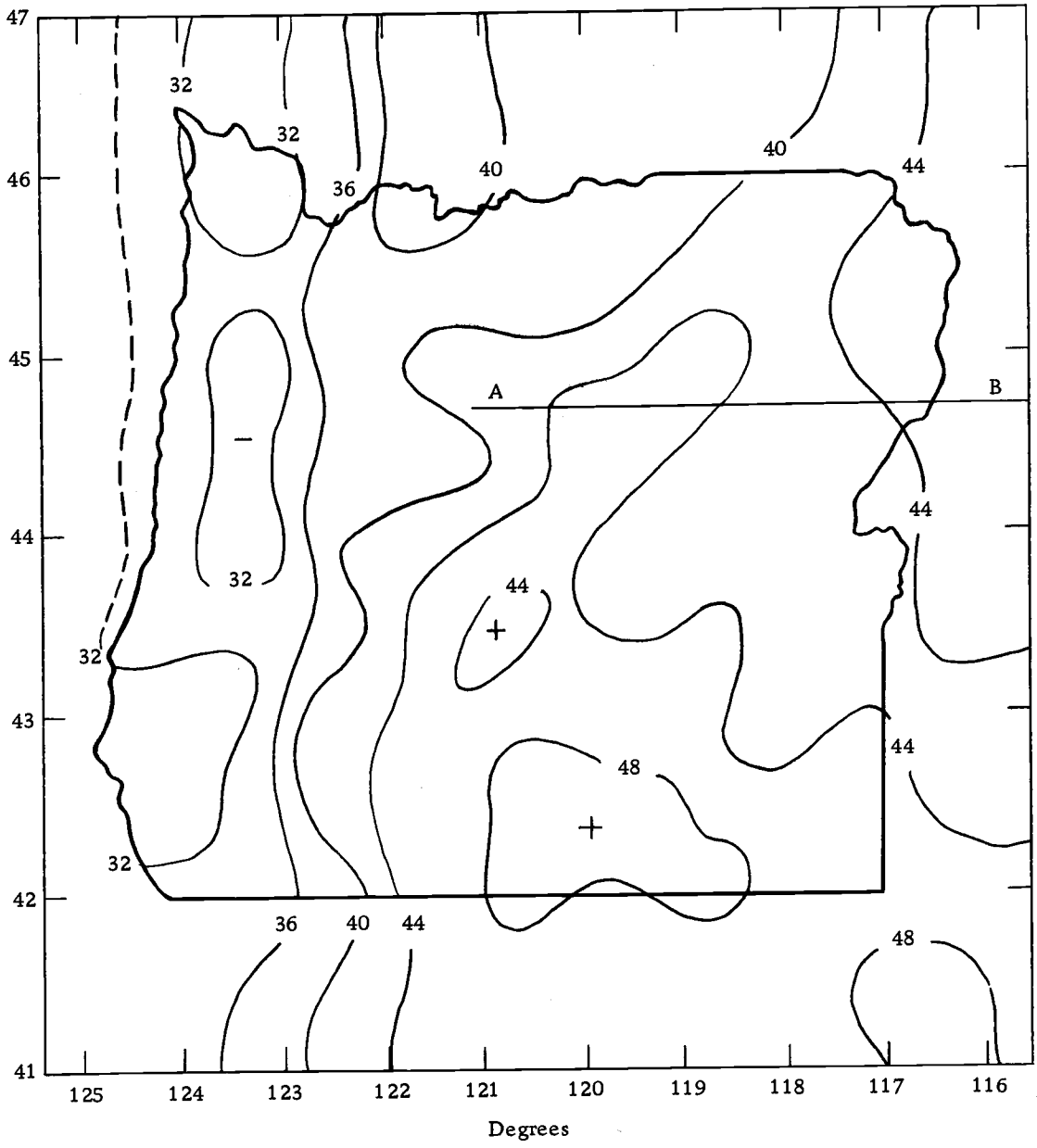

Figure 16a. Crustal thickness profiles for d = 30 km and $\Delta\rho$ = 0.45 gm/cc obtained by the second derivative approximation method. Contour interval: 4 km.

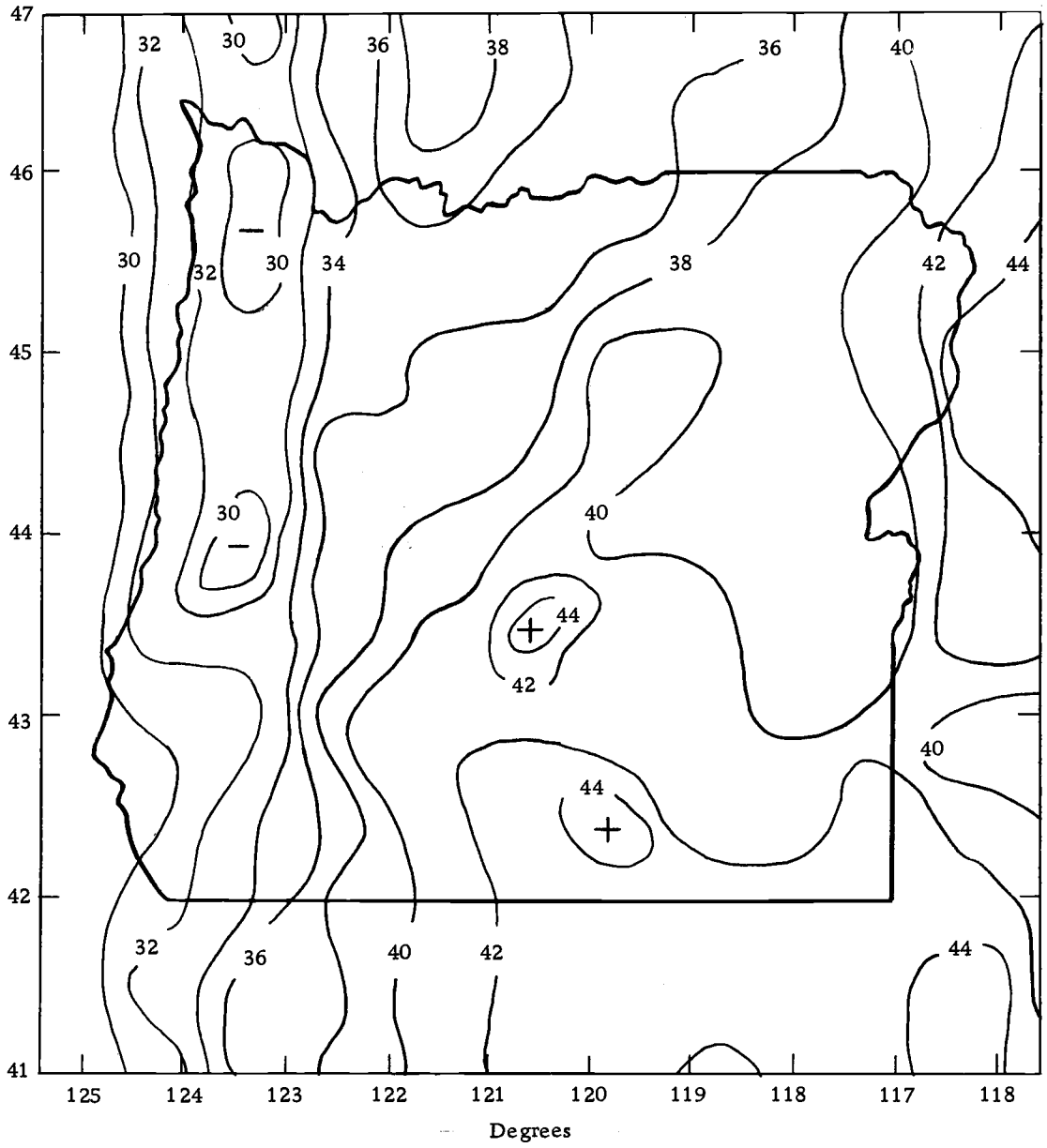

Figure 16b. Crustal thickness profiles for d = 30 km and $\Delta\rho$ = 0.60 gm/cc obtained by the second derivative approximation method. Contour interval: 2 km.

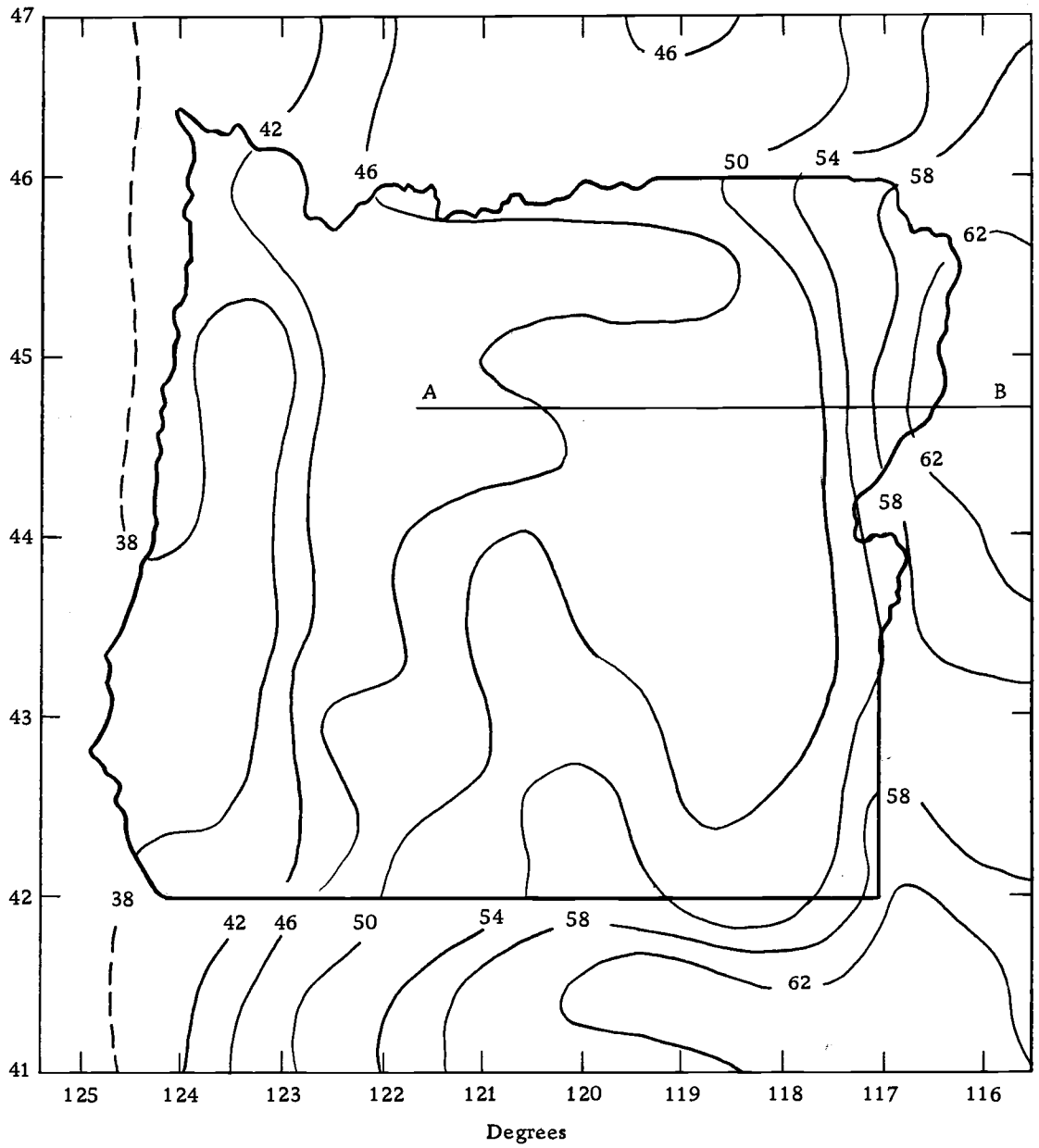

Figure 17a. Crustal thickness profiles for d = 35 km and $\Delta\rho$ = 0.45 gm/cc obtained by the second derivative approximation method. Contour interval: 4 km.

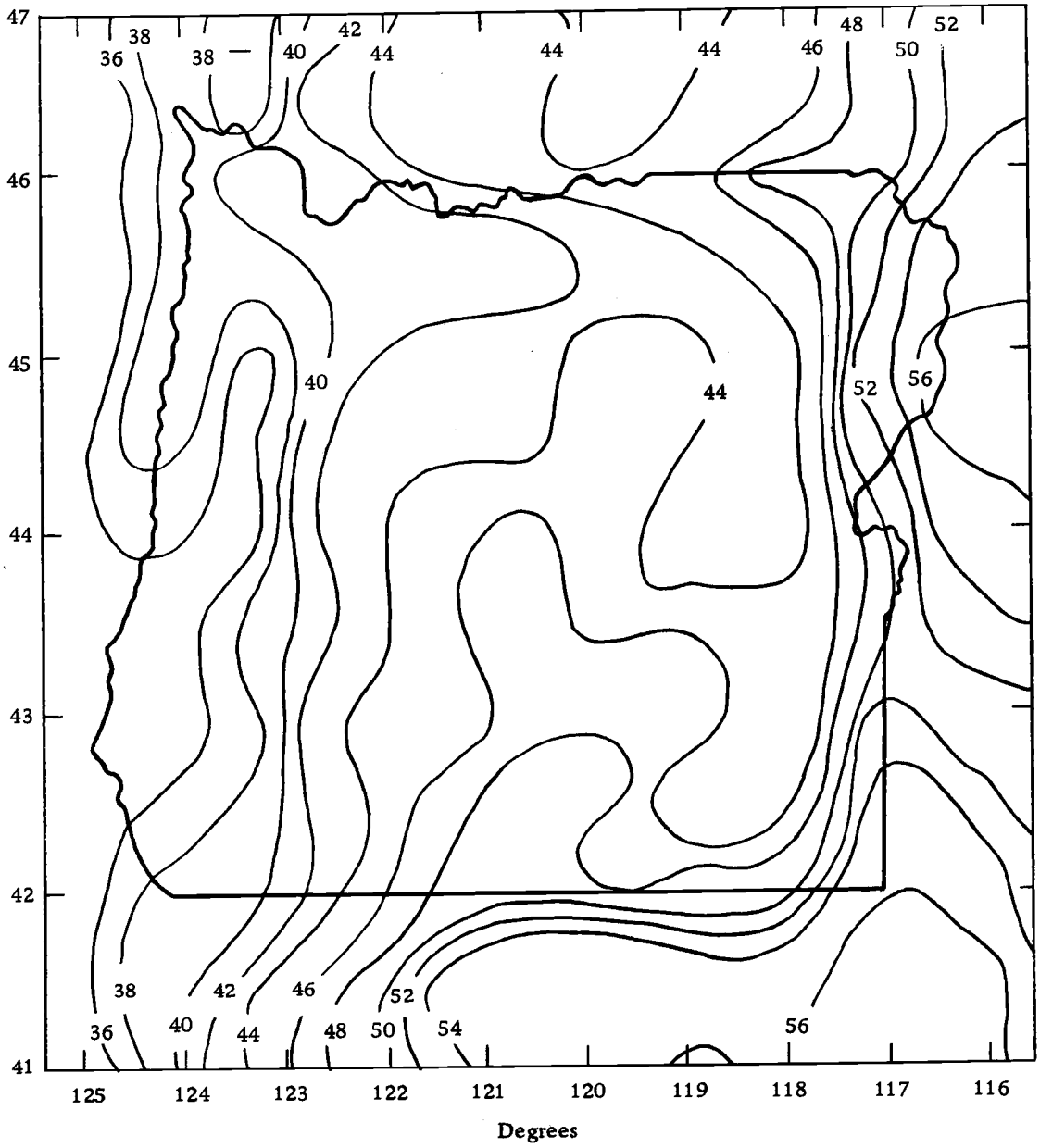

Figure 17b. Crustal thickness profiles for d = 35 km and $\Delta\rho$ = 0.60 gm/cc obtained by the second derivative approximation method. Contour interval: 2 km.

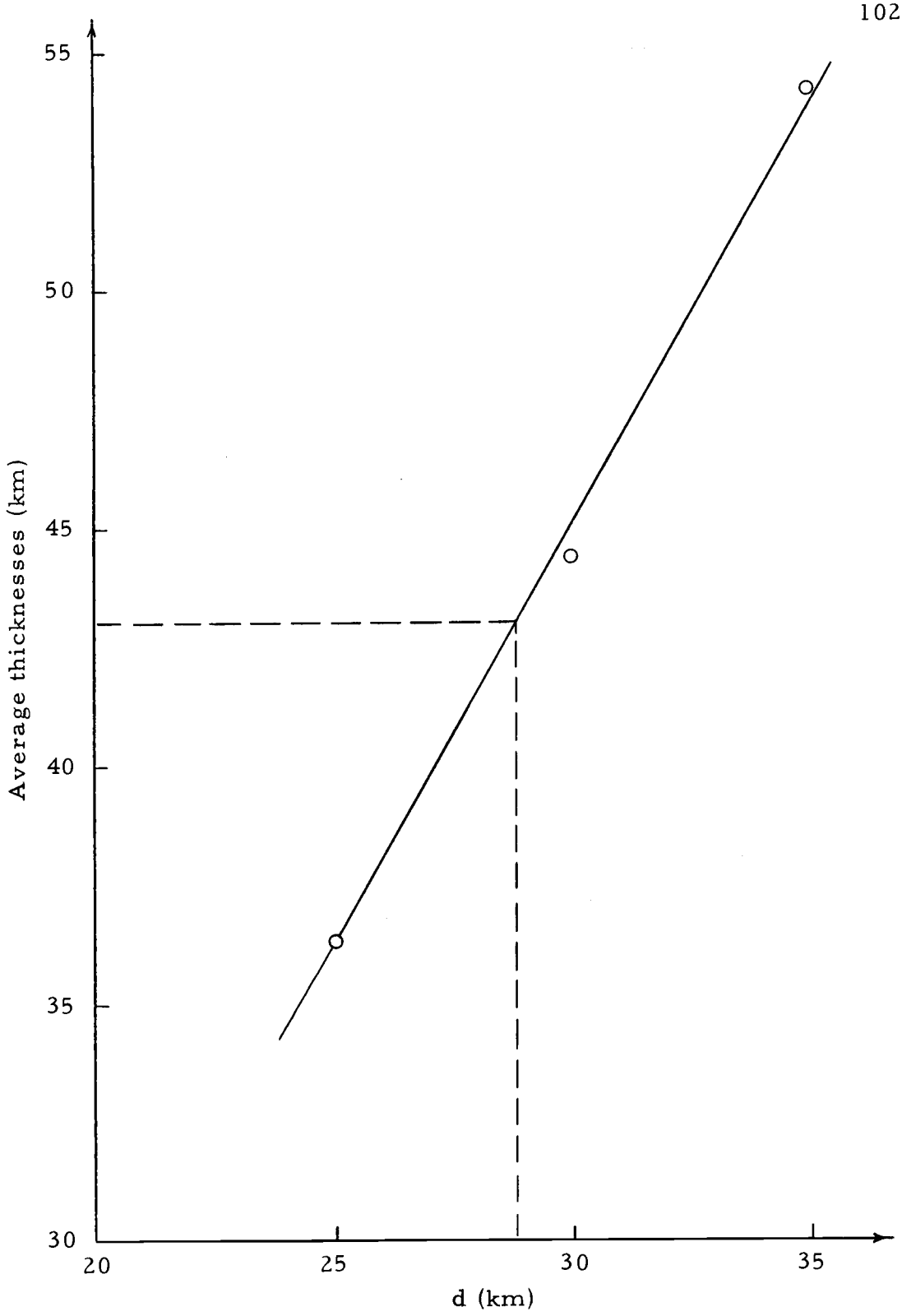

Figure 18. Graph of average thicknesses against assumed values of d, with $\rho = 0.45$ gm/cc.

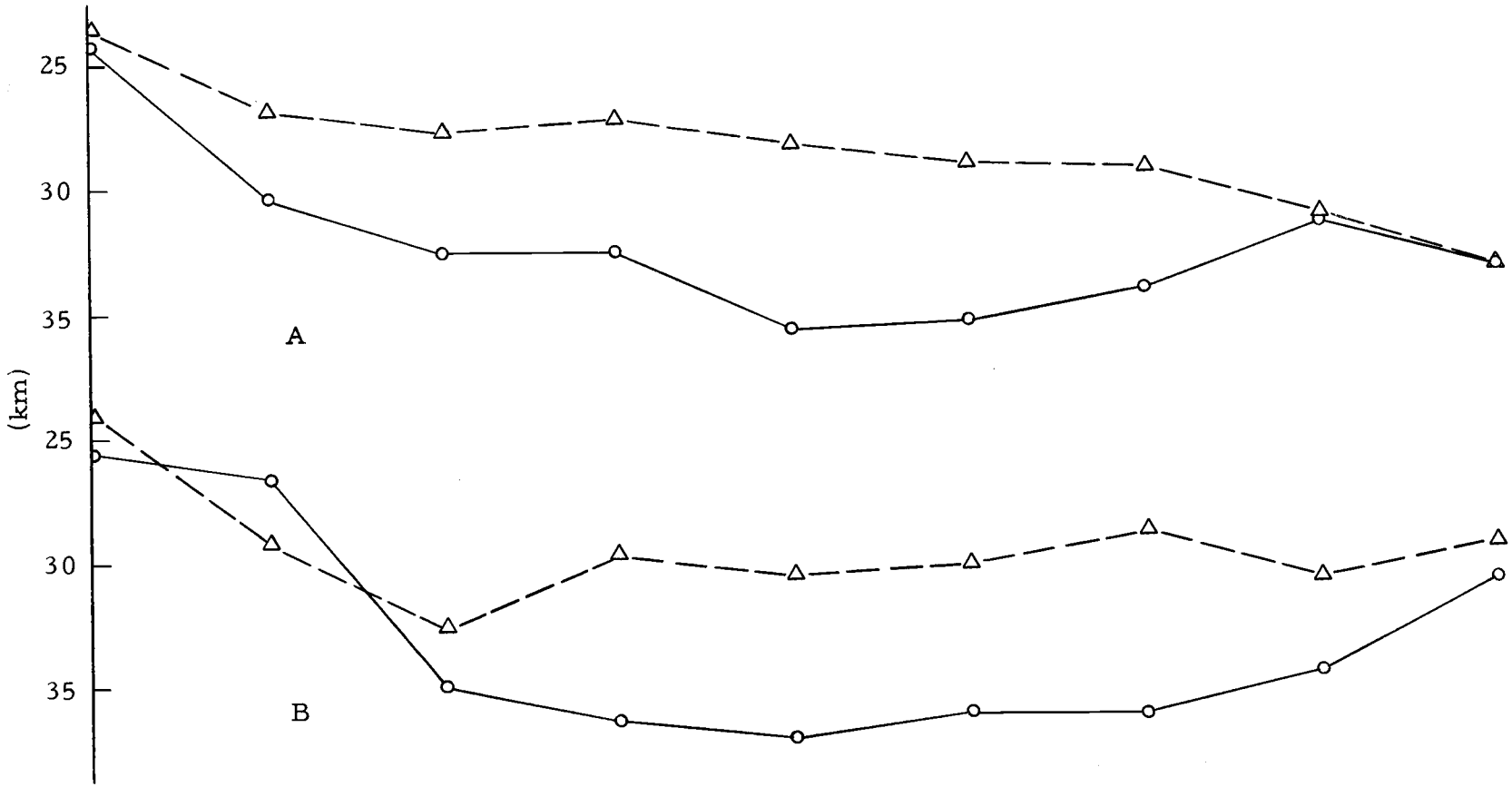

Figure 19. Cross-sections along latitudes 45°N (A) and 43°N (B), from longitude 116°30' to 123°30', through Figure 6b (broken curve) and Figure 15b (full curve).

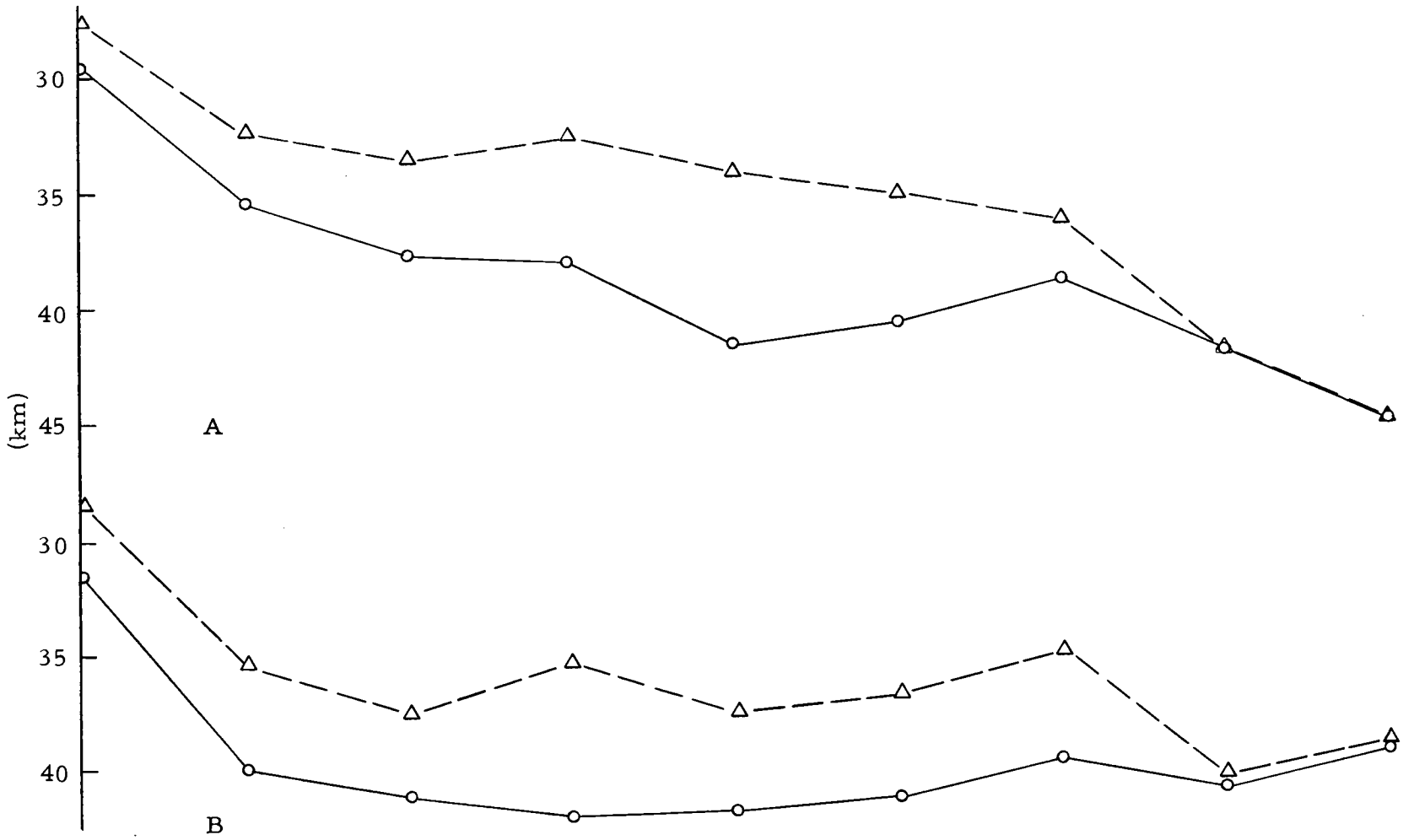

Figure 20. Cross-sections along latitudes 45°N (A) and 43°N (B), from longitude 116°30' to 123°30', through Figure 7b (broken curve) and Figure 16b (full curve).

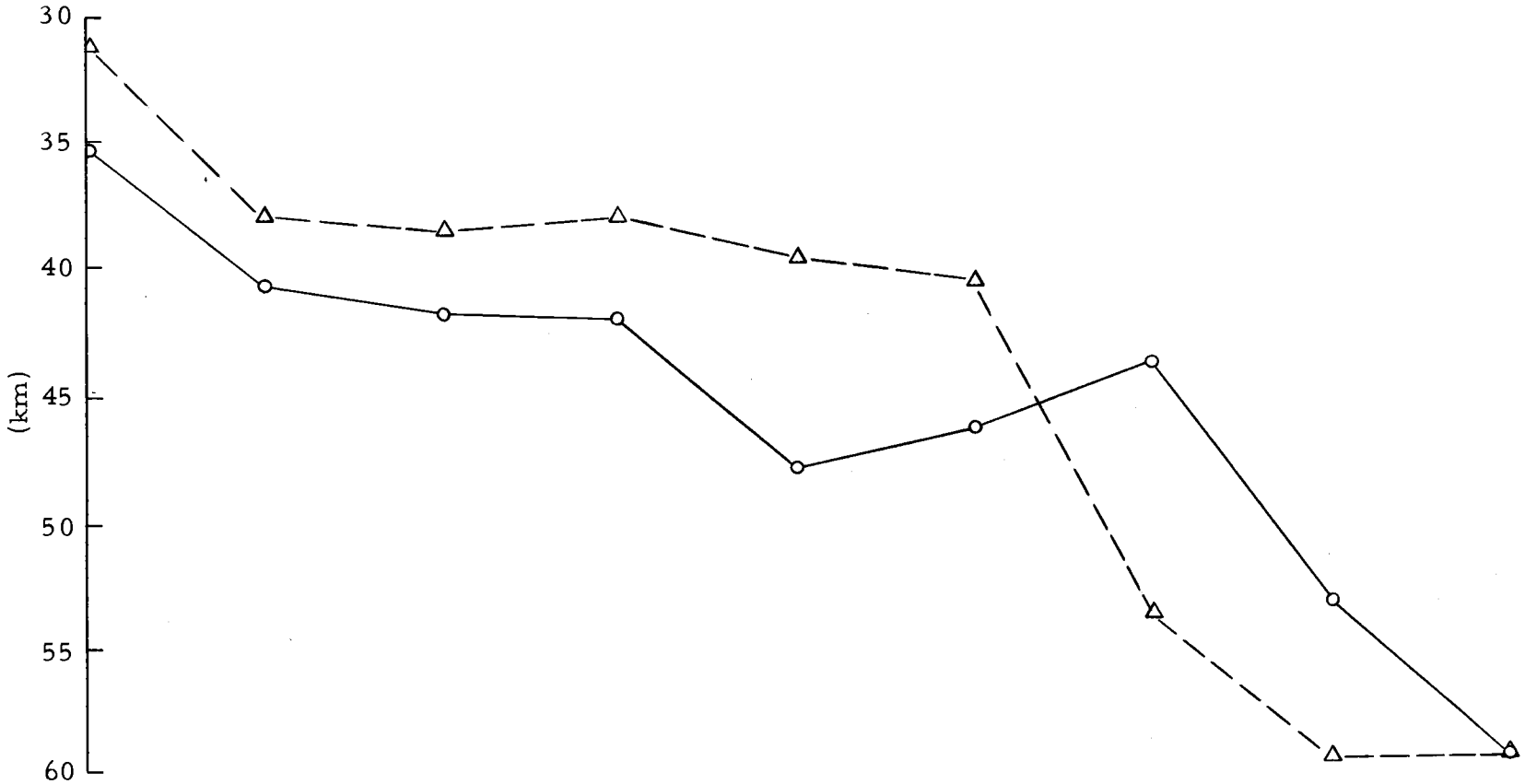

Figure 21a. Cross-sections along latitude 45°N, from longitude 116°30' to 123°30', through Figure 8b (broken curve) and Figure 17b (full curve).

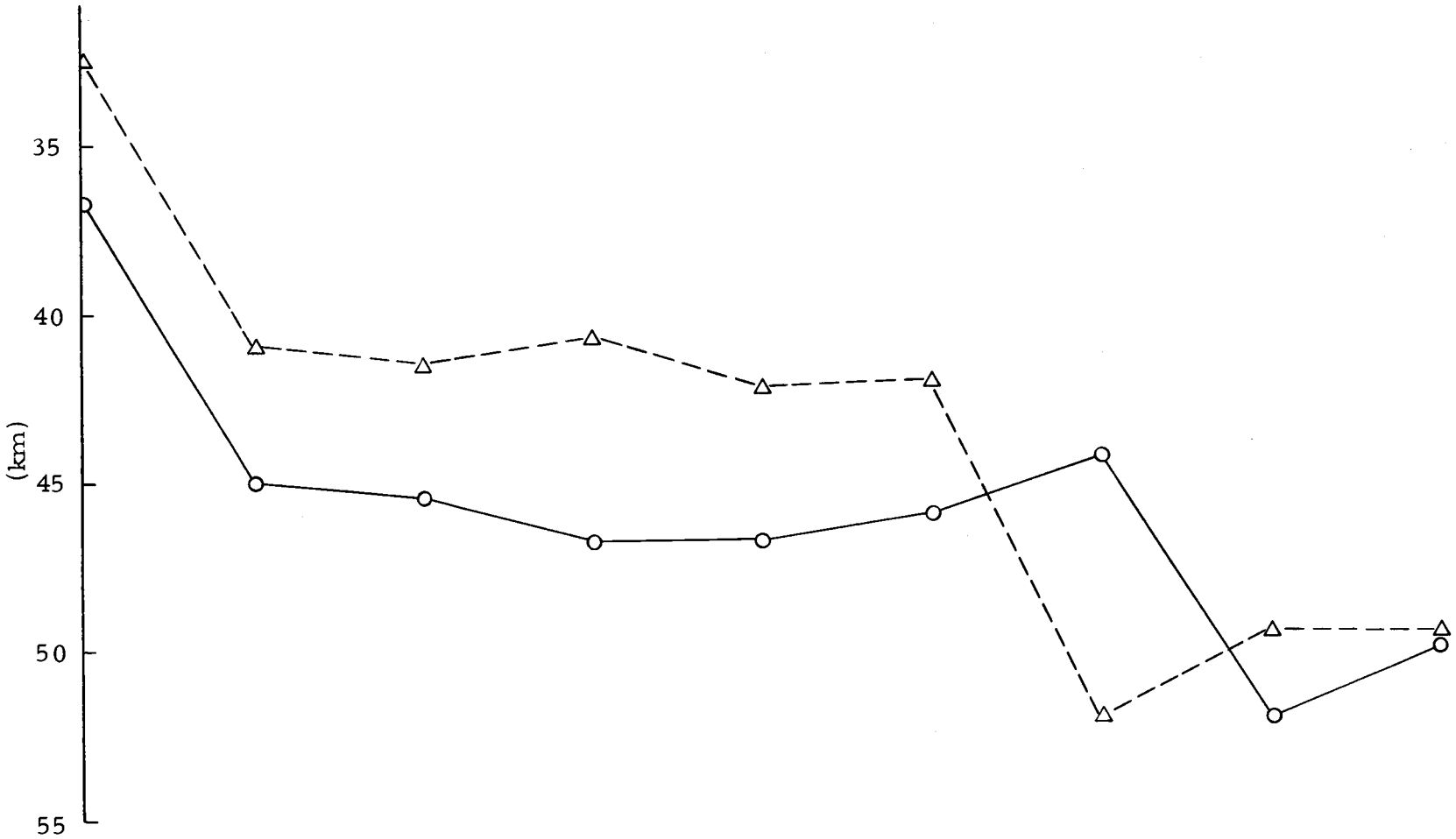

Figure 21b. Cross-sections along latitude 43°N, from longitude 116°30' to 123°30', through Figure 8b (broken curve) and Figure 17b (full curve).

CONCLUSION

The algebraic and the second derivative approximation methods provide two approaches to the study of the crustal thickness and its variation. The two methods are adaptable to a high speed computer and produce results rapidly. In this respect, they may often be preferable to the indirect method of interpretation. It is concluded that the algebraic approach can be extended to the study of the shapes of massive anomalous bodies.

In so far as each assumed value of d, the average crustal thickness, produces its own thickness profiles, the results yielded by the two methods are not absolute. However, when an absolute value of the average crustal thickness is known from a seismic profile, this value should be used for d so as to obtain the best approximation to absolute thicknesses. In this way the two methods, although based on a simple model of a homogeneous crust and a homogeneous upper mantle, provide a convenient and economical way of combining the gravitational and seismic methods for regional studies of crustal thickness in regions in which a few seismic profiles are available.

BIBLIOGRAPHY

Airy, G. B. 1855. On the computation of the effect of the attraction of mountain masses. Philosophical Transactions of the Royal Society, series B, 145:101-104.

Arfken, G. 1966. Mathematical methods of physicists. New York, Academic Press. 704 p.

Baker, C. T. H., L. Fox, D. F. Mayers and K. Wright. 1964. Numerical solution of Fredholm integral equations of the first kind. Computer Journal 7:141-148.

Baldwin, E. M. 1964. Geology of Oregon. Eugene, University of Oregon Cooperative Book Store. 165 p.

Bateman, H. 1946. Some integral equations of potential theory. Journal of Applied Physics 17:91-102.

Berg, J. W. et al. 1966. Crustal refraction profile, Oregon Coast Range. Bulletin of the Seismological Society of America 56:1357-1362.

Bodvarsson, G. 1966. Corvallis, Department of Mathematics, Oregon State University. Lecture notes on theoretical and mathematical methods in geophysics.

Bodvarsson, G. 1969. Numerical interpretation of potential field data. Corvallis, Department of Oceanography, Oregon State University. Unpublished.

Bodvarsson, G. 1971. Approximation methods for equivalent strata. Corvallis, Department of Oceanography, Oregon State University. Unpublished.

Blank, H. R. 1965. Southern Oregon gravity data. Menlo Park, California, U. S. Geological Survey. Open file report. 63 p.

Bullard, E.C. and R.I.B. Cooper. 1948. The determination of the masses necessary to produce a given gravitational field. Royal Society of London, Proceedings, series A, Mathematical and Physical Sciences 194:332-347.

Byerly, P. 1937. The Sierra Nevada in the light of isostasy. Bulletin of the Geological Society of America 48:2025-2031.

Chapman, S. and J. Bartels. 1940. Geomagnetism, Vol. 1. Oxford, Clarendon Press. 542 p.

Chiburis, E.F. 1966. Crustal structures in the Pacific Northwest States from phase-velocity dispersion of seismic surface waves. Ph.D. thesis. Corvallis, Department of Oceanography, Oregon State University. 170 p.

Couch, R.W. and R. Whitsett. 1969. The North Powder earthquake of August 14, 1969. The ORE BIN 31:239-243.

Coulomb, J. and G. Jobert. 1963. The physical constitution of the earth, tr. by A.E.M. Nairn. Edinburgh, Oliver and Boyd. 328 p.

Danes, Z.F. and L.A. Oncley. 1962. An analysis of some second-derivative method of gravity interpretation. Geophysics 27:611-615.

Dehlinger, P., E.F. Chiburis and M.M. Collver. 1965. Local travel-time curves and their geologic implications for the Pacific Northwest States. Bulletin of the Seismological Society of America 55:587-607.

Dehlinger, P., R.W. Couch and M. Gemperle. 1968. Continental and oceanic structure from the Oregon coast westward across the Juan de Fuca Ridge. Canadian Journal of Earth Sciences 5:1079-1090.

Dix, C.H. 1964. Use of the function sin x/x in gravity problems. Proceedings of the Japan Academy 40:276-278.

Dobrin, M.B. 1960. Introduction to geophysical prospecting. New York, McGraw-Hill. 446 p.

Duff, G.F.D. and D. Naylor. 1966. Differential equations of applied mathematics. New York, John Wiley. 423 p.

Elkins, T.A. 1951. The second derivative method for gravity interpretation. Geophysics 16:29-50.

Emilia, D.A. 1968. Numerical methods in the direct interpretation of marine magnetic anomalies. Ph.D. thesis. Corvallis, Department of Oceanography, Oregon State University. 100 p.

Faddeeva, D.K. and V.N. Faddeeva. 1963. Computational methods of linear algebra, tr. by R.C. Williams. San Francisco, W.H. Freeman and Company. 621 p.

Faddeeva, V.N. 1959. Computational methods of linear algebra, tr. by D.C. Benster. New York, Dover. 252 p.

Forsythe, G.E. and C.B. Moller. 1967. Computer solution of linear algebraic systems. Englewood Cliffs, N.J., Prentice Hall. 148 p.

Garland, G.D. 1965. The earth's shape and gravity. New York, Pergamon Press. 183 p.

Grant, F.S. and G.F. West. 1965. Interpretation theory in applied geophysics. New York, McGraw-Hill. 584 p.

Griffin, W.R. 1949. Residual gravity in theory and practice. Geophysics 14:39-56.

Gutemberg, P. 1943. Seismological evidence for roots of mountains. Bulletin of the Geological Society of America 54:473-498.

Hammer, S. 1939. Terrain corrections for gravimetric stations. Geophysics 4:184-194.

Hayford, J.F. 1906. Geodetic evidence of isostasy. Proceedings of the Washington Academy of Science 8:25-40.

Heiskanen, W.A. and F.A. Vening Meinesz. 1958. The earth and its gravity field. New York, McGraw-Hill. 470 p.

Henderson, R.A. and I. Zietz. 1949. Computation of second derivatives of geomagnetic fields. Geophysics 14:517-534.

Hertling, J. 1969. Assistant Professor of Mathematics, Oregon State University. Personal communication.

Hill, D.P. 1970. Crustal structure of the Columbia Plateau from the EDZOE events. Unpublished.

Hill, D.P. and L.C. Pakiser. 1966. Crustal structure between the Nevada Test Site and Boise, Idaho, from seismic refraction measurements, in the earth beneath the continents. American Geophysical Union Geophysical Monograph 10. 663 p.

Kantorovich, L.V. and V.I. Krylov. 1958. Approximate methods of higher analysis, tr. by C.D. Benster. New York, Interscience Publishers. 681 p.

Kellogg, O.D. 1929. Foundations of potential theory. New York, Dover. 384 p.

Kreisel, G. 1949. Some remarks on integral equations with kernels: $L(y_1-x_1, \ldots, y_n-x_n; a)$. Royal Society of London, Proceedings, series A, Mathematical and Physical Sciences 197:160-183.

MacMillan, W.D. 1958. The theory of the potential. New York, Dover. 469 p.

Mesko, C.A. 1965. Some notes concerning the frequency analysis for gravity interpretation. Geophysical Prospecting 13:475-488.

Mesko, C.A. 1966. Two-dimensional filtering and the second derivative method. Geophysics 31:606-617.

Morse, P.M. and H. Feshbach. 1953. Methods of theoretical physics. New York, McGraw-Hill. 2 vols.

Nettleton, L.L. 1954. Regionals, residuals and structures. Geophysics 19:10-22.

Pakiser, L.C. and D.P. Hill. 1963. Crustal structure in Nevada and sourthern Idaho from nuclear explosions. Journal of Geophysical Research 68:5757-5766.

Peters, L.J. 1949. The direct approach to magnetic interpretation and its practical application. Geophysics 14:290-320.

Philips, D.L. 1962. A technique for the numerical solution of certain integral equations of the first kind. Association for Computing Machinery, Journal 9:84-97.

Pratt, J.H. 1857. On the deflection of the plumbline in India, caused by the attraction of the Himalayan mountains. Philosophical Transactions of the Royal Society, series B 149:745-778.

Putnam, G.P. and C.M. Gilbert. 1895. Results of a trans-continental series of gravity measures. Bulletin of the Philosophical Society of Washington 13:31-76.

Reid, H.F. 1911. Isostasy and mountain ranges. Proceedings of the American Philosophical Society 50:444-451.

Rosenbach, O. 1953. A contribution to the computation of the second derivative from gravity data. Geophysics 18:894-912.

Scarborough, J.B. 1966. Numerical mathematical analysis. Baltimore, Johns Hopkins Press. 600 p.

Shih, K.G. 1967. On the reduction and interpretation of ocean floor temperature and heat flow data. Corvallis, Oceanography Department, Oregon State University. Ph.D. thesis. 103 p.

Simpson, S.M. 1954. Least square polynomial fitting to gravitational data and density plotting by digital computers. Geophysics 19:255-269.

Skeels, D.C. 1967. What is residual gravity? Geophysics 32:872-876.

Snow, C. 1923. Spectrum analysis of radio signals. Scientific Papers, Bureau of Standard 19:231-261.

Sobolev, S.L. 1964. Partial differential equations of mathematical physics, tr. by E.R. Dawson. Oxford, Pergamon Press. 427 p.

Sutton, O.G. 1953. Micrometeorology. New York, McGraw-Hill. 333 p.

Tanner, J.G. 1967. An automated method of gravity interpretation. Geophysical Journal of the Royal Astronomical Society 13:339-347.

Thiruvathukal, J.V. 1968. Regional gravity of Oregon. Ph.D. thesis. Corvallis, Department of Oceanography, Oregon State University.

Tomoda, Y. and K. Aki. 1955. Use of the function sin x/x in gravity problems. Proceedings of the Japan Academy 31:443-448.

Tsuboi, Chuji. 1938. Gravity anomalies and the corresponding subterranean mass distribution. Proceedings of the Imperial Academy of Japan 14:170-175.

Tsuboi, C. and T. Fuchida. 1937. Relations between gravity values and corresponding subterranean mass distribution. Bulletin of the Earthquake Research Institute 15:636-650.

Vening Meinesz, F.A. 1931. Une nouvelle méthode pour la réduction isostatique régionale de l'intensité de la pesanteur. Bulletin Géodésique 29:33-51.

Washington, H.S. 1922. Isostasy and rock density. Bulletin of the Geological Society of America 33:375-410.

Woollard, G.P. 1962. The relation of gravity anomalies to surface elevation, crustal structure and geology. Madison, Department of Geology, The University of Wisconsin, Research Report Series, Part V. 74 p.

Woollard, G.P. 1969. Standardization of gravity measurements, in the Earth's crust and upper mantle. American Geophysical Union. Geophysical Monograph 13. 735 p.

Woollard, G.P. and J.C. Rose. 1963. International gravity measurements. Society of Exploration Geophysicists. 518 p.

APPENDICES

APPENDIX A
PROGRAM GRAVCALC

```
OS3 FORTRAN  VERSION 2.1                11/11/70  1400
      PROGRAM GRAVCALC                                                  00001
      COMMON K1(45,45),K2(45,45),C(45,45),H(45),UG(45),X(45),RHS(45)    00002
      REAL K1,K2                                                        00003
      INTEGER ROW,COL                                                   00004
      GAMMA=6.67E-8                                                     00005
      PHO=0.6                                                           00006
      DO 50 I = 1,6                                                     00007
      D = 25.E5                                                         00008
      DETA = 100.E5                                                     00009
      DPSI = 1 * D / 2.                                                 00010
      CK2=GAMMA*PHO*DPSI*DETA/2.0E-3                                    00011
      IPT=0                                                             00012
      READ (1,9999) DG                                                  00013
 9999 FORMAT (X,8E10.2,/,X,7E10.2)                                      00014
      PP=0.0                                                            00015
      PP3=3.0*PP                                                        00016
      CK1=CK2*2.0*D                                                     00017
      ROW=0                                                             00018
      X=0.0                                                             00019
      DO 6 I=1,15                                                       00020
      Y=0.0                                                             00021
      DO 5 J=1,3                                                        00022
      ROW=ROW+1                                                         00023
      COL=0                                                             00024
      PSI=0.0                                                           00025
      DO 4 K=1,15                                                       00026
      PP=(X-PSI)*(X-PSI)+D*D                                            00027
      ETA=0.0                                                           00028
      DO 3 L=1,3                                                        00029
      COL=COL+1                                                         00030
      P2=PP+(Y-ETA)*(Y-ETA)                                             00031
      P3=SQRT(P2)*P2                                                    00032
      C(ROW,COL)=K1(ROW,COL)=CK1/P3                                     00033
      K2(ROW,COL)=CK2*(PP3-P2)/P3/P2                                    00034
      ETA=ETA+DETA                                                      00035
 3    CONTINUE                                                          00036
      PSI=PSI+DPSI                                                      00037
 4    CONTINUE                                                          00038
      RHS(ROW)=DG(ROW)                                                  00039
      Y=Y+DETA                                                          00040
 5    CONTINUE                                                          00041
      X=X+DPSI                                                          00042
 6    CONTINUE                                                          00043
      ACC=GS(C,45,45,H,RHS,-20,1.0E-3)                                  00044
      WRITE(3,1001) ACC                                                 00045
 1001 FORMAT(* INITIAL SOLUTION OBTAINED TO*E12.4* ACCURACY*)           00046
      L=1                                                               00047
 7    CONTINUE                                                          00048
      DO 9 I=1,45                                                       00049
      Y=UG(I)                                                           00050
      DO 8 J=1,45                                                       00051
      C(I,J)=K1(I,J)+2.0*K2(I,J)*H(J)                                   00052
      Y=Y-H(J)*(K1(I,J)+H(J)*K2(I,J))                                   00053
 8    CONTINUE                                                          00054
      RHS(I)=Y                                                          00055
 9    CONTINUE                                                          00056
      ACC=GS(C,45,45,X,RHS,-10,1.0E-3)                                  00057
      IF(ACC.GT.1.0E-3) WRITE(3,1002) ACC,L                             00058
 1002 FORMAT(* ONLY CONVERGED TO*E12.4* ON STEP*I3)                     00059
      IF(L.GT.20) GO TO 11                                              00060

OS3 FORTRAN  VERSION 2.1  GRAVCALC  11/11/70  1400
      L=L+1                                                             00061
      Y=0.0                                                             00062
      DO 10 I=1,45                                                      00063
      Y=Y+ABS(H(I))                                                     00064
      D=D+ABS(X(I))                                                     00065
      H(I)=H(I)+X(I)                                                    00066
 10   CONTINUE                                                          00067
      IF(D.GT.1.0E-3*Y) GO TO 7                                         00068
      D=D/Y                                                             00069
 11   CONTINUE                                                          00070
      WRITE(2,1003) L,D,H                                               00071
 1003 FORMAT(* AFTER*I3* ITERATIONS, WITH RELATIVE ERROR*E12.4* H IS*/  00072
     1 3(/ *,8F10.2,/,* *,7F10.2))                                      00073
      END                                                               00074
                                                                        00075
```

```
OS3 FORTRAN  VERSION 2.1                11/11/70  1400
      FUNCTION GS(R,NS,N,X,Y,ITCNT,TOL)                                 00076
      DIMENSION R(1),Y(1),X(1)                                          00077
      VALUE NS,N,ITCNT,TOL                                              00078
C                                                                       00079
C                                                                       00080
C     GAUS-SIEDEL ITERATION FOR SOLVING LINEAR SYSTEMS OF               00081
C     EQUATIONS.                                                        00082
C         R=R(NS,--) IN DIMENSIONING STATEMENT                          00083
C          =R(N,N) IN PROGRAM USAGE                                     00084
C         X=SOLUTION VECTOR                                             00085
C         Y=RIGHT HAND SIDE VECTOR                                      00086
C     ITCNT=NUMBER OF ITERATIONS ALLOWED.  IF NEGATIVE                  00087
C           USE Y AS INTIAL VALUE AND TRANSFORM SYSTEM TO               00088
C           ONE WITH ZERO DIAGONAL.  IF POSITIVE USE X AS THE           00089
C           INITIAL VALUE AND DON#T TRANSFORM SYSTEM.                   00090
C   TOL=CONVERGENCE VALUE(IN DIGIT ANSWER 10**(-N))                     00091
C                                                                       00092
C                                                                       00093
C     GS WILL BE THE NORM OF THE DIFFERENCE DIVIDED BY THE              00094
C     NORM OF THE SOLUTION VECTOR ON RETURN                             00095
C                                                                       00096
C                                                                       00097
      IF(ITCNT.GE.0) GO TO 3                                            00098
C                                                                       00099
C     TRANSFORM SYSTEM                                                  00100
C                                                                       00101
      ID=1                                                              00102
      DO 2 J=1,N                                                        00103
      RII=R(ID)                                                         00104
      Y(J)=X(J)=Y(J)/RII                                                00105
      IF=J                                                              00106
      DO 1 K=1,N                                                        00107
      R(IF)=-R(IF)/RII                                                  00108
      IF=IF+NS                                                          00109
1     CONTINUE                                                          00110
      R(ID)=0.                                                          00111
      ID=ID+NS+1                                                        00112
2     CONTINUE                                                          00113
      ITCNT=-ITCNT                                                      00114
C                                                                       00115
C     BEGIN G-S ITERATIONS                                              00116
C                                                                       00117
3     CONTINUE                                                          00118
      ID=0                                                              00119
4     CONTINUE                                                          00120
      XN=XD=0.                                                          00121
      DO 6 I=1,N                                                        00122
      J=I                                                               00123
      RII=Y(I)                                                          00124
      XN=XN+ABS(X(I))                                                   00125
      DO 5 K=1,N                                                        00126
      RII=RII+R(J)*X(K)                                                 00127
      J=J+NS                                                            00128
5     CONTINUE                                                          00129
      XD=XD+ABS(RII-X(I))                                               00130
      X(I)=RII                                                          00131
6     CONTINUE                                                          00132
      ID=ID+1                                                           00133
      IF(ID.GE.ITCNT) GO TO 7                                           00134
      IF(XD.LE.TOL*XN) 7,4                                              00135

OS3 FORTRAN  VERSION 2.1  GS        11/11/70  1400
7     CONTINUE                                                          00136
      GS=XD/XN                                                          00137
      END                                                               00138
                                                                        00139
```

APPENDIX B

PROGRAM UPWARD

```
OS3 FORTRAN  VERSION 2.1            04/20/71  1330
      PROGRAM UPWARD                                                    00001
      DIMENSION H(15,15), G(15,15), DG(15,15)                           00002
      READ (1,99) D, D2                                                 00003
   99 FORMAT (2F10.5)                                                   00004
      CONST1 = -D / ( 4. * 3.14159)                                     00005
      READ (1,102) ((G(I1,I2),I1=1,10),I2=1,15)                         00006
      READ (1,103) ((G(I1,I2),I1=11,15),I2=1,15)                        00007
  102 FORMAT (X,10E10.3)                                                00008
  103 FORMAT (X,5E10.3)                                                 00009
      D2SQ = D2 * D2                                                    00010
      DSQ = D * D                                                       00011
      DO 50 I1 = 1,15                                                   00012
      DO 50 I2 = 1,15                                                   00013
      SUM = 0.                                                          00014
      DO 40 I3 = 1,15                                                   00015
      DO 40 I4 = 1,15                                                   00016
      RSQ = ((D2 * (I1 - I3)) ** 2 + (D2 * (I2 - I4)) ** 2 +DSQ) ** 1.5 00017
      SUM = SUM + (G(I3,I4) * D2SQ) / RSQ                               00018
   40 CONTINUE                                                          00019
      DG(I1,I2) = CONST1 * SUM                                          00020
   50 CONTINUE                                                          00021
      WRITE (2,100) ((DG(I1,I2),I1=1,10),I2=1,15)                       00022
      WRITE (2,101) ((DG(I1,I2),I1=11,15),I2=1,15)                      00023
  100 FORMAT (#1#,/,15(# #,10E10.3,/))                                  00024
  101 FORMAT (# #,/,15(# #,5E10.3,/))                                   00025
      END                                                               00026
```

APPENDIX C
PROGRAM SUM

```
OS3 FORTRAN  VERSION 2.1              08/13/70  1024
      PROGRAM SUM                                                          00001
      DIMENSION Q1(21,21), Q2(21,21), Q3(21,21), H(21,21), DG(21,21)       00002
      DIMENSION  GC(21,21), GS(21,21), RESULT(21,21)                       00003
      PI = 3.14159                                                         00004
      CONST = 1. / (PI * 6.67 * .60)                                       00005
C  LUN 1 HAS INPUT TO WMP#S PROGRAM                                        00006
      READ (1,101) ((Q1(I,J),I=1,10),J=1,21)                               00007
      READ (1,105) ((Q1(I,J),I=11,21),J=1,21)                              00008
  101 FORMAT (10E10.3)                                                     00009
  105 FORMAT (11E10.3)                                                     00010
C  LUN 2 HAS GC ON IT                                                      00011
C  LUN 3 HAS GS ON IT                                                      00012
      DO 10 I = 1,21                                                       00013
      DO 10 J = 1,21                                                       00014
      GC (I,J) = Q1 (I,J)                                                  00015
   10 CONTINUE                                                             00016
      READ (3,102) ((GS(I,J),I=1,10),J=1,21)                               00017
      READ (3,106) ((GS(I,J),I=11,21),J=1,21)                              00018
  102 FORMAT (F5.3,X,F5.3,8F7.3)                                           00019
  106 FORMAT (F6.3,10F7.3)                                                 00020
      D = 25.                                                              00021
C  LUN 4 HAS DG ON IT (OUTPUT FROM DARRAY)                                 00022
      READ (4,104) ((DG(I,J),I=1,10),J=1,21)                               00023
      READ (4,107) ((DG(I,J),I=11,21),J=1,21)                              00024
  104 FORMAT (10E10.4)                                                     00025
  107 FORMAT (X,11E10.4)                                                   00026
      DO 30 J = 1,21                                                       00027
      DO 30 I = 1,21                                                       00028
      Q2 (I,J) = 2. * D * D / 900. * (GC(I,J) - GS(I,J))                   00029
      GS(I,J) = GS(I,J) * D / (2. * 3.14159)                               00030
      Q3 (I,J) = D / (4. * PI) * DG (I,J)                                  00031
      RESULT (I,J) = D -CONST * ( Q1 (I,J) - Q2 (I,J) - Q3 (I,J))          00032
   30 CONTINUE                                                             00033
      WRITE (2,103) D                                                      00034
  103 FORMAT (#1DEPTH =#,E15.4)                                            00035
      WRITE (2,100) ((RESULT (I,J),I=1,21),J=1,21)                         00036
  100 FORMAT (#1RE=#,/,8(X,7E9.2,/))                                       00037
      END                                                                  00038
```